2017

Characterization Of Subgrade Resilient Modulus For MEPDG And The Effects On Pavement Rutting

Md Mostaqur Rahman
University of South Carolina

CHARACTERIZATION OF SUBGRADE RESILIENT MODULUS FOR MEPDG AND THE EFFECTS ON PAVEMENT RUTTING

by

Md Mostaqur Rahman

Bachelor of Science
Bangladesh University of Engineering and Technology, 2009

Master of Science
University of New Mexico, 2012

Submitted in Partial Fulfillment of the Requirements

For the Degree of Doctor of Philosophy in

Civil Engineering

College of Engineering and Computing

University of South Carolina

2017

Accepted by:

Sarah Gassman, Major Professor

Charles Pierce, Committee Member

Inthuorn Sasanakul, Committee Member

Andrew Johnson, Committee Member

Cheryl L. Addy, Vice Provost and Dean of the Graduate School

DEDICATION

To my beloved parents: Mr. Md Bazlar Rahman & Mrs. Masuda Rahman, and grandparents: Late Solaiman Ali & Late Morium Nesa, Late Mokbul Ali & Mrs. Sahanara Khanam.

ACKNOWLEDGEMENTS

I wish to express my deepest gratitude and appreciation to my advisor and chair of my dissertation committee, Dr. Sarah Gassman, for her guidance and encouragement for this study and for her time and support throughout my Ph.D. career.

I would like to thank the members of my dissertation committee, Dr. Charles Pierce, Dr. Inthuorn Sasanakul, and Dr. Andrew Johnson for their valuable recommendations pertaining to this study and assistance to my professional development.

I also acknowledge to the Office of Materials and Research, South Carolina Department of Transportation (SCDOT) for the funding to pursue this research. I specially would like to thank Mr. Jay Thompson, Mr. Luke Gibson, Mr. Mike Lockman, and Mr. Chad Rawls for their assistance in field data and sample collections.

Cooperation and encouragement from my lab mates are highly appreciated. I would like to express gratitude to Dr. Emad Gheibi for assistance with the soil index tests for this study. Special thank goes to Dr. Mike Hasek, Mr. Ryan Starcher, Mr. William Villamil, Mr. Muwafaq Awad, and Mr. Md Majbah Uddin for their sincere effort and help in laboratory testing.

ABSTRACT

In 2008, the American Association of State Highway and Transportation Officials (AASHTO) released a modified pavement design method (i.e., the Mechanistic Empirical Pavement Design Guide (MEPDG)) based on Long Term Pavement Performance (LTPP) data from all over the United States. The MEPDG default design parameters developed from the LTPP database are expected to be significantly different than those for South Carolina material, traffic and weather conditions, thus the default design parameters may not be accurate for South Carolina. Therefore, the new pavement design method should be calibrated for South Carolina conditions by performing MEPDG local calibration.

Different input variables should be studied to run the pavement design program to minimize the difference between the measured and predicted distresses of pavements. Rutting is one of the most important asphalt pavement distresses because it is responsible for both the functional and structural condition degradation of the flexible pavement. There are limited studies on the effect of resilient modulus (M_R) of subgrade on pavement rutting in the MEPDG. Therefore, the purpose of this study was to characterize the subgrade M_R and study the effects of subgrade M_R on pavement rutting.

Firstly, pavement performance evaluation models were developed in this study using data from primary and interstate highway systems in the state of South Carolina, USA. Twenty pavement sections were selected from across the state and historical pavement performance data for those sections was collected. A total of 9 models were developed based on regression techniques, which include 5 for Asphalt Concrete (AC)

pavements and 4 for Jointed Plain Concrete Pavements (JPCP). Five different performance indicators were considered as response variables in the statistical analysis: Present Serviceability Index (PSI), Pavement Distress Index (PDI), Pavement Quality Index (PQI), International Roughness Index (IRI), and AC pavement rutting. Annual Average Daily Traffic (AADT), Free Flow Speed (FFS), precipitation, temperature, and soil type (soil Type A from Blue Ridge and Piedmont Region, and soil Type B from Coastal Plain and Sediment Region) were considered as predictor variables. Results showed that Type A soil produced statistically higher PDI, PQI ($p < 0.01$), and rutting ($p < 0.001$) compared to Type B soil on AC pavements; whereas, Type A soil produced statistically higher IRI and lower PSI ($p < 0.001$) compared to Type B soil on JPCP pavements. Using the developed models, local transportation agencies could estimate future corrective actions, such as maintenance and rehabilitation, as well as future pavement performances.

Next, resilient modulus (M_R) of subgrade soils for different geographic regions in South Carolina was characterized in this study. Shelby tube samples of subgrade soils were collected from existing pavements in different regions: SC-93 in Pickens county (Upstate Area), US-521 in Georgetown county (Coastal Plain), and US-321 in Orangeburg county (Coastal Plain, near the fall line). Statistical analysis was performed to develop M_R estimation models for undisturbed soils using soil index properties. A correlation between laboratory measured M_R with the modulus from Falling Weight Deflectometer tests was also developed. Finally, the effects of M_R on subgrade rutting were studied using MEPDG. Results showed that the developed models offer higher reliability than the universal Long-Term Pavement Performance models in estimating the resilient modulus of undisturbed soils and predicting subgrade rutting for South Carolina.

Pavement rutting depends largely on subgrade soil stiffness, which is a function of the in-situ moisture content and soil index properties. The subgrade soil moisture content may vary from the specified condition due to variations in the compaction procedure during construction and fluctuations in the ground water table from seasonal changes. The resilient modulus (M_R) is used to define the subgrade soil stiffness, and is one of the most important material inputs for the Mechanistic-Empirical (M-E) pavement design method. In this study, California Bearing Ratio (CBR) tests and laboratory M_R tests were performed on remolded samples of soils collected from different regions in South Carolina. The samples were prepared at moisture contents above and below the optimum moisture content (w_{opt}). Correlations between the results from the two tests were developed as a function of moisture content and statistical models were developed to correlate generalized constitutive M_R model parameters with soil index properties. Furthermore, pavement rutting was studied using the resilient modulus determined for the subgrade soils compacted at w_{opt} and $\pm 2\% w_{opt}$. Statistical analysis showed that a slight change in moisture content during compaction has a significant effect on pavement rutting. The peak value of both CBR and M_R was found on the dry side of optimum and at a dry density less than the maximum. It is also found that the subgrade soil moisture condition has a significant influence on subgrade rutting if graded aggregate base is used. However, if a higher strength base layer is used (i.e., cement stabilized base or asphalt treated aggregate base), the effect of moisture content is less significant.

PREFACE

This Ph.D. dissertation is organized in the following order. The first chapter presents the background and objectives of the research. All subsequent chapters are prepared in a format to facilitate the writing and submission of journal papers. The paper related to Chapter 2 has been accepted to the KSCE Journal of Civil Engineering. The paper related to Chapter 3 has been accepted to the International Journal of Geotechnical Engineering. The paper related to Chapter 4 is submitted to Transportation Research Record: Journal of Transportation Research Board. Chapter 5 presents the conclusions and recommendations of this study.

This dissertation is primarily based on research supported by the SCDOT and the Federal Highway Administration (FHWA) under contract SPR 708: Calibration of the AASHTO Pavement Design Guide to South Carolina Conditions – Phase I. The opinions, findings and conclusions expressed herein are those of the authors and not necessarily those of SCDOT or FHWA.

TABLE OF CONTENTS

LIST OF FIGURES

LIST OF TABLES

CHAPTER 1

INTRODUCTION

1.1 PROBLEM STATEMENT

Resilient and permanent deformation occurs with time in different pavement layers due to repeated traffic load application on pavement materials in different weather conditions (Behzadi and Yandell, 1996). Rutting is the pavement surface depression in the wheel paths and is caused by the permanent deformation of the pavement layers or subgrade layers. It originates from the lateral movement of pavement material due to cumulative traffic loading. Rutting is categorized as a structural distress that affects both the riding quality and pavement structural health. Therefore, rutting within the pavement layers is considered to be a major failure mode in flexible pavement that can cause structural failure of the pavement (Shahin, 2005). Traffic conditions (Zaghloul et al., 2006; Jadoun and Kim, 2012), climate conditions (Zaghloul et al., 2006; Johanneck and Kazanovich, 2010; Zapata et al., 2007) and the pavement and subgrade materials (Singh et al., 2011; Saxena et al., 2010; Xu et al., 2013; Hossain et al., 2011; Wu and Yang, 2012; Graves and Mahboub, 2006) all have a significant influence on the structural life of a pavement.

The Mechanistic Empirical Pavement Design Guide (MEPDG) is the latest pavement design method that was developed using data from the Strategic Highway Research Program (SHRP) Long-Term Pavement Performance (LTPP) study (AASHTO, 2008). The two fundamental differences between the previously used design method

(Guide for Design of Pavement Structures, AASHTO, 1993) and the MEPDG are that the MEPDG predicts multiple performance indicators and it provides a direct tie between materials, structural design, construction, climate, traffic, and pavement management systems. This is a change from an empirical based method to a mechanistic based method. MEPDG is recently being adopted throughout the United States (U.S.) for pavement design because of its ability to account for the mechanistic behavior of in-situ materials, new materials and changing load types (Souliman et al., 2010). Local calibration of MEPDG is required because MEPDG is developed using national data that does not necessarily represent the material and climate conditions for each state, such as those in South Carolina. Currently state departments of transportation in the U.S. (e.g. Texas (Banerjee et al., 2009), New Mexico (Tarefder and Rodriguez-Ruiz, 2013), and North Carolina (Jadoun and Kim, 2012)) are performing local calibrations of the MEPDG.

Previous studies have shown different pavement layer characteristics (i.e. asphalt concrete dynamic modulus, coefficient of thermal expansion of Portland cement concrete layer, resilient modulus of unbound base and subgrade layer) are the key input parameters of pavement design and performance evaluation (El-Badawy, 2012; Hossain et al., 2011; Khazanovich et al., 2006; and Saxena et al., 2010; Singh et al., 2013; Xu et al., 2013). These pavement layer characteristics are required to run different transfer models in MEPDG. Transfer models are used to predict pavement deformation (i.e., rutting) of different structural layers. Wu and Yang (2012) evaluated MEPDG flexible pavement design using pavement management system data for Louisiana. A special optimization approach was introduced to determine a set of preliminary local calibration factors for the MEPDG rutting models for flexible pavements. Waseem and Yuan (2013) also performed

the local calibration of MEPDG rutting models for flexible pavements. They proposed a set of percentage contributions to the total rutting from different pavement layers based on previous empirical studies and computation observations. One particular study by Orobio and Zaniewski (2011) examined each of the pavement material characteristics and determined the sampling based sensitivity analysis of the MEPDG applied to material input. They found that the Resilient Modulus (M_R) of subgrade had the largest effect on the rutting predicted from MEPDG. Baus and Stires (2010) also performed a sensitivity analysis and reported similar findings regarding material inputs. Their study suggested subgrade M_R had a significant influence on pavement roughness measured as International Roughness Index (IRI), total rutting, alligator cracking and longitudinal cracking for pavements in several South Carolina counties. Therefore, they recommended a comprehensive subgrade investigation to determine M_R for South Carolina.

1.2 BACKGROUND

The research framework for this study is shown in Figure 1.1 in the form of a concept map. Three different types of inputs should be considered to perform the design in MEPDG: local material, local climate and local traffic. MEPDG compares the output or the predicted distress with the original distress to minimize the residual error and to determine the calibration factors. These calibration factors are adjustments applied to the coefficients and/or exponents of the transfer function or the distress prediction equations to eliminate bias between the predicted and measured pavement distress (AASHTO, 2008). Two calibration factors are used in the MEPDG: global and local calibration factors.

A typical asphalt pavement structure has three layers: asphalt layer, base layer and the subgrade layer. All of these layers have important material characteristics (i.e. asphalt

concrete dynamic modulus, coefficient of thermal expansion of Portland cement concrete layer, resilient modulus of unbound base and subgrade layer) that influence MEPDG local calibration. Cooper et al. (2012) emphasized the parametric evaluation of design input parameters (i.e. traffic level, hot-mix asphalt or HMA thickness, asphalt concrete dynamic modulus, base course thickness and subgrade type) on MEPDG predicted performance. A sensitivity analysis was conducted to identify the input parameters with the greatest effects on the predicted pavement performance from the MEPDG. Results showed that traffic level and the HMA thickness are the two main influential input parameters for pavement rutting. Another study considered the environmental and traffic impacts on MEPDG (Zaghloul et al., 2006). The potential impacts of the accuracy of the Enhanced Integrated Climate Model (EICM) predictions on MEPDG-predicted damage and hence on expected pavement service life was investigated.

Orobio and Zaniewski (2011) examined each of the pavement material characteristics and determined the sampling based sensitivity analysis of the MEPDG applied to material input. They studied 30 parameters for pavement structures that contained asphalt concrete layers of 2 in., 3 in. and 10 in. at the top of one 3 in. asphalt treated base layer and the subgrade. Figure 1.2 shows the effects of the 11 material inputs that showed significant effects on pavement rutting. The bar indicates the regression coefficients for different material properties. Five of the 11 significant parameters have negative regression coefficients, and the other six significant parameters showed positive relations. A positive regression coefficient indicates that MEPDG rutting increases with increasing input values; whereas, a negative regression coefficient indicates that, as the

parameter increases, pavement rutting decreases. The study found that M_R of subgrade had the largest effect on the rutting predicted from MEPDG.

Simulation of the base layer material resilient modulus effects on MEPDG was studied by Xu et al. (2013). In performing the sensitivity analysis in MEPDG software, pavement rutting and fatigue cracking were considered. Monte-Carlo simulation was performed in the sensitivity analysis. Results showed that the relationship between the layer design thickness and M_R varies from almost linear to nonlinear, which is highly dependent on the pavement structure and material properties. Characterization and performance modeling of a cement stabilized base layer in MEPDG was performed by Saxena et al. (2010) in another study. The current characterization of cement stabilized materials (CSMs) was evaluated and issues with CSM modeling and characterization in the MEPDG were discussed.

Behzadi and Yandell (1996) studied the effect of subgrade M_R on pavement performance in terms of rutting. In that study, a preliminary step in the prediction of rutting and cracking in a number of accelerated loading facility trials were presented. The residual and resilient properties of a silty clay subgrade material were measured using a repeated load triaxial testing machine. A constitutive equation was developed to predict the amount of plastic strain after any number of load repetitions at any specific stress level. Both the elastic and permanent parameters were measured for accurate prediction of rutting and cracking. In another literature, a model to predict the subgrade resilient modulus for MEPDG was developed by Khazanovich et al. (2006). They used two standard test methods for laboratory testing: NCHRP Project I-28 or Harmonized Test Methods for Laboratory Determination of M_R for Flexible Pavement design (NCHRP, 2004) and

AASHTO T 307 for determining the M_R of soil. Sensitivity analysis was then performed with MEPDG to evaluate the resilient modulus for Minnesota subgrade. The resilient modulus tests were performed on fabricated samples of the unbound material and subgrade in both of these studies.

Effects of additives such as lime, fly ash, and cement kiln dust on subgrade resilient modulus have been studied by Hossain et al. (2012). Resilient modulus data for stabilized subgrade from 139 samples from four types (i.e., Carnasaw, Port, Kingfisher, and Vernon series) of soils from Oklahoma were evaluated. Different stress based regression models were evaluated using statistical software. A significant increase in M_R values was observed for the three selected additives. The extent of increase in the M_R value depends on the type of soil, and type and amount of additive.

The resilient modulus of subgrade soils has also been found through correlation to other in situ and laboratory tests. Falling weight deflectometer (FWD) has been used to determine the in-situ modulus (e.g., Nazzal and Mohammad, 2010; Flintsch et al., 2003; and Ksaibati et al., 2000. The dynamic cone penetrometer test was used to evaluate base and subgrade layers by Chen et al. (2001). Determination of subgrade M_R using bender elements in the laboratory was shown in a study by Baig and Nazarian (1995). AASHTO design guide also proposed a correlation between California Bearing Ratio (CBR) and resilient modulus for fine-grained soils (Heukelom and Klomp, 1962). However, the studies conducted on the estimation of resilient modulus from CBR test results showed that the reliability of prediction models are not statistically satisfactory which is due to the structural differences between these two tests (Coleri, 2007).

Pavement material characteristics for different pavement layers are prone to change with different temperature and moisture content; therefore, several studies have been performed to determine the seasonal variation of the subgrade M_R (Ceratti et al., 2004; Khoury and Zaman, 2004; Heydinger, 2003; and Guan et al., 1998). Evaluation of MEPDG seasonal adjustment factors for the moduli of unbound layer has been shown in a study (Nassiri and Bayat, 2013). It was found that the FWD back calculated subgrade moduli in different seasons, excluding the freezing season, fits the MEPDG-predicted subgrade moduli at depth 910 mm with a R-squared of 80 percent.

In South Carolina, some limited data on the seasonal variation of subgrade strength was obtained by Chu (1972). In that study, field tests were performed to examine subgrade moisture variations under existing pavements in South Carolina. Field studies indicate that the finer the soil, the greater the difference between the equilibrium and optimum moisture content. Through their field work, they observed that moisture contents varied with season, soil type, and location in the pavement system and the height of the water table influenced subgrade moisture content. They found a strong correlation between subgrade moisture content and high groundwater table for pavement systems in South Carolina as shown in Figure 1.3. The study recommended a complete moisture variation study below South Carolina pavements in connection with pavement performance and design. Baus and Johnson (1992) performed bi-monthly FWD testing to develop a database of FWD deflection basins. That study included the establishment of 16 pavement test sections located throughout South Carolina. Table 1.1 shows the list of site location and soil type of 16 pavement test sections. Figure 1.4 shows the backcalculated moduli using drop number 5 at station 0 for US 321 of Fairfield County. The data shows a significant variation

in computed layer moduli (E_1 and E_2 in Figure 1.4 represent the Young's modulus of the asphalt-bound material as the surface layer and the unbound or cement modified material as the second layer, respectively) for different back-calculation programs; however, there was little seasonal variation of the subgrade soil moduli (E_{sg} in Figure 1.4 represents Young's modulus of subgrade materials as the infinite elastic half-space). A significant variation in overall pavement structure stiffness was also observed (E_e in Figure 1.4). Similar results were observed for the other test sections in South Carolina.

Ceratti et al. (2004) performed both laboratory tests and in situ tests to determine the seasonal variation of subgrade soil M_R in Southern Brazil. Laboratory testing was carried out to establish the relationship between water content and soil suction. The M_R was found for soil specimens submitted to drying, wetting, or wetting-after-drying paths. Jet-filled tensiometers were used to determine soil suction in different pavement test sections. A traffic simulator was also used in this study to measure the deflection. A relation between M_R, moisture variation and soil suction for subgrade soils was developed by Khoury and Zaman (2004). Heydinger (2003) evaluated the seasonal variation of subgrade soil for Ohio as part of LTPP instrumentation project seasonal monitoring program (SMP).

There have been limited studies to characterize the resilient modulus of subgrade soils (Hossain, 2008; Titi et al., 2006; George, 2004; Mohammad et al., 2007; Behzadi and Yandell, 1996) and only a single study focused on the effect of subgrade M_R on the pavement permanent deformation or rutting (Behzadi and Yandell, 1996). In the studies by Hossain (2008) and Titi et al., (2006) remolded samples (which do not necessarily represent actual field conditions) were used. For the studies by George (2004) and Mohammad et al. (2007); undisturbed soil samples were obtained from the field for the M_R

tests; however, the M_R results were not related to the MEPDG rutting model. Therefore, a comprehensive research program is necessary to study the effect of in-situ or undisturbed subgrade M_R on pavement performance and rutting. The behavior of subgrade soil in different temperature and climate regions with different moisture variations also requires study.

Using the available literature on MEPDG local calibration with material inputs, research gaps that need to be filled were identified for the local calibration process. These findings were then used to develop a research question aimed to understand the relationship between subgrade strength and pavement performance in MEPDG. The developed research questions are: How is pavement rutting influenced by the M_R of subgrade soils in South Carolina? What are the effects of moisture variation of subgrade resilient modulus on pavement rutting?

1.3 OBJECTIVES

The primary objectives of this research are to:

- Characterize the resilient modulus (M_R) of subgrade soil from different climate regions of South Carolina.
- Study the effect of subgrade resilient modulus on pavement rutting using the Mechanistic Empirical Pavement Design Guide (MEPDG).

To meet these objectives, the following tasks were performed:

Task 1. Development of pavement performance evaluation models to investigate the effect of different variables (traffic, climate, soil type) on different distress indicators (Present Serviceability Index (PSI), Pavement Quality Index (PQI), Pavement Distress Index (PDI), International

Roughness Index (IRI), and pavement rutting) for South Carolina pavements. Pavement performance for Asphalt Concrete (AC) and Portland Cement Concrete (PCC) pavements are compared for two unbound materials: soil Type A from the Blue Ridge and Piedmont Region, and soil Type B from Coastal Plain and Sediment Region.

Task 2. Determining the subgrade M_R using high quality soil samples collected from different regions of South Carolina by conducting laboratory M_R tests with appropriate test sequences. The effect of cyclic stress, confining stress and the moisture content on subgrade soil is addressed. Model parameters for the bulk stress model and the generalized constitutive resilient modulus model are established for South Carolina soils to use in MEPDG. Constitutive models are developed between soil index properties and the resilient modulus model parameters for undisturbed soils. FWD model is developed relating laboratory measured M_R with FWD modulus. The developed models (constitutive model and FWD model) are compared to the LTPP models for estimating M_R of South Carolina soils and the effect of M_R obtained from different models on pavement subgrade rutting is studied using MEPDG.

Task 3. California Bearing Ratio (CBR) tests for subgrade soils of different regions in South Carolina are evaluated at different moisture contents. Correlations are made between the laboratory remolded M_R values with CBR test results from the similar subgrade soil. Finally, the effect of

moisture variation of subgrade resilient modulus (M_R) on pavement rutting is studied for different moisture content.

1.4 DISSERTATION OUTLINE

Following the problem statement, background and objectives that have been presented in Chapter 1, the next four chapters are organized based on each of the three tasks and the conclusion. Each of next three chapters has an introduction, literature review, objectives, methodology, and result section. Chapter 2 presents the results from Task 1 to develop pavement performance evaluation models. Effects of different traffic, climate and material inputs on pavement performance are discussed. Chapter 3 presents the results from the field and laboratory study conducted to characterize the subgrade resilient modulus for Task 2. Different M_R models are discussed and the effect of cyclic stress, deviator stress and moisture content on M_R is also presented. Chapter 4 is based on Task 3 where the M_R found from laboratory testing in Task 2 is compared to CBR test results. The effect of moisture variation of subgrade M_R on pavement rutting models from Task 3 will be also presented in Chapter 4. Chapter 5 will summarize the findings and culminates with conclusions and recommendations from this study.

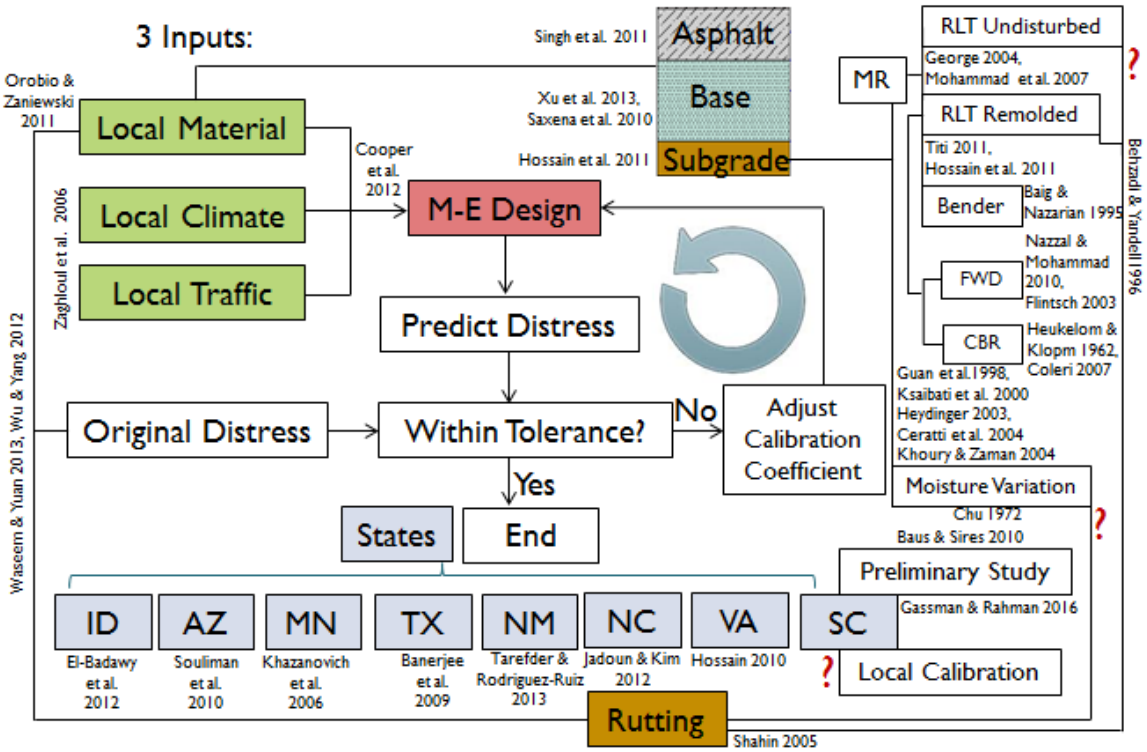

Figure 1.1 MEPDG Local Calibration Process with Concept Map

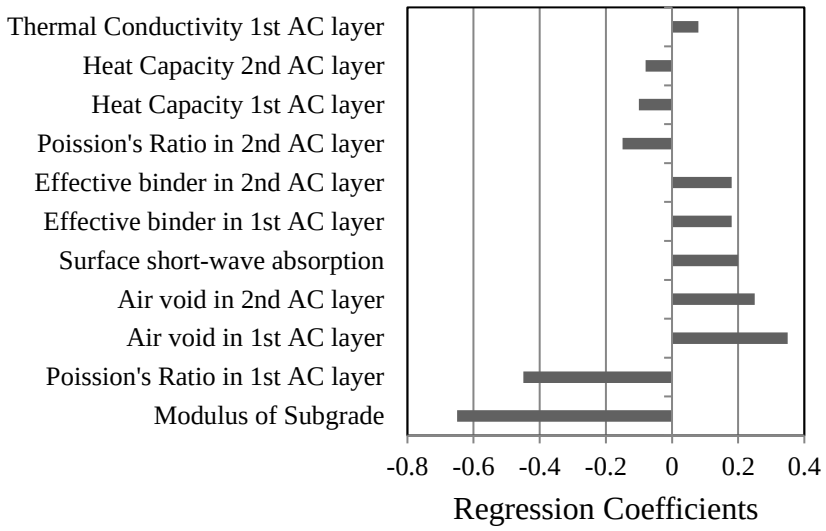

Figure 1.2 Effects of Material Inputs on MEPDG by Orobio and Zaniewski (2011)

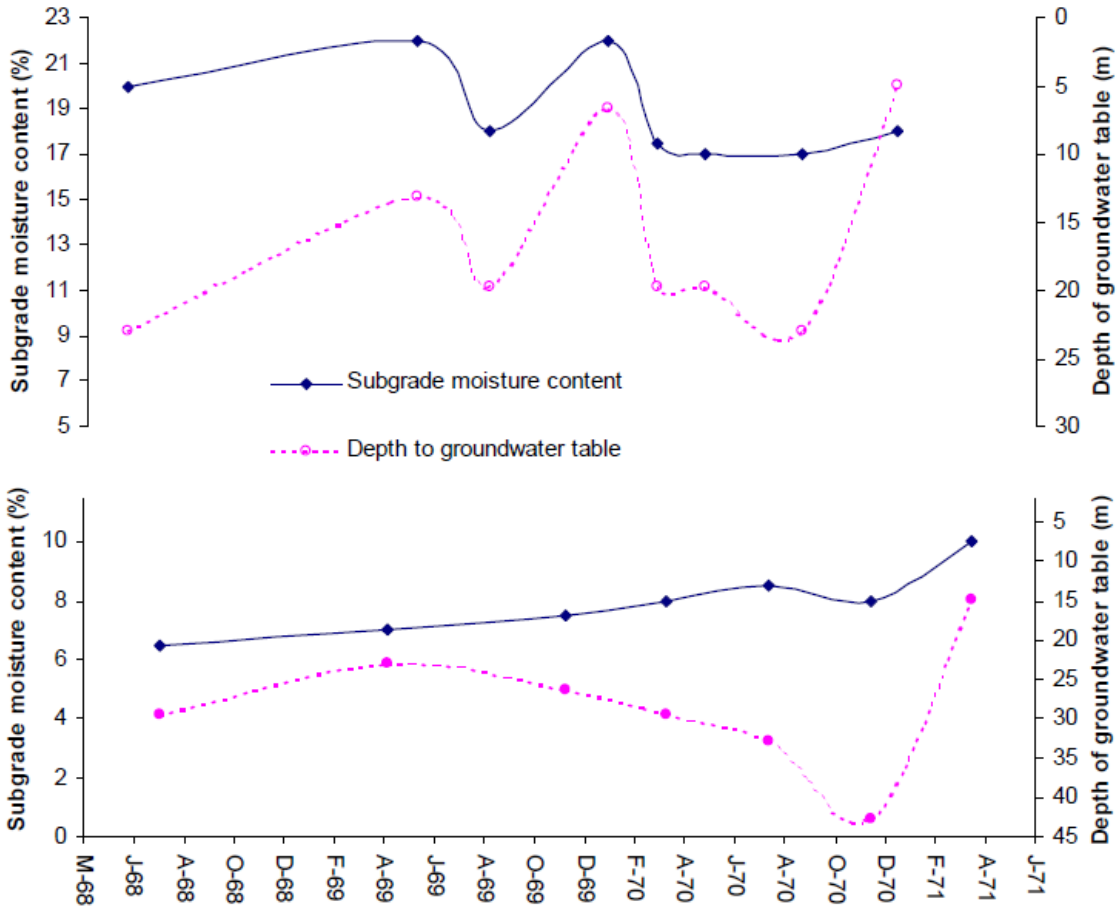

Figure 1.3 Variations in Moisture Content with Fluctuations in Ground Water Table (after Chu et al., 1972)

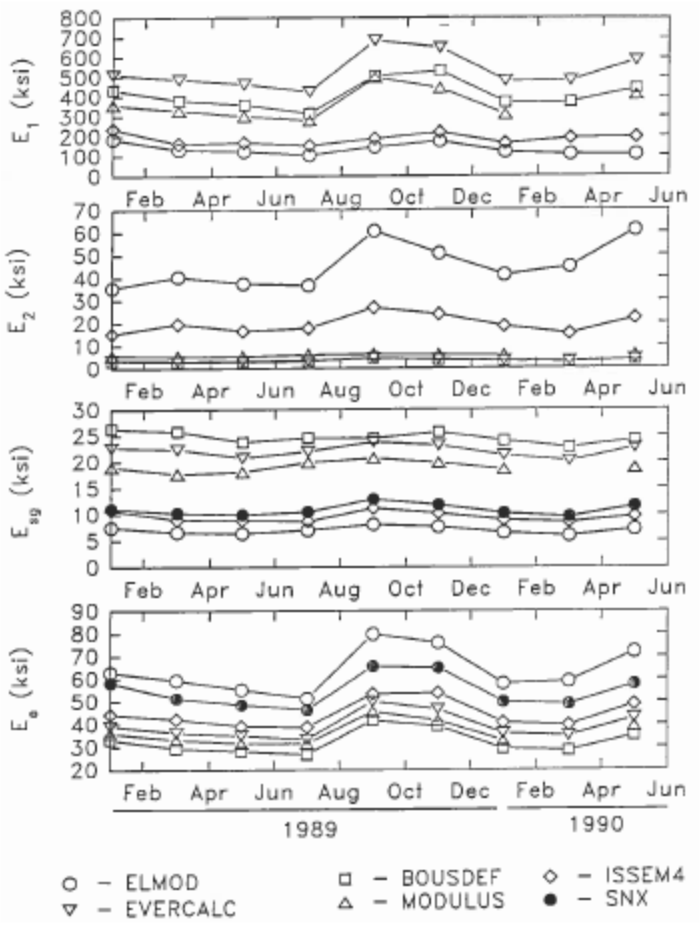

ELMOD (ELMOD, 1985), BOUSDEF (Zhou et al., 1990), ISSEM4 (ISSEM4, 1987), EVERCALC (EVERCALC, 1990), MODULUS (Scullion et al., 1990). SNX (Baus and Johnson, 1992).

E_1 = Young's modulus of asphalt-bound material layer or surface layer,
E_2 = Young's modulus of unbound or cement modified material layer or second layer,
E_{sg} = Young's modulus of the subgrade or the infinite elastic half-space,
E_e = overall pavement structure stiffness.

Figure 1.4 Backcalculated Moduli for US 321 of Fairfield (after Baus and Johnson, 1992)

Table 1.1 FWD Test Site Data by Baus and Johnson (1992)

Site No.	Road	County	Subgrade Classification
1	I 26	Calhoun	A-1-b
2	I 26	Orangeburg	A-1-b
3	SC 31	Charleston	A-2-4
4	US 17	Charleston	A-3
5	US 17	Charleston	A-3
6	US 321	Fairfield	A-3
7	SC 9	Chester	A-2-5
8	I 26	Newberry	A-2-4
9	I 77	Richland	A-1-b
10	S 1623	Lexington	A-1-b
11	I 20	Lexington	A-1-b
12	US 76/378	Sumter	A-1-b
13	US 76/378	Marion	A-7-6
14	US 76/301	Florence	A-2-6
15	I 385	Greenville	A-2-7
16	US 176	Union	A-3

CHAPTER 2

PAVEMENT PERFORMANCE EVALUATION MODELS FOR SOUTH CAROLINA[1]

[1]Adapted from Rahman, M. M., M. M., Uddin, and S. L. Gassman. Accepted by *KSCE Journal of Civil Engineering*. Reprinted here with permission of publisher (see APPENDIX C), 01/23/2017.

2.1 GENERAL

This chapter develops pavement performance evaluation models using data from primary and interstate highway systems in the state of South Carolina, USA. Twenty pavement sections are selected from across the state, and historical pavement performance data of those sections are collected. A total of 9 models were developed based on regression techniques, which include 5 for Asphalt Concrete (AC) pavements and 4 for Jointed Plain Concrete Pavements (JPCP). Five different performance indicators are considered as response variables in the statistical analysis: Present Serviceability Index (PSI), Pavement Distress Index (PDI), Pavement Quality Index (PQI), International Roughness Index (IRI), and AC pavement rutting. Annual Average Daily Traffic (AADT), Free Flow Speed (FFS), precipitation, temperature, and soil type (soil Type A from Blue Ridge and Piedmont Region, and soil Type B from Coastal Plain and Sediment Region) are considered as predictor variables. Results showed that AADT, FFS, and precipitation have statistically significant effects on PSI and IRI for both JPCP and AC pavements. Temperature showed significant effect on PDI, PQI ($p < 0.01$), and rutting ($p < 0.05$) for AC pavements. Considering soil type, Type A soil produced statistically higher PDI, PQI ($p < 0.01$), and rutting ($p < 0.001$) compared to Type B soil on AC pavements; whereas, Type A soil produced statistically higher IRI and lower PSI ($p < 0.001$) compared to Type B soil on JPCP pavements. Using the developed models, local transportation agencies could estimate future corrective actions, such as maintenance and rehabilitation, as well as future pavement performances.

2.2 INTRODUCTION

The South Carolina Department of Transportation (SCDOT) is currently conducting the first phase of research on Mechanistic-Empirical Pavement Design Guide (MEPDG) local calibration for the state of South Carolina, USA. The purpose of this research is to identify sources of data within SCDOT for calibration and to identify in-service pavement sections suitable for calibration studies. Selection of the hierarchical input level for each input parameter is necessary for pavement sections. The new MEPDG requires input data in four major categories: climate, traffic, materials, and pavement performance. The biggest challenge to use the performance data from SCDOT's specific pavement management system is the incompatibility of the SCDOT pavement performance data collection protocols with the new MEPDG distress identification protocol. Hence, there is a need for developing performance evaluation models for the South Carolina pavements, by taking into account both local and MEPDG distress indices.

Pavement performance prediction is essential for rationally allocating resources at the network level (Meegoda and Gao, 2014), including resources for future maintenance and rehabilitation actions. Transportation agencies can save money by reducing the pavement deterioration prediction error (Madanat, 1993). To determine the future performance of pavements, the present condition of the pavement and the variables that control the pavement deterioration must be known. Pavement condition in South Carolina is assessed by network level pavement roughness and surface distress data annually collected on the interstate and the primary highway systems by the SCDOT. Collected condition data includes roughness, rutting, fatigue cracking, transverse cracking,

longitudinal cracking, raveling and patching. These condition data are used to determine different pavement performance indicators: Present Serviceability Index (PSI), Pavement Distress Index (PDI), Pavement Quality Index (PQI), International Roughness Index (IRI), and rutting. IRI and PSI are functions of roughness, PDI is a function of different distresses, PQI is a function of both pavement serviceability and distresses, and rutting is the surface depression under wheel path. Factors that affect pavement condition and performance indicators can be categorized into three groups: factors related to traffic, factors related to climate and factors related to material. The effect of these factors on pavement deterioration and performance indicators varies as described in a few previous literatures (Archilla and Madanat, 2001; Cooper et al., 2012; and Orobio and Zaniewski, 2011).

Truck traffic volume, climate (e.g., temperature, precipitation), and pavement structural condition have been shown to contribute most significantly to the deterioration of pavement (Meegoda and Gao, 2014). The magnitude and the number of wheel load passes is the main contributor to deteriorate the pavement surface (Isa et al., 2005). Usually medium truck loading is used to predict pavement deterioration in terms of annual average daily traffic (AADT). In South Carolina, about 10,000 large freight trucks (typically, weighing more than 10,000 pounds) traveled on the major interstates each day in 2007 (Uddin and Huynh, 2015). Moreover, South Carolina pavements are exposed to extreme summer temperatures that average near 32 °C (90 °F) during the day and the precipitation is primarily in the form of rainfall that averages about 127 cm/year (50 inch/year) (NCEI, 2015). With the change of temperature and moisture content, pavement material characteristics for different pavement layers are prone to change (Nassiri and Bayat, 2013). If the deformations of one or more of the components in a typical pavement (e.g., surface

layer, base layer and subgrade layer) are sufficiently large to cause cracking of the surfacing material, a pavement may be considered as failed (Seed et al., 1962). South Carolina soils that serve as the subgrade layer can be divided into two regions separated by the geological fall line: the Blue Ridge/Piedmont Region and the Coastal Plain/Sediment Region. The soils in each region have different characteristics and thus are expected to have different impacts on pavement condition and performance indices.

Prior to MEPDG local calibration, a statistical study is required to assess the influence of various climatic, traffic and material inputs on pavement deterioration as related to pavement roughness and pavement distress indicators. Thus, the purpose of this study is to develop performance evaluation models using regression techniques for two of the MEPDG performance indicators: International Roughness Index (IRI), and rutting; and three of the SCDOT pavement performance indices: PSI, PDI and PQI. To achieve this, five different design inputs are considered for the study: AADT, Free Flow Speed (FFS), precipitation, temperature, and soil type. These inputs are selected based on their importance on pavement performance and availability in the SCDOT database.

2.3 LITERATURE REVIEW

Pavement performance evaluation models have been developed for several states in the USA. These include the pavement performance models that were developed for the Delaware Department of Transportation (DelDOT) using the pavement inventory data of their pavement management system (Mills et al., 2012). The variables they considered were pavement age, geometry, functional class, type of overlay, pavement condition rating, and the annual average volume of traffic. Simple and multiple regression analysis were used to develop performance models for their pavements. Performance models for flexible

pavement were developed for Georgia using regression technique (Kim and Kim, 2006). The researchers found that linear regression models are effective to forecast pavement performance if Average Annual Daily Traffic (AADT) is considered as a predictor. Gulen et al. (2001) developed regression models to predict the performance of pavements in Indiana, where they considered pavement roughness as the response variable, and pavement age and AADT as predictor variables. Performance models were also developed using regression techniques for Minnesota pavements (Prozzi and Madanat, 2004). A network level pavement performance model was developed using 20 years of historical pavement condition data for approximately 19,000 highway sections maintained by the New York State Department of Transportation (NYSDOT) (DeLisle et al., 2003). In a study by the Michigan Department of Transportation (MDOT), pavement distress data was used to assess the impact of construction (smoothness, early completion of construction, and nuclear density) on pavement performance (Chang et al., 2001). Pavement performance model was also developed using Pavement Condition Rating for North Carolina Department of Transportation (NCDOT) (Chan et al., 1997); and an overall distress index, a structural index with roughness index for North Dakota Department of Transportation (NDDOT) (Johnson and Cation, 1992).

In addition to aforementioned studies in the USA, some other countries have developed performance models for their respective pavement systems: Malaysia (Isa et al., 2005), Portugal (Ferreira et al., 2010), Canada (Hong and Wang, 2003), and New Zealand (Henning et al., 2004). Isa et al. (2005) used regression techniques to develop pavement performance models for federal roads of Malaysia. Ferreira et al. (2010) tested two pavement performance models, the AASHTO model and the Nevada model for Portugal

through the use of the strategic evaluation tool (SET) based on deterministic segment-linked optimization model and solved by a method developed using generic algorithm method. A simple probabilistic approach was developed for Ontario pavement based on nonhomogeneous continuous Markov chain by Hong and Wang (2003). In New Zealand, data from 63 Long Term Pavement Performance (LTPP) sites was used to calibrate the pavement deterioration models currently used on the state highway network (Henning et al., 2004).

Different statistical and regression techniques have been used to develop pavement evaluation models and to study the effects of different factors on pavement performance. Thyagarajan et al. (2010) studied the critical input parameters of MEPDG to investigate the effect of variability in key input parameters. The influence of project specific input uncertainties were evaluated on predicted pavement performance and distresses. They found Tornado plots and extreme tail analysis are useful statistical tools that can assist design engineers to identify the relative importance of input parameters and the effect of their variability on design reliability. Salama et al. (2006) investigated the effect of different axle and truck types on flexible pavement damage. Condition evaluation models were developed for Distress Index (DI), Ride Quality Index, and rutting. A relative comparison of different variables was carried out using simple, multiple and stepwise regression technique. An auto regression approach for predicting pavement DI was developed, in other study, with limited data (Ahmed et al., 2010). Gulen et al. (2001) also used regression techniques to develop improved performance prediction models. IRI was used as a response variable, while the age of the pavement and the current AADT were predictor variables. The data from their randomly selected road test sections did not yield

statistically strong models. Xu et al. (2014) used linear regression and artificial neural networks to predict the deterioration of Wheel Path Cracking (WPC) over a one year period. The extent and severity of WPC along with age and AADT were used as input variables in the study. An empirical comparison of nine representative statistical pavement performance models was conducted by Chu and Durango-Cohen (2008) using serviceability data from the AASHTO road test. The purpose of the study was to understand the effect of different statistical assumptions and estimation techniques on the models predictive capabilities. Rahman and Tarefder used system dynamic approaches to develop functional and structural condition based pavement evaluation model (2015). Both functional and structural condition of the pavement are equally important from an engineering perspective (Tarefder and Rahman, 2016). Good correlation between functional and structural condition index was observed for New Mexico pavements. Recently, Gupta et al. (2012) performed a critical review of the literature related to flexible pavement performance models. The paper presented a detailed review of various pavement performance models to examine the roles of factors related to pavement materials, environmental conditions, and type of traffic and volume of traffic. They concluded from other literatures that age and traffic are the most important variables to predicting pavement distress. Moreover, climate factors affect the structural properties of the pavements which are responsible for the deterioration of the pavements. Since these factors are uncertain in nature and vary from place to place, they considered them as important in analyzing the performance of pavement.

A minimum of 20 pavement test sections was recommended by Baus and Stires (2010) for calibrating and validating distress predictions. Hence, 20 pavement sections

were selected from 15 counties in South Carolina to serve as a representative sample—14 Asphalt Concrete (AC) sections of average length 5.3 miles and 6 Portland Cement Concrete (PCC) pavement sections of average length 5.8 miles. In the state of South Carolina, the mostly used PCC pavement type is Jointed Plain Concrete Pavement (JPCP) and all the 6 selected PCC sections are JPCP. None of the selected pavement sections are Continuously Reinforced Concrete Pavement or Jointed Reinforced Concrete Pavement.

2.4 OBJECTIVES OF STUDY

The objectives of this study are to:

1. Develop performance evaluation models for AC pavements and JPCP using multiple regression techniques for different distress indicators: PSI, PDI, PQI, IRI, and rutting.
2. Investigate the effect of different variables (AADT, FFS, precipitation, temperature, and soil type) on AC and JPCP pavement performances.
3. Compare AC and JPCP pavement performance for two unbound materials: soil type A from the Blue Ridge and Piedmont Region, and soil type B from Coastal Plain and Sediment Region

2.5 PAVEMENT SECTIONS, DATA AND VARIABLES

2.5.1 Pavement Sections Selections

Table 2.1 lists the selected pavement sections with their location, pavement type, surface course type and thickness, base course type and thickness, pavement length, and date of construction. Figure 2.1 shows the location of the selected pavement sections. To select the in-service sections, the following guidelines were in consideration.

1. The pavement sections are primary or interstate routes located in Coastal Plain and Piedmont Regions in South Carolina.
2. Both flexible and rigid pavements with typical layer configuration and material selection, including traditional and new materials, are included.
3. Different service times for different types of pavements are included.
4. Priority is given to the initially selected sections with historical data, including climate, materials, traffic, and performance data.
5. Selected sections are not overlaid or rehabilitated, and are suitable for MEPDG local calibration.

2.5.2 Performance Data

Historic performance data for the selected pavement sections were collected using the pavement viewer of SCDOT's Integrated Transportation Management System (ITMS). Available performance data for the past 10 years were collected and summarized. The data included five main performance measures: (1) PSI, (2) PDI, (3) PQI, (4) IRI, and (5) rutting. A total of 160 data points, representing each performance indicator, were collected for the 20 pavement sections. The number of samples collected for the AC pavements was 103, and that of the JPCP pavements was 57. Descriptive statistics of the numerical variables are presented in Table 2.2. The performance indicators are described next, along with their value ranges.

2.5.2.1 Present Serviceability Index (PSI)

PSI represents the riding quality of the pavement and is calculated from the mean IRI. SCDOT uses the following equation developed by Paterson (1986) for estimating PSI.

$$PSI = 5.0e^{(-0.002841 \times IRI)} \quad (2.1)$$

where IRI is in inch/ mile and PSI is a dimensionless index ranging from 0 to 5; 5 represents perfect condition and 0 represents failed condition. In the SCDOT pavement management system, a newly constructed pavement is assigned a PSI value of 4.5.

2.5.2.2 Pavement Distress Index (PDI)

PDI describes the observed surface distresses for PCC pavements and observed surface distress with mean rut depth for AC pavements. For PCC pavements observed surface distress includes: punchouts, spalling, pumping, patching, transverse cracking, longitudinal cracking, faulting, and surface deterioration. For AC pavements observed surface distress includes: raveling, fatigue cracking, patching, transverse cracking, and longitudinal cracking. To determine PDI, SCDOT uses the following equation (PMS, 1990).

$$PDI = 5.0 - ADV \tag{2.2}$$

where ADV is the adjusted distress value. Description of the ADV can be found in different literatures (e.g., Wang, 2002). Newly constructed pavements are assumed to be distress free, meaning that the ADV is initially zero. Therefore, those pavements are assigned a PDI of 5.0. PDI ranges from 0 to 5, where 5 represents perfect condition and 0 represents failed condition. PDI is a dimensionless index similar to PSI.

2.5.2.3 Pavement Quality Index (PQI)

PQI is the combination of PSI and PDI, which represents the overall condition of the pavement. SCDOT determines PQI using following equation (PMS, 1990).

$$PQI = 1.158 + 0.138 \times PSI \times PDI \tag{2.3}$$

where PQI is a dimensionless index and ranges from 0 to 5. In the SCDOT pavement management system, newly constructed pavement is assigned a PQI value of 4.3.

2.5.2.4 International Roughness Index (IRI)

IRI is an index for roughness measurement obtained by road meters installed on vehicles or trailers. In South Carolina, IRI values are derived from wheel path profiles obtained using non-contacting inertial profilers. Typically, data readings are taken continuously and data from each 0.10 mile intervals are reported (Baus and Hong, 2004). IRI values less than 170 inch/mile are acceptable and any IRI value less than 95 inch/mile indicates good roughness condition of the pavement (FHWA, 2004; Shahin, 2005).

2.5.2.5 Rutting

Rutting is a longitudinal surface depression in the wheel path resulting from plastic or permanent deformation in each pavement layer. It is the primary load related distress in flexible pavement. SCDOT measures rutting using a three-point automated profiler. The unit used for rut depths is inch where less than 0.5 inches rut depth is considered as less severe (Shahin, 2005).

2.5.3 Predictor Variables

In this study, effects of the following five predictor variables are investigated: (1) Annual Average Daily Traffic (AADT), (2) Free flow speed (FFS), (3) Precipitation, (4) Temperature, and (5) Soil type. Variables (1) to (4) are numerical, and variable (5) is categorical.

2.5.3.1 Annual Average Daily Traffic (AADT)

AADT is the average daily traffic on a roadway section for all days of the week during a period of one year, expressed in vehicle per day (veh/d). The number of repeated traffic is solely responsible for the load related pavement distresses. AADT data were collected for the pavement sections for the period from 2005 to 2014.

2.5.3.2 Free Flow Speed (FFS)

FSS affects the pavement roughness and surface friction. The following equations (Dowling, 1997) were used to calculate the FFS of the pavement sections.

$$\text{FFS} = (0.88 * \text{Link Speed Limit} + 14); \text{for speed limit} > 50 \text{ mph} \quad (2.4)$$

$$\text{FFS} = (0.79 * \text{Link Speed Limit} + 12); \text{for speed limit} \leq 50 \text{ mph} \quad (2.5)$$

2.5.3.3 Precipitation

Moisture content is an environmentally driven variable that can affect the pavement layer properties, such as degradation of material quality, loss of bond between layers and softening of the subgrade layer (ARA, 2004). Hence, precipitation could affect the pavement performances. The mean annual precipitations of the pavement sections were taken from their corresponding counties, found from the National Climate Data Center database (NCEI, 2015), for the years 2005 to 2014.

2.5.3.4 Temperature

Temperature is another environmental factor, which affect pavement performance. For the selected pavements sections, temperature information was collected for their respective counties from the National Climate Data Center database (NCEI, 2015). Specifically, yearly mean temperature data were collected for the years 2005 to 2014. The summary of the precipitation and temperature data for different selected counties are shown in Table 2.3. Table 2.3 indicates that coastal region has both higher average annual precipitation and higher mean annual temperature than upstate region for the period of 2005 to 2014.

2.5.3.5 Soil Type

Subgrade soil strength for the selected pavement sections is currently not available; therefore, different soil types have been chosen as an alternative. Two types of soils are selected: Type A and Type B. South Carolina soils can be divided into two regions separated by the geological fall line as shown in Figure 2.1: (i) Upstate Area or Blue Ridge and Piedmont Region (Type A), and (ii) Coastal Plain and Sediment Region (Type B) (SCDOT, 2010).

Type A soils are described as micaceous clayey silts and micaceous sandy silts, clays, and silty soils in partially drained condition; Type B soils include fine sand that is difficult to compact. In terms of AASHTO classifications, Type B soils are primarily A-1 to A-4 and Type A soils are predominately A-5 or higher (Pierce et al., 2011). The AASHTO system classifies soils into eight groups: A-1 through A-8 where A-1 to A-3 are granular soils, A-4 to A-7 are fine grained soils, and A-8 represents organic soils (AASHTO, 2008).

2.6 METHODOLOGY

To formulate pavement performance evaluation models, multiple linear regression analysis was conducted. Specifically, using multiple linear regression analysis, for performance measures/indicators, two separate models were formed for each performance indicator. The first model describes the effects of predictor variables on the indicators if the pavement is AC, and the second model describes the effects if the pavement is JPCP. The results of the models will be compared with each other and the best model will be suggested for the performance evaluation. A brief description on multiple linear regression and its assumptions are provided next.

2.6.1 Multiple Linear Regression

A linear regression model that contains more than one predictor/independent variable is called a multiple linear regression model. It takes into account the effect of all specified predictor/independent variables at the same time. Suppose the response variable Y is quantitative and at least one predictor variable X_i is quantitative, then the multiple linear regression models have the following form.

$$Y = \beta_0 + \beta_1 X_1 + \beta_2 X_2 + \cdots + \beta_i X_i \quad (2.6)$$

where Y = response variable (e.g., IRI, rutting, PDI, PQI, and PSI); β_0= intercept; β_i= coefficients; and X_i = predictor variables (e.g., $log_{10}AADT$, Temperature, Precipitation, FFS, and Soil Type). The intercept β_0 defines the value of Y when all X_i's are 0. The regression coefficient β_k represents the change in the mean response corresponding to a unit change in X_k when all other X_i's are held constant, $k \in i$.

2.6.1.1 Assumptions

Multiple linear regression analysis makes several key assumptions. The principal assumptions (Keith, 2015) are described here.

1. Dependent and independent variables are linearly related through regression coefficients. An appropriate transformation of the variable must be incorporated in the model if there is non-linearity.
2. Each observation should be drawn independently from the population. This means that the errors for each observation are independent from those of others.
3. There must be equal variance of errors across all levels of the independent variables, which refer to as homoscedasticity.

4. The errors are normally distributed. This assumption is only vital in case of small samples.
5. There is little or no multicollinearity in the data. Multicollinearity occurs when several independent variables correlate at high levels with one another.

2.6.1.2 Standard Regression Coefficients

To compare the relative importance of different predictor variables, standardized coefficients values are often utilized. Standardized coefficients are determined by converting all variables into Z scores, which in turn, convert the distribution mean to zero and standard deviation to one. The standardized multiple linear regression is specified as the following.

$$Y' = \beta_1' X_1' + \beta_2' X_2' + \cdots + \beta_i' X_i' \quad (2.7)$$

$$Y' = Z_y = \frac{\bar{Y} - Y}{\sigma_y} \quad (2.8)$$

$$X_i' = Z_{x_i} = \frac{\bar{X}_i - X_i}{\sigma_{x_i}} \quad (2.9)$$

where $Y' =$ standardized response variable; β_i' = standardized coefficients; X_i'= standardized predictor variables; $\bar{Y}$ = average value of response variable; σ_y= standard deviation of response variable; $\bar{X}_i$= average value of predictor variables; and σ_{x_i}= standard deviation of predictor variables.

2.6.1 Analysis

The statistical analysis was started with a bivariate analysis to examine the Pearson intercorrelation among a distress indicator (e.g., PSI, IRI, PDI, and rutting) and the predictor variables. Bivariate analysis also involved the assessment of multicollinearity of

the predictor variables. To do this, a variance inflation factor (VIF) was introduced. VIF measures how much the variance of a coefficient is increased due to multicollinearity, and a VIF $\geq$ 10 indicates a serious multicollinearity problem (Neter and Wasserman, 1996). Next, a multiple regression analysis was conducted to predict the values of response variable based on the value of predictor variables. Then, unstandardized and standardized coefficients for each predictor variables were analyzed to determine precisely the level of change in the response variable accounted for by a change in the predictor variable. The overall R^2 and adjusted $R^2$of the regression model were calculated to assess the percentage of the variance in the distress indicator that was explained by the predictor variables. The aforementioned procedure was followed for each distress indicator and both pavement types. The procedure was repeated 9 times. All analyses were performed in IBM SPSS Statistics software (v 12).

2.7 RESULTS

Results of the Pearson intercorrelation analysis of the PSI with the predictor variables, in case of AC pavements, are presented in Table 2.4. The correlation between PSI and predictor variables are found as low to large, with the Pearson correlation values (r) ranging from 0.05 to 0.58. FFS is the strongest related predictor of PSI (r = 0.58, p < 0.01). The table also shows that some of the predictor variables have strong correlations with each other. For instance, AADT is strongly correlated with Precipitation (r = 0.39, p < 0.01) and with Temperature (r = -0.62, p < 0.01). In contrast, the correlation between FFS and Temperature, and Soil type and Precipitation are found as low. Lastly, VIF values of predictors suggest that there is no serious multicollinearity problem in the data. Similar outputs are found from the Pearson intercorrelation analysis of the other distress indicators

with the predictor variables. For the sake of brevity, those outputs are not presented here. However, all of the correlation and VIF values are within acceptable range (VIF < 10).

Performance evaluation models for PSI, PDI, PQI, IRI, and rutting are reported in Table 2.5 through Table 2.9, respectively. Except rutting, each performance indicator has two different models: one for AC pavements and another one for JPCP. The rutting model is only developed for AC pavements, because PCC pavements do not show rut in the wheel path. Each model shows different statistical results from the analyses; which include unstandardized regression coefficients (β), standardized regression coefficients (β′), coefficient of determination (R^2), and overall model significance (F-test). In the analysis, soil type B is considered as the reference soil type. Nine evaluation models were fitted; and each model was found overall statistically highly significant after the F-test, except for the PDI model for AC pavements ($p < 0.01$) and rutting model for AC pavements ($p < 0.01$).

The effects of different independent variables on PSI for AC pavements and JPCP are shown in Table 2.5. In the PSI model for AC pavements, FFS, AADT and precipitation were found to have statistically significant effects on PSI. FFS showed positive effects on PSI, β = 0.021; $p < 0.001$. In contrast, AADT poses negative effects on PSI, β = -0.151; $p < 0.01$. Precipitation also showed negative effects on PSI, β = 0.006; $p < 0.05$. FFS showed higher absolute standardized regression coefficient (β′ = 0.684) than AADT (β′ = -0.301) or precipitation (β′ = -0.211). This indicates that FFS has more importance to explain PSI of AC pavements than AADT or precipitation. The model was overall statistically significant, F (5, 94) = 14.913; $p < 0.001$, and the model explained 44.2% of total variation in PSI (R^2 = 0.442).

For JPCP, four independent variables showed statistically significant effects on PSI. Among those variables, FFS showed positive effects on PSI (β = 0.038), whereas AADT (β = -0.809), precipitation (β = -0.005) and soil types (β= -0.560) showed negative effects on PSI. In JPCP, AADT, FFS and soil types showed the highest absolute standardized regression coefficient (β' = -1.057, β' = 1.044 and β' = -1.018 respectively). This means, among all the variables considered, these three have more importance to explain PSI of JPCP. Statistically significant unstandardized regression coefficient of soil type (β = -0.560) indicates that soil type A acts significantly to attain lower PSI measure than soil type B for JPCP. Like AC pavements, JPCP also showed overall statistically significant model, F (5, 50) = 65.865; $p < 0.001$. Moreover, the model fit is very satisfactory with explaining 86.8% of total variation in PSI (R^2 = 0.868). AADT, FFS and precipitation showed statistically significant effects on PSI for both AC and JPCP models. Several literatures also found reduction in PSI due to traffic (e.g., Lu et al., 1974; Mikhail and Mamlouk, 1999).

Table 2.6 shows the effects of different predictor variables on PDI for AC pavements and JPCP. In the PDI model for AC pavements, FFS, temperature and soil types were found to have statistically significant effects on PDI. FFS showed positive effects on PDI, β = -0.033; $p < 0.001$. Temperature and soil type (A vs B) also showed positive effects on PDI (β= 0.104, β = 0.787, respectively). The model was overall moderately statistically significant, F (5, 95) = 3.938; $p < 0.001$, and the model explained 17.2% of total variation in PDI, (R^2 = 0.172). Hence, the selected variables of this study are less capable of explaining PDI than PSI (R^2 = 0.442) for AC pavements. Results of PDI model agree with

Hasan et al. (2015). They found that the mean annual temperature has a great influence on pavement distresses.

For JPCP, precipitation and AADT showed statistically significant effects on PDI. Both variables showed negative impact on PDI (β = -0.007 and β= -0.443 respectively). Unlike AC pavements, JPCP did not show any significant effect of temperature on PDI, β = -0.012; $p > 0.05$. JPCP showed an overall statistically significant model, F (5, 51) = 18.071; $p < 0.001$. Moreover, the model satisfactorily explained 63.9% of the total variation in PDI ($R^2 = 0.639$).

Table 2.7 shows the effects of different predictor variables on PQI, which is a function of PSI and PDI (Eq. (2)). For AC pavements, FFS, temperature and soil type showed statistically significant effects on PQI. The model was overall statistically significant, F (5, 95) = 4.591; $p < 0.001$, and the model explained 19.5% of the total variation in PDI, ($R^2 = 0.195$). For JPCP, precipitation, AADT, FFS and soil type showed statistically significant effects on PQI. Unlike AC pavements, JPCP did not show any significant effect of temperature. JPCP showed overall statistically significant model, F (5, 51) = 27.470; $p < 0.001$. Moreover, the model explained 72.9% of total variation in PQI ($R^2 = 0.729$).

The regression results for IRI models are found in Table 2.8. For both AC and JPCP, precipitation, AADT and FFS showed statistically significant influence on IRI. Precipitation and AADT showed positive impact on IRI while FFS showed negative impact on IRI. In addition, soil type showed statistically significant influence on IRI for JPCP. This is similar to the findings of Al-Mansour et al. (1994). Like AADT, they found traffic count had a significant influence on pavement roughness. Moreover, another study also

reported a negative effect of vehicle operational speed on IRI (Li et al., 2014), and Wang et al. (2014) found that pavement roughness has a very small effect on FFS. Temperature did not have a significant influence on IRI for either type of pavement, which agrees with the results from Hasan et al. (2015). Results also indicate that unlike AC pavements, soil type has a significant effect on IRI for JPCP.

The statistical results for rutting on AC pavements are found in Table 2.9. Note that the variable Rutting is transformed into $\log_{10}$Rutting. Soil types (β = -0.227; $p < 0.001$) showed highly significant impact on rutting. FFS (β = -0.008; $p < 0.01$) and temperature (β = -0.021; $p < 0.05$) showed moderately and low statistically significant effect respectively on rutting. Neither traffic nor precipitation showed any significant influence on pavement rutting. However, some previous studies found significant effects of these two variables on rutting (Li et al., 2014; Mfinanga et al., 1996; and Ramos Garcia and Castro, 2011). Although the model was overall statistically significant according to F-test, the model explained only 17.9% of total variation in rutting (R^2 = 0.179). This indicates that there might be other influential variables to better evaluate pavement rutting or some potential sources of variation in SCDOT rutting measurement are responsible.

2.7.1 Model Comparison

Comparisons of measured and estimated distress indicator values for the AC pavements are presented in Figure 2.2 and for the JPCP in Figure 2.3. The figures illustrate how the measured distress indicators are consistent with the model estimates for each data record. For AC pavements, the figures show that the estimates from the models are generally well matched with the measured distress values, although those for PDI, PQI,

and rut show more outliers than the other two distress indicators. For JPCP, the figures indicate a good match between model estimates and measured distress values.

Table 2.10 compares the mean values of measured and estimated distress indicators for both AC and JPCP. It can be seen that the estimated mean values are close to the measured mean values except rutting. To verify whether there is a statistical difference between the estimated and measured mean of distress values, pairwise *t* tests were conducted. The null hypothesis (H_0) was that there is no obvious difference between measured and estimated distress values, and the alternative hypothesis (H_1) was that there is a significant difference between them. We do not reject the null hypothesis at the 5% level of significance for all distress indicators except rutting model. Thus, it can concluded that there is no significant difference between the estimated distress values obtained from the models and the measured distress values for all distress indicators, for both AC and JPCP except AC rutting model.

2.7.2 Model Limitations

Similar to any other pavement performance evaluation model, the model developed in this paper is only an approximation of the actual physical phenomenon of pavement performance. However, the estimated and measured distress indicators show the applicability of the developed models for pavement performance evaluation in South Carolina. There were still some limitations to the size of the data sample, which might have occurred a few not-so-accurate estimates, especially in the case of AC pavement PDI, and rutting. A possible approach to overcome this limitation would be to obtain more pavement performance data so that the models could be updated. Furthermore, data from other available sources could be considered. By doing so, in addition to have a relatively

large data set, a few more new variables could also be incorporated in the evaluation models, which may help to reduce potential bias and estimation error. However, one should apply engineering judgement before investigating additional variables for the models. Another limitation of the developed models is that they are of an empirical nature. That means the applicability of them outside of South Carolina is limited. To be used for areas outside of South Carolina, it is required to develop calibration process for the models.

2.7.3 Limitations of SCDOT Rutting Measurement Technique

Reliable model for AC rutting was not developed and, AADT did not show any significant effect on pavement rutting as expected. This is because the rut data measured by SCDOT may not be accurate. SCDOT uses the same three-point laser profiler to measure IRI and rutting. Those profilers are calibrated for a reference plane which all measurements are taken from. IRI is taken using the two lasers in the wheel paths. IRI is a cumulative measure of in./mi, so the lasers measure and sum the variations in the measured surface heights as the profiler moves down the road. An algorithm in the software converts these measures to an IRI value. Rutting is collected using the same two wheel path lasers, with an additional center mounted laser to provide a moving surface reference point different from the reference plane established during calibration. Rutting values are taken approximately every 3 inches and are then averaged across 0.10 miles segments.

SCDOT uses three-point profilers but a study by the FHWA (FHWA, 2001) showed that the three-point measurement systems do not necessarily provide a measurement of the rut depth that is similar to the total amount of rutting as measured manually by the wire line method. Moreover, the transverse location of the rut bar significantly affects the rutting measurement. Therefore, consistent lateral placement of the survey vehicle is essential to

repeatable rut depth measurements. As three-point profilers do not provide adequate network-level rut depths for pavement management systems, are not recommended to use by FHWA. Although the five-point rut depths are more highly correlated with the wire line rut depths, they consistently underestimate the mean wire line rut depth. Due to the high variability in the rut depth measurement using the three-point or five-point method, consistent year-to-year measurements may be difficult to achieve. FHWA observed that the correlation coefficient of wireline rut depth with the three-point and five-point profiler are 0.41 and 0.79 respectively. If a five-point profiler is used to collect network-level data collection, FHWA recommends additional care to ensure that the transverse location of the rut bar is consistent from year to year and that the mean values are adjusted to reflect more realistic rut depth values. Recently, 3D systems, which allow more accurate assessment of the road performance at both the network and project levels, are being used by DOTs for rut measurements (Serigos, et al., 2013).

2.8 CONCLUSIONS

The following conclusions can be made based on the analyses of performance data from in-service pavements in South Carolina.

- For the IRI models developed for AC and JPCP, AADT, FFS and precipitation showed statistically significant effects on IRI ($p < 0.01$). AADT and precipitation have positive effects on IRI, whereas FFS has negative effects on IRI for both AC and JPCP. That means IRI increases with increasing AADT and increasing precipitation. However, IRI decreases with increasing FFS.
- For the PSI models developed for AC and JPCP, AADT, FFS and precipitation showed statistically significant effects on PSI ($p < 0.01$). AADT and precipitation

have negative effects on PSI, whereas FFS has positive effects on PSI for both AC and JPCP. That means PSI decreases with increasing AADT and increasing precipitation. However, PSI increases with increasing FFS. As PSI is a function of only IRI, different models for these two dependent variables showed similar results.

- Temperature does not show any significant effect on IRI or PSI. Temperature showed significant effect only on AC pavement PDI and PQI ($p < 0.01$) and rutting ($p < 0.05$). Moreover, positive effect of temperature on AC pavement PDI and PQI means these indices increase with increasing temperature. Negative effect of temperature on AC pavement rutting means these indices decreases with increasing temperature.
- Precipitation was found to be a significant predictor for PSI on both types of pavement, JPCP PDI and PQI, and AC and JPCP IRI ($p < 0.05$). Therefore, the climate input precipitation was found to be more important than temperature for predicting different pavement performance in South Carolina.
- Considering soil type, Type A soil produced statistically higher PDI, PQI ($p < 0.01$), rutting ($p < 0.001$) compared to Type B soil on AC pavements; whereas, Type A soil produced statistically higher IRI and lower PSI ($p < 0.001$) compared to Type B soil on JPCP. Therefore, effects of soil types on pavement performance should be further investigated by performing in-situ tests of subgrade strength.
- Temperature, FFS and soil type showed statistically significant effect on AC pavement PDI and PQI. However, for JPCP PDI and PQI, AADT and precipitation were found as significant variables. AC pavements and JPCP showed different significant variables for PDI and PQI. AADT did not show any significant effects

on AC pavement PDI and PQI. Very low regression coefficients obtained from AC pavement PDI model (Adjusted R^2 = 0.128) and AC pavement PQI model (Adjusted R^2 = 0.152). This result was not expected and may be a result of routine maintenance performed by the SCDOT on AC pavements which was not considered in this study and/or there might be some inconsistencies in the SCDOT's manual survey techniques for distress measurements.

- In this study, performance evaluation models were developed for the South Carolina pavements, taking into account both local and MEPDG distress indices. Therefore, using the developed performance evaluation models, different local pavement performance indicators for a given climatic (temperature and precipitation), traffic (AADT) and material (soil type A or B, pavement type AC or JPCP) condition can be predicted. Additionally, developed performance evaluation models for IRI would also be a useful tool for MEPDG local calibration, to predict IRI in different climatic, traffic and material conditions.
- Rutting models showed very low coefficient of determination (R^2 = 0.179) and AADT had no significant influence ($p > 0.05$). South Carolina soil type A produced statistically higher rutting ($p < 0.001$).

2.9 FUTURE STUDIES

One of the key findings of this study is that two different types of soil have statistically significant effects on South Carolina pavement performance. Therefore, the difference in their subgrade strength needs to be further investigated. In future studies, resilient modulus of subgrade soil would be determined for both Type A and Type B and the results would be compared. Moreover, precipitation might be considered as a more

important climate input than temperature in MEPDG local calibration for South Carolina. Furthermore, the IRI models of this study would be compared with the IRI models developed using MEPDG for both AC and JPCP to better understand the roughness behavior of South Carolina pavements.

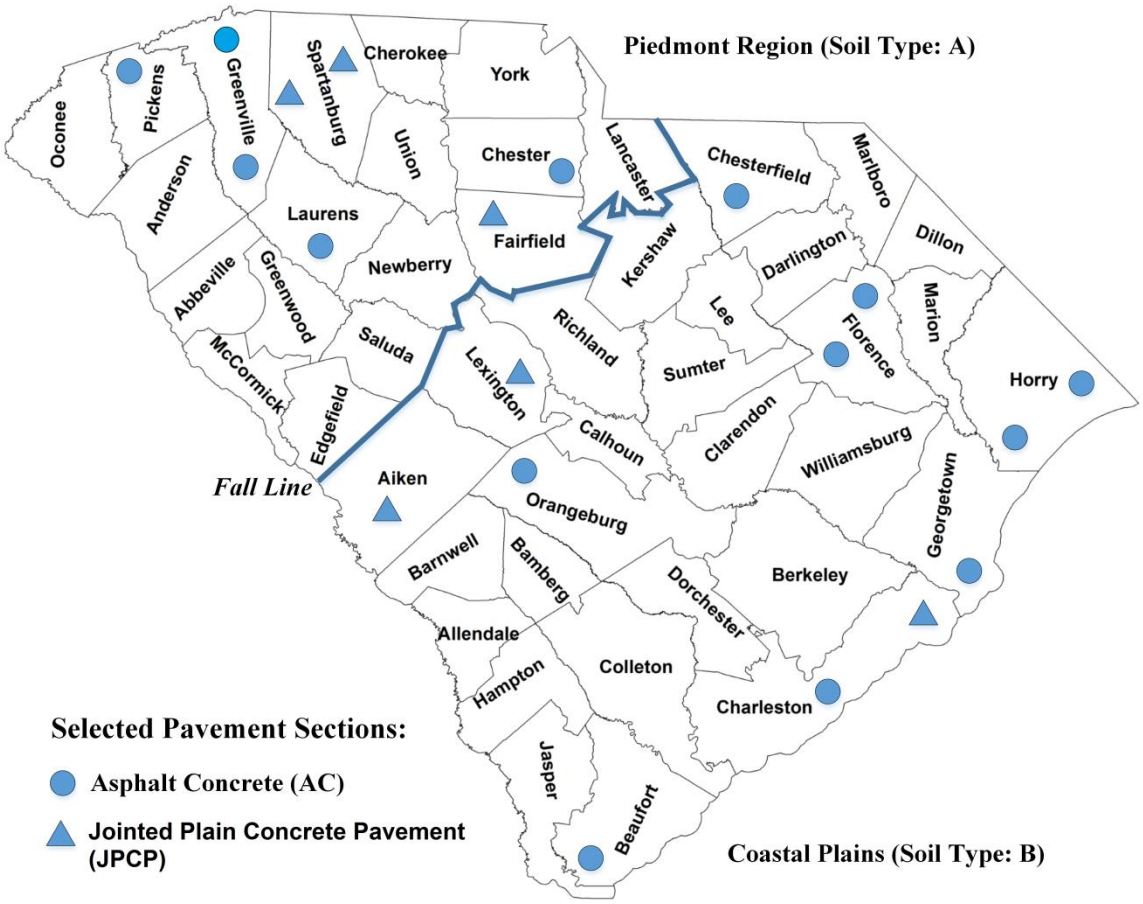

Figure 2.1 Selected Pavement Sections

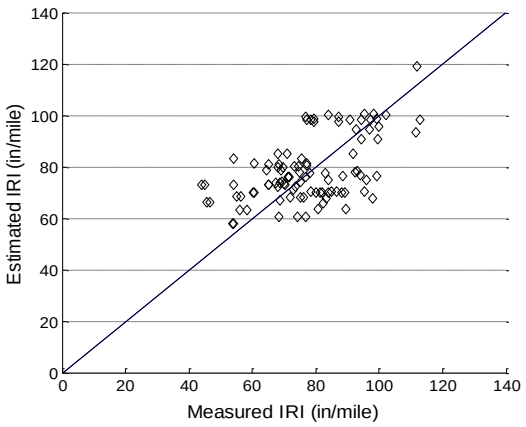

(a) IRI

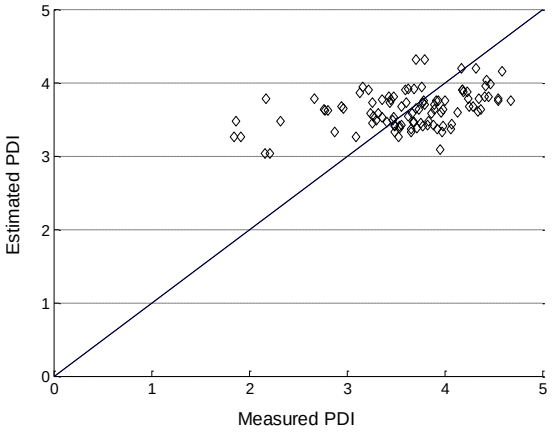

(b) PDI

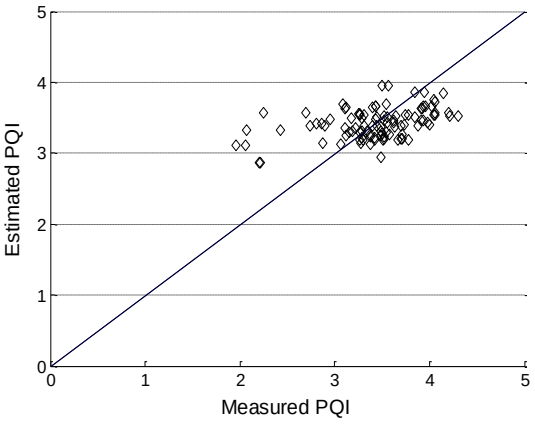

(c) PQI

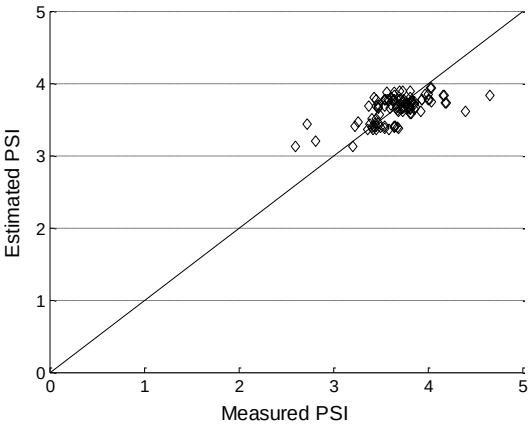

(d) PSI

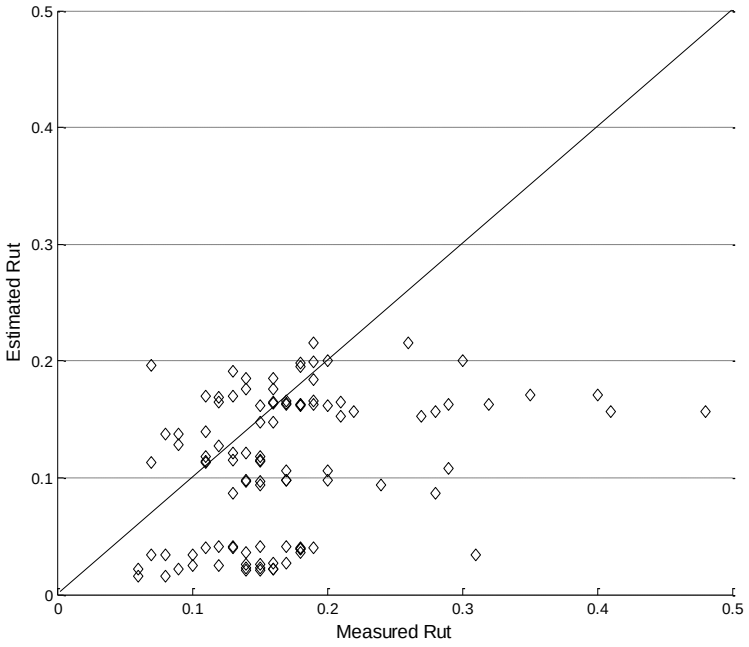

(e) Rut (in.)

Figure 2.2 Comparison of Estimated and Measured Performance Indicators for AC Pavements

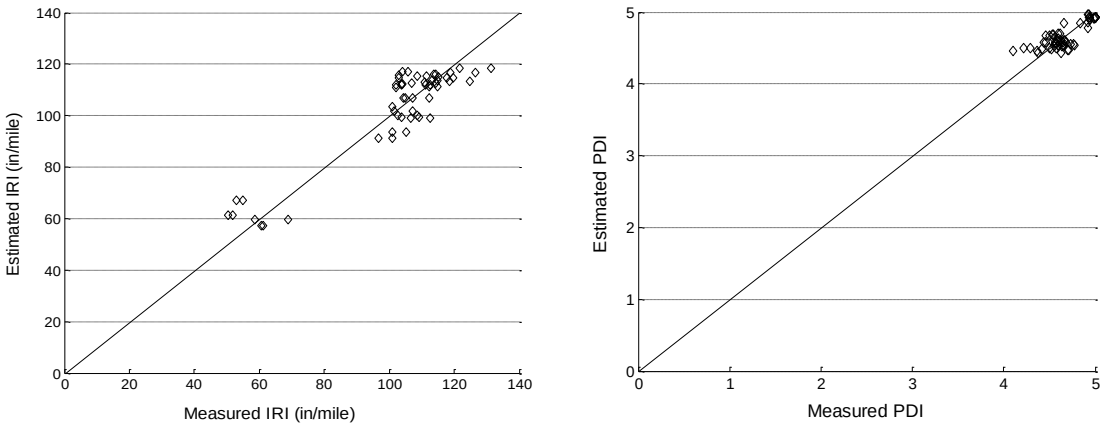

(a) IRI

(b) PDI

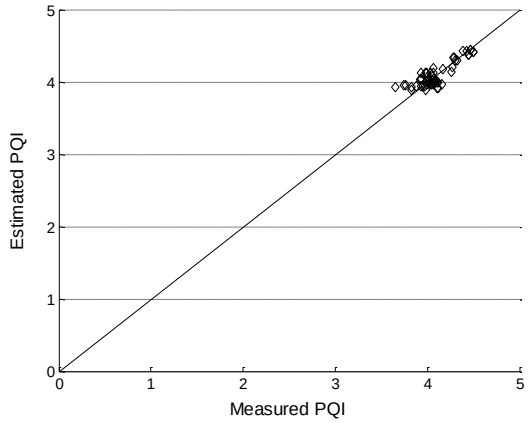

(c) PQI

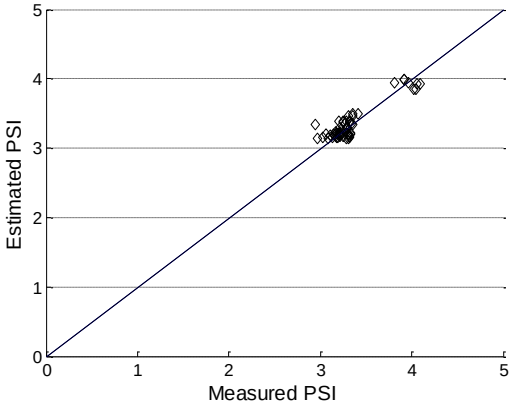

(d) PSI

Figure 2.3 Comparison of Estimated and Measured Performance Indicators for JPCP Pavements

Table 2.1 Selected Pavement Sections

County	Location	Type	Surface Course Thickness (in.)	Base Course Type	Base Course Thickness (in.)	Length (miles)	Let Date
Aiken	I 520	JPCP	11	AA + GAB	1.5 + 8	5.35	7/25/2008
Beaufort	US 278	AC	3.6	AA + GAB	3.2 + 6	1.56	3/13/1998
Charleston	SC 461	AC	5.7	AA + SAB	2.7 + 8	2.48	5/21/1996
Charleston	I 526	JPCP	11	CSM + CMS	6 + 6	2.39	6/25/1991
Chester	SC 9	AC	6.1	GAB	8	7.12	10/1/1999
Chesterfield	SC 151	AC	3.9	AA + Sand Clay	2.7 + 8	5.36	12/15/1999
Fairfield	I 77	JPCP	10	LC + CMS	6 + 6	14.17	10/21/1980
Florence	SC 327	AC	6.9	Macadam	8	5.09	2/25/1992
Florence	US 301	AC	3.8	GAB + CMS	8 + 6	2.38	9/30/2003
Georgetown	US 521	AC	3.8	GAB + CMS	8 + 6	4.07	6/1/2003
Greenville	I 385	AC	16.6	CSM	6	7.65	8/28/2000
Greenville	I 85	AC	3.9	AA	7.7	1.00	8/31/2005
Horry	SC 22	AC	3.8	AA + GAB	5.5 + 8	24.35	10/12/2001
Horry	SC 31	AC	3.8	AA + GAB	2.7 + 8	3.98	1/31/2005
Laurens	SC 72	AC	3.6	AA	6.8	5.99	3/1/2002
Lexington	S 378	JPCP	9	GAB	6	1.47	11/1/2001
Orangeburg	US 321	AC	5.6	GAB	6	6.17	7/1/2004
Pickens	SC 93	AC	3.4	AA	5.8	1.34	4/10/2001
Spartanburg	SC 80	JPCP	10	GAB	5	3.30	6/1/2000
Spartanburg	I 85	JPCP	12	AA + CMS	4 + 6	6.29	6/11/1997

Note: I, US, and SC represent Interstate highways, United States routes, and South Carolina routes, respectively. AC = Asphalt Concrete, JPCP = Jointed Plain Concrete Pavement, AA = Asphalt Aggregate Base, GAB = Graded Aggregate Base, SAB = Stabilized Aggregate Base, CSM = Cement Stabilized Macadam, CMS = Cement Modified Subbase, LC =Lean Concrete, Let date = Date of construction.

Table 2.2 Descriptive Statistics of the Numerical Variables in the Evaluation Models

		AC pavements			JPCP pavements		
Variable	Unit	Min	Max	Std. dev.	Min	Max	Std. dev.
PSI	–	2.6	4.7	0.3	2.9	4.1	0.3
PDI	–	1.9	4.7	0.6	4.1	5.0	0.2
PQI	–	2.0	4.3	0.5	3.7	4.5	0.2
IRI	inch/mile	43.9	112.9	15.2	50.5	137.4	20.2
Rutting	inch	0.06	0.48	0.07			
$\log_{10}$AADT	veh/d	3.4	5.0	0.5	3.8	4.9	0.4
FFS	mph	39.7	71.2	7.9	47.6	75.6	7.7
Precipitation	mm	31.8	68.5	8.5	31.7	54.7	6.2
Temperature	°F	54.1	66.7	3.4	59.2	68.3	2.7

Table 2.3 Summary of Precipitation and Temperature Data for Years 2005 to 2014

Region	County	Average Annual Precipitation (mm)		Yearly Mean Temperature (°F)	
		Mean	Standard Deviation	Mean	Standard Deviation
Upstate	Chester	41.4	5.5	60.3	1.0
	Fairfield	42.4	6.5	61.6	0.9
	Greenville	52.4	7.2	61.6	0.9
	Laurens	40.7	7.7	61.6	0.9
	Pickens	47.0	5.6	61.6	0.9
	Spartanburg	41.4	6.5	60.0	0.7
	Average	*44.2*	*6.5*	*61.1*	*0.9*
Coastal	Aiken	40.6	3.4	64.7	1.7
	Beaufort	55.2	7.6	64.6	0.8
	Charleston	45.7	5.8	66.8	0.8
	Chesterfield	50.9	9.3	66.8	0.8
	Florence	47.0	4.0	66.8	0.8
	Georgetown	48.4	7.7	66.8	0.8
	Horry	44.5	7.7	63.9	0.6
	Lexington	46.3	5.1	63.2	0.9
	Orangeburg	46.3	2.7	63.7	1.5
	Average	*47.2*	*5.9*	*65.3*	*1.0*

Table 2.4 Correlations for PSI and Predictor Variables, and VIF (AC Pavements)

	Pearson correlation (*r*)						
	PSI	Precipitation	Temperature	$\log_{10}$AADT	FFS	Soil type	VIF
PSI	1.00						
Precipitation	-0.13	1.00					1.40
Temperature	0.05	-0.27**	1.00				4.58
$\log_{10}$AADT	-0.04	0.39**	-0.62**	1.00			2.09
FFS	0.58**	0.18	-0.04	0.34**	1.00		1.55
Soil type	-0.20*	-0.01	-0.81**	0.43**	-0.26**	1.00	4.41

*$p < 0.05$; **$p < 0.01$

Table 2.5 Effects of Predictor Variables on PSI

	AC pavements		JPCP pavements	
Predictors	β	β′	β	β′
Intercept	4.397***		6.229***	
Precipitation	-0.006*	-0.211	-0.005*	-0.115
Temperature	-0.019	-0.249	-0.021	-0.202
$\log_{10}$AADT	-0.151**	-0.301	-0.809***	-1.057
FFS	0.021***	0.684	0.038***	1.044
Soil type (A vs B)	-0.047	-0.094	-0.560***	-1.018
R^2	0.442		0.868	
Adjusted R^2	0.413		0.855	
Overall model significance	F(5, 94) = 14.913***		F(5, 50) = 65.865***	

*$p < 0.05$; **$p < 0.01$; ***$p < 0.001$

Table 2.6 Effects of Predictor Variables on PDI

	AC pavements		JPCP pavements	
Predictors	β	β′	β	β′
Intercept	-4.565		7.576***	
Precipitation	0.000	-0.006	-0.007*	-0.191
Temperature	0.104**	0.577	-0.012	-0.155
$\log_{10}$AADT	-0.160	0.131	-0.443***	-0.751
FFS	0.033***	0.428	0.003	0.107
Soil type (A vs B)	0.787**	0.641	-0.114	-0.271
R^2	0.172		0.639	
Adjusted R^2	0.128		0.604	
Overall model significance	F(5, 95) = 3.938**		F(5, 51) = 18.071***	

*$p < 0.05$; **$p < 0.01$; ***$p < 0.001$

Table 2.7 Effects of Predictor Variables on PQI

	AC pavements		JPCP pavements	
Predictors	β	β′	β	β′
Intercept	-2.683		6.882***	
Precipitation	-0.002	-0.037	-0.006*	-0.199
Temperature	0.076**	0.530	-0.015	-0.200
$\log_{10}$AADT	0.145	-0.150	-0.491***	-0.889
FFS	0.029***	0.479	0.011**	0.423
Soil type (A vs B)	0.604**	0.620	-0.220*	0.557
R^2	0.195		0.729	
Adjusted R^2	0.152		0.703	
Overall model significance	F(5, 95) = 4.591***		F(5, 51) = 27.470***	

*$p < 0.05$; **$p < 0.01$; ***$p < 0.001$

Table 2.8 Effects of Predictor Variables on IRI

	AC pavements		JPCP pavements	
Predictors	β	β′	β	β′
Intercept	-4.876		-116.797*	
Precipitation	0.474*	0.190	0.379*	0.118
Temperature	1.852	0.296	1.648	0.225
$\log_{10}$AADT	14.686**	0.349	57.820***	1.053
FFS	-1.789***	-0.669	-2.666***	-1.032
Soil type (A vs B)	0.800	0.019	39.592***	1.003
R^2	0.407		0.859	
Adjusted R^2	0.376		0.845	
Overall model significance	F(5, 97) = 13.315***		F(5, 50) = 61.109***	

*$p < 0.05$; **$p < 0.01$; ***$p < 0.001$

Table 2.9 Effects of Predictor Variables on Rutting

Model		AC Pavements	
		β	β′
Independent Variables	Intercept	1.206	
	Precipitation	-0.002	-0.112
	Temperature	-0.021*	-0.405
	$\log_{10}$AADT	-0.009	-0.025
	FFS	-0.008**	-0.343
	Soil Type (A vs B)	-0.227***	-0.659
R^2		0.179	
Adjusted R^2		0.136	
Overall Model Significance		F(5, 97) = 4.221**	

*p < 0.05; **p < 0.01; ***p < 0.001

Table 2.10 Paired Comparisons between Measured and Estimated Distress Indicators

Model		Mean		Paired comparison (α = 0.05)	
		Measured	Estimated	*p*-Value	Test result
AC pavements	IRI	77.78 in./mile	78.74 in./mile	0.47	Do not reject H_0
	PDI	3.63	3.63	0.93	Do not reject H_0
	PQI	3.43	3.42	0.85	Do not reject H_0
	PSI	3.68	3.65	0.18	Do not reject H_0
	Rutting	0.17	0.11	0.00	Reject H_0
JPCP pavements	IRI	102.33 in./mile	102.37 in./mile	0.97	Do not reject H_0
	PDI	4.66	4.66	0.68	Do not reject H_0
	PQI	4.09	4.09	0.98	Do not reject H_0
	PSI	3.34	3.35	0.42	Do not reject H_0

CHAPTER 3

EFFECT OF RESILIENT MODULUS OF UNDISTURBED SUBGRADE SOILS ON PAVEMENT RUTTING[1]

[1]Adapted from Rahman, M. M., and S. L. Gassman. Accepted by *International Journal of Geotechnical Engineering*. Reprinted here with permission of publisher (see APPENDIX C), 05/17/2017.

3.1 GENERAL

This chapter presents the results from a test program to characterize resilient modulus (M_R) of subgrade soils for different geographic regions in South Carolina. Soils in South Carolina can be divided into two regions separated by the geological fall line (i) Upstate Area or Blue Ridge and Piedmont Region, and (ii) Coastal Plain and Sediment Region. For this study, Shelby tube samples of subgrade soils were collected from existing pavements in each region: SC-93 in Pickens county (Upstate Area), US-521 in Georgetown county (Coastal Plain), and US-321 in Orangeburg county (Coastal Plain, near the fall line). Resilient modulus tests were performed on the collected soil samples following AASHTO T 307. Model parameters were obtained using both the bulk stress model and the generalized constitutive resilient modulus model, which can be used as Level 2 input parameters for the Mechanistic Empirical Pavement Design Guide (MEPDG). Statistical analysis was performed to develop M_R estimation models for undisturbed soils using soils index properties. A correlation between laboratory measured M_R with the modulus from Falling Weight Deflectometer tests was also developed. These models can be used to produce Level 3 input parameters. Finally, the effects of M_R on subgrade rutting were studied using MEPDG. Results showed that the developed models offer higher reliability than the universal Long-Term Pavement Performance models in estimating the resilient modulus of undisturbed soils and predicting subgrade rutting for South Carolina.

3.2 INTRODUCTION

Traditionally, pavement structures have been designed empirically using the Guide for Design of Pavement Structures (AASHTO, 1993), which was developed based on past experience and AASHTO Road Test data (Archilla and Madanat, 2001). Currently, a new

approach using the Mechanistic Empirical Pavement Design Guide (MEPDG) is being implemented throughout the United States (US) because of its ability to account for different material behavior, in-situ materials, new materials, changing load types and pavement distresses (Souliman et al., 2010). The change in pavement design from an empirical based method to a mechanistic-empirical based method is recent, and therefore, departments of transportation in the US are performing local calibration of MEPDG for their states. Recently, the South Carolina Department of Transportation (SCDOT) began Phase I of the calibration of the AASHTO Pavement Design Guide to South Carolina Conditions. To fully implement the MEPDG in South Carolina, characterization of local subgrade soils is required.

Resilient modulus (M_R) is used to characterize the stress-strain behavior of subgrade soil and is one of the most important material inputs for MEPDG. M_R represents not only the elastic behavior, but also the load carrying capacity of subgrade soils under dynamic traffic loading. An accurate quantification of M_R is required for designing an optimum pavement thickness (Rahman and Tarefder, 2015). Moreover, accurate prediction of flexible pavement performance is highly dependent on the accuracy of M_R value (Ng et al., 2016). This study represents a comprehensive test program to characterize M_R for different geographic regions in South Carolina which can be used to perform MEPDG local calibration. Soils in South Carolina can be divided into two regions separated by the geological fall line (i) Upstate Area or Blue Ridge and Piedmont Region (i.e. micaceous clayey or sandy silts, and clays), and (ii) Coastal Plain and Sediment Region (i.e. fine sand) (SCDOT, 2010). Rahman et al. (2016) recently developed pavement performance evaluation models for South Carolina, and they found that difference in these two soil types

has statistically significant effects on South Carolina pavement performance. Therefore, the variation in subgrade strength of different South Carolina soil needs to be further investigated. For this study, Shelby tube (undisturbed) samples of subgrade soil were collected from existing pavements in each region of South Carolina. M_R tests were performed on the collected samples following AASHTO T 307. Model parameters were obtained for both the bulk stress model and the generalized constitutive resilient modulus model using repeated load triaxial tests to characterize the stress-strain behavior of different types of South Carolina subgrade soil.

Determination of M_R using repeated load triaxial tests is often time consuming and requires extensive efforts and sensitive equipment. Therefore, correlations between physical properties and repeated load resilient modulus tests have been developed for unbound materials and soils within the Long-Term Pavement Performance (LTPP) program by Yau and Quintus (2004). In addition, Titi et al. (2015) developed correlations between basic soil properties and M_R constitutive model parameters for Wisconsin fine-grained soils using regression analysis techniques. In both cases, laboratory remolded soil samples were used rather than undisturbed samples of natural soil. Thus, given the differences in soil structure and water content between laboratory remolded soil samples and natural soils, this study was performed to develop M_R estimation models between soil index properties and M_R obtained using undisturbed samples of natural soils in South Carolina. Models were developed for both granular materials and silty-clay materials using multiple linear regression analysis and were compared to the universal LTPP models.

Both remolded and undisturbed soil samples have been used to perform resilient modulus tests in different studies (Mohammad et al., 2007; Hossain et al., 2011). However,

undisturbed soil samples better represent the in-situ soil structure underneath the pavement as those are obtained from the test site with minimum structural disturbance during sample preparation before M_R tests. Whereas, undisturbed soil samples better represent the in-situ soil structure underneath the pavement as those are obtained from the test site with minimum structural disturbance during the sampling process. Burczyk et al. (1994) observed that sample disturbance has influence on soil resilient modulus. Yau and Von Quintus (2004) reported that sampling technique (disturbed/undisturbed test specimens) of subgrade soils has an effect on the resilient modulus test results for all soil groups (gravel, silt, and clay) except sand. Dai and Zollars (2002) concluded that, characterization of resilient modulus using undisturbed subgrade soil samples may be more appropriate than using disturbed samples for studying pavement response. Laboratory remolded subgrade soil samples have been widely used to study subgrade resilient modulus, primarily due to difficulties in collecting undisturbed samples. For developing prediction models, remolded test specimen test results have been used by different studies (Malla and Joshi, 2008; George, 2004). Significant improvement in correlation between M_R and soil physical properties were observed when remolded and undisturbed samples were separated for model prediction by Von Quintus and Killingsworth (1998). Therefore, undisturbed soil samples are used to determine M_R and to develop correlation with soil index properties in this study.

Determination of soil physical properties requires considerable effort and laboratory facilities. Therefore, nondestructive test methods such as the Falling Weight Deflectometer (FWD) are often conducted to predict M_R from correlations between M_R and FWD modulus. FWD is used to back calculate the modulus from pavement deflections,

and is widely used to predict pavement stiffness (Zhou, 2000; and Meshkani et al., 2003). Correlations between FWD modulus and laboratory resilient modulus have been developed (Von Quintus and Killingsworth, 1997; Nazzal and Mohammad, 2010; and Ji et al., 2015); however, correlations from different studies have not been shown to be consistent due to material variability and differences in FWD equipment and analysis methods used. In this study, FWD tests were performed at locations near each boring location from where the Shelby tube samples were collected. Then correlations between laboratory measured M_R on undisturbed soil samples and FWD modulus were developed for different soil types.

Only a few studies have been published about the effect of subgrade strength on the deformation or rutting models in MEPDG (Wu and Yang, 2012; and Khazanovich et al., 2006) and more studies are needed (Graves and Mahboub, 2006). The study by Wu and Yang (2012) examined the effect of subgrade M_R on pavement rutting for different local conditions based on MEPDG. However, they used laboratory prepared remolded samples to determine subgrade M_R. In this chapter, subgrade rutting based on MEPDG was studied using the M_R found from undisturbed soils. These results were compared to the subgrade rutting predicted using the two models developed in this study (constitutive model and FWD model) and LTPP models.

3.3 BACKGROUND

3.3.1 Determination of Resilient Modulus

M_r represents the stiffness of an unbound or a subgrade layer of a highway pavement subjected to repeated traffic loading. Resilient modulus is defined as the ratio of the amplitude of the repeated maximum axial cyclic stress to the amplitude of the resultant recoverable or resilient axial strain. Resilient modulus is analogous to the modulus of elasticity (E) of soil as both are related to the basic theory of elasticity. However, modulus of elasticity is measured due to static force, whereas, resilient modulus is determined due to dynamic loading condition.

$$M_r = \frac{\sigma_{cyclic}}{\varepsilon_r} \tag{3.1}$$

where, σ_{cyclic} is the maximum axial cyclic stress and ε_r is the recoverable strain due to σ_{cyclic}.

In the laboratory, resilient modulus is determined by performing a repeated load triaxial compression test. In the test, a repeated axial cyclic stress of fixed magnitude, load duration, and cycle duration is applied to a cylindrical test specimen. During testing, the specimen is subjected to a dynamic cyclic stress and a static-confining pressure provided by means of a triaxial pressure chamber. The total resilient or recoverable axial deformation response of the specimen is measured and used to calculate the resilient modulus (AASHTO, 2003).

The current protocol to determine the resilient modulus of soil and aggregate material is AASHTO T 307. According to this test protocol, a haversine-shaped loading waveform as shown in Figure 3.1 is repeatedly applied on top of a cylindrical specimen under confining pressure (see Figure 3.2). A schematic showing a soil specimen in a triaxial

chamber is shown in Figure 3.3. The total load cycle duration is 1 sec which includes a 0.1 sec load duration and a 0.9 sec rest period. The test sequence for subgrade soil is shown in Table 3.1, where Sequence 0 represents the conditioning phase before the actual test. Conditioning consists of applying 500 to 1000 cycles of load according to AASHTO T 307, and is performed to eliminate the effect of the interval between compaction and loading and to eliminate the effect of initial loading versus reloading. The conditioning also helps in minimizing the effects of initial imperfect contact between the sample cap and the base plate and the test specimen. Therefore, another purpose of conditioning is to ensure proper contact of the sample to the cap before loading sequences No. 1 to 15 are applied. A large time interval between compaction and loading may change the moisture condition and void ratio of soil and therefore, more plastic deformation may occur in the initial loading unloading curve without conditioning.

After conditioning is completed; each of the 15 main test sequences are applied in 100 load repetitions having haversine-shaped load pulse and the average recoverable deformation for the last five cycles of each sequence are recorded. The maximum cyclic deviator stress, the contact stress and the total recoverable strain are used to calculate resilient modulus. Figure 3.3(a) shows an example of the stress and strain for one load cycle and Figure 3.3(b) shows an example of stress versus strain for the 15 test sequences or the 1500 load cycle.

3.3.2 Factors Affecting Resilient Modulus of Soils

3.3.2.1 Moisture Content

Research studies have shown that subgrade M_R decreases with an increase in moisture content or degree of saturation (Butalia et al. 2003; Drumm et al., 1997; Fredlund et al.,

1977; Heydinger 2003; Huang, 2001; Mohammad et al., 1994; and Titi et al., 2006). Butalia et al. (2003) observed a reduction in resilient modulus due to an increase in positive pore pressure with an increase in moisture content for unsaturated cohesive soils. Drumm et al. (1997) found that the resilient modulus decreases as the degree of saturation increases for soil samples compacted at maximum dry unit weight. Figure 3.4 shows the effect of degree of saturation on resilient modulus of fine grained subgrades (Drumm et al. 1997)

3.3.2.2 Unit Weight

The effects of unit weight on subgrade resilient modulus have been investigated on some previous studies (Chou 1976; and Titi 2006; Smith and Nair 1973; Allen 1996; Drumm 1997, Seed et al. 1962). Test results indicated that at a constant moisture content, the resilient modulus increases with the increase of the dry unit weight (density) of the soil. According to Seed et al. (1962), at low moisture contents, a lower density will give a lower resilient modulus. The relationship is reversed for high moisture contents (Figure 3.5).

3.3.2.3 Deviator Stress

The resilient modulus of cohesive soils decreases with an increase in deviator stress due to the softening effect (Rahman and Tarefder, 2015). Cohesive soils if normally consolidated soften while sheared and remolded. A decrease in stress is observed at strains beyond the peak stress and therefore, resilient modulus decreases.

For loose granular soils, the resilient modulus increases with an increase in deviator stress, which indicates strain hardening (granular interlock) due to particle reorientation into denser state (Maher et al. 2000). Granular soils are most efficiently compacted or densified by vibration both in the laboratory and in the field which results in higher density and higher resilient modulus. Figure 3.6 (a) and Figure 3.6 (b) show the effect of deviator

stress on resilient modulus for coarse grain (A-1-b) and fine grain (A-6) soils respectively (Ng. et al. 2015). Figure 3.6 indicates that, the coarse grained soil (A-1-b) has a positive relationship between resilient modulus and deviator stress, while the fine grained soil (A-6) has a negative relationship between resilient modulus and deviator stress. However, resilient modulus for both soils increase with the higher confining stresses.

3.3.2.4 Confining Pressure

In general, for subgrade soils, resilient modulus increases with increasing confining pressure (Butalia et al. 2003, Seed et al. 1962, and Titi et al. 2006). However, the effect of confining stress is more significant in granular soils than cohesive soils (Titi et al. 2006). Thomson and Robnett (1979) concluded that the resilient modulus of fine-grained soils does not depend on the confining pressures. Resilient modulus of granular soils is usually described as a function of bulk stress. On the other hand, for cohesive soils, resilient modulus is usually described as a function of deviator stress. Figure 3.6 shows that resilient modulus increases with the increasing confining stress for both coarse grained and fine grained soils as a higher resilient modulus was found for 6 psi confining pressure compared to 2 psi confining pressure.

3.3.2.5 Compaction

Compaction methods and soil type also influence the resilient modulus. Seed et al. (1962) reported samples compacted statically showed higher resilient modulus compared to those compacted by kneading compaction. Drumm et al. (1997) found higher resilient modulus for the soil which was compacted on the dry side of optimum than the soil compacted at the wet side of optimum.

3.3.2.6 Soil Type

Thomson and Robnett (1979) found that low clay content and high silt content results in lower resilient modulus compared to high clay content and low silt content. They also found that low plasticity index and liquid limit, low specific gravity, and high organic content results in lower resilient modulus. Lekarp et al. (2000) reported that the resilient modulus decreases if the amount of fines increases of the granular material; whereas, Chou (1976) found that amount of fines has no general trend on the resilient modulus of granular soil.

3.3.3 Resilient Modulus Models

3.3.3.1 Bulk Stress Model

Bulk stress (θ or σ_b) is the sum of the three principal stresses (σ_1, σ_2, and σ_3) and is widely used for estimating the resilient modulus (M_R) of coarse-grained soils (Hicks and Monismith, 1971).

$$M_R = k_1\theta^{k_2} \tag{3.2}$$

where k_1 and k_2 are material constants.

One of the limitations of the bulk stress model is that this model does not consider shear stress, shear strain or volumetric strain. It also does not separately consider the deviatoric stress to account for the actual field stress state.

May and Witczak (1981) modified the bulk stress model as follows (Titi et al. 2006):

$$M_R = K_1 k_1\theta^{k_2} \tag{3.3}$$

where K_1 is a function of the pavement structure, test load and developed shear strain.

3.3.3.2 Deviatoric Stress "Semi-log" Model

The deviator stress is the cyclic stress in excess of the confining pressure and it is an important factor for the resilient modulus of cohesive soils. Therefore, AASHTO recommended the following deviatoric model for cohesive soils (Titi et al. 2006):

$$M_R = k_3 {\sigma_d}^{k_4} \tag{3.4}$$

where where σ_d is the deviator stress and k_3 and k_4 are material constants. This model is typically used for fine-grained soil because the confining pressure has a less significant effect than the deviator stress for cohesive soils. The disadvantage of the deviator stress model is that it does not consider the effect of confining pressure.

3.3.3.3 Uzan Model

Uzan (1985) developed a model to overcome the limitations of the bulk stress model by considering the deviatoric stress to account for the actual field stress state. Uzan model is given below:

$$M_R = k_1 \theta^{k_2} \sigma_d^{k_3} \tag{3.5}$$

where k_1, k_2, and k_3 are material constants and θ and σ_d are the bulk and deviatoric stresses respectively. By normalizing the resilient modulus and stresses in the above models, it can be written as follows (Titi et al. 2006):

$$M_R = k_1 P_a \left[\frac{\theta}{P_a}\right]^{k_2} \left[\frac{\sigma_d}{P_a}\right]^{k_3} \tag{3.6}$$

where P_a is the atmospheric pressure, expressed in the same unit as M_R, θ and σ_d.

Uzan (1985) also suggested that this model can be used for all types of soils. This model reduces to the bulk stress model and the Deviatoric Stress model by setting k_3 and k_2 setting to zero.

3.3.3.4 Octahedral Shear Stress Model

Witzak and Uzan (1988) modified the Uzan (1985) model by replacing the deviator stress with octahedral shear stress as follows:

$$M_R = k_1 P_a \left[\frac{\theta}{P_a}\right]^{k_2} \left[\frac{\tau_{oct}}{P_a}\right]^{k_3} \quad (3.7)$$

where τ_{oct} is the octahedral shear stress, P_a is the atmospheric pressure, and k_1, k_2, and k_3 are material constants. The advantage of this model is that the octahedral shear stress considers all three (major, intermediate, and minor) principal stresses.

3.3.3.5 AASHTO Mechanistic-Empirical Pavement Design Models

The general constitutive equation for resilient modulus selected for implementation in the MEPDG was developed through the National Cooperative Highway Research Program (NCHRP) project 1-28A as follows:

$$M_R = k_1 P_a \left[\frac{\sigma_b}{P_a}\right]^{k_2} \left[\frac{\tau_{oct}}{P_a} + 1\right]^{k_3} \quad (3.8)$$

where P_a is atmospheric pressure (101.325 kPa), σ_b is bulk stress = $\sigma_1 + \sigma_2 + \sigma_3$, σ_1 is major principal stress, σ_2 is intermediate principal stress and is equal to σ_3 for axisymmetric condition (triaxial test), σ_3 is minor principal stress (or confining pressure in the repeated load triaxial test), τ_{oct} is octahedral shear stress, and k_1, k_2 and k_3 are model parameters or material constants. This model can be used for any type of soil.

3.4 RESEARCH OBJECTIVES

The objectives of this study are to:

1. Determine the subgrade M_R for different regions of South Carolina by conducting repeated load triaxial tests on high quality Shelby tube samples.

2. Investigate the effect of soil type, deviator stress, confining stress, moisture content, and unit weight on the M_R of the subgrade soil.
3. Establish model parameters for the bulk stress model and the generalized constitutive resilient modulus model for South Carolina soils to use in MEPDG.
4. Develop constitutive models between soil index properties and the resilient modulus model parameters for undisturbed soils.
5. Develop FWD model relating laboratory measured M_R with FWD modulus.
6. Compare developed models (constitutive model and FWD model) with LTPP models for estimating M_R of South Carolina soils, and study the effect of M_R obtained from different models on pavement subgrade rutting using MEPDG.

3.5 METHODOLOGY

3.5.1 Site Selection and Sample Collection

Three pavement sections were selected for this study: US-321 in Orangeburg County (Coastal Plain, near the fall line), US-521 in Georgetown County (Coastal Plain), and SC-93 in Pickens County (Upstate Area). These sites were selected to represent different soil regions above and below the fall line as shown in Figure 3.7. Also, these locations are suitable for field FWD testing and asphalt coring due to their low traffic activity; and thus were sites where disruptions to traffic flow from lane closures would be minimal. For this study, Shelby tube (undisturbed) samples of subgrade soil were collected at 1500-3000 ft intervals along a 6.17 mi pavement section on US-321 in Orangeburg County (37 samples from 13 boreholes), along a 4.07 mi pavement section on US-521 in Georgetown County (19 samples from 7 boreholes), and along a 1.34 mi pavement section on SC-93 in Pickens County (26 samples from 5 boreholes). At each borehole location,

FWD tests were performed; and asphalt cores and bulk samples were collected. The spacing and number of tests and samples for each are shown in Table 3.2.

Maps showing the location of each pavement section, the locations of the FWD tests and boring locations along each pavement section, and a photograph showing the surface pavement conditions at each of the three sites are shown in Figure 3.8. The plan and profile views of a typical soil boring are shown in Figure 3.9. Photographs of field sample collection and laboratory testing are shown in Figure 3.10. At each site, 6 in. diameter asphalt cores were collected from the center of the right lane (Figure 3.10(a)) and high quality soil samples were collected from the same holes in 3 ft. long and 3 in. diameter Shelby tubes (Figure 3.10(b)). Bulk samples of soil were collected from an adjacent hole (Figure 3.10(c))

3.5.2 Soil Index Property Tests

Bulk soil samples were used to determine soil index properties by performing different laboratory tests: conduct grain size analysis (ASTM D 6913/AASHTO T 311), Atterberg Limits (ASTM D 4318/AASHTO T 90), specific gravity (ASTM D 854/ AASHTO T 100), maximum dry density and optimum water content (ASTM D 698/AASHTO T 99), and moisture content tests (ASTM D 2216/AASHTO T 265) in the laboratory. Soils were classified according to USCS (ASTM D 2488) and AASHTO (AASHTO M 145).

3.5.3 Field FWD Tests

FWD tests were performed at each boring location on the same day prior to coring the asphalt. At each FWD test location, four different loads are dropped ranging from 6000 lbs. to 14000 lbs. and deflections due to those load applications are measured. The FWD

equipment has seven different sensors to measure the deflections at prescribed distances from the load. Sensors are located at 0 inch, 7.9 inch, 11.8 inch, 17.7 inch, 23.6 inch, 35.4 inch, and 47.2 inch from the location of the load pedestal. Two different software packages are used to back-calculate elastic modulus from the deflection data: SCDOT program (developed by Johnson, 1992), and BACKFAA (backcalculation software developed by Federal Aviation Administration, FAA, 2002). The back-calculated modulus values from these two different software packages showed similar results because both programs were developed based on layered elastic analysis principals. Results obtained from the SCDOT program is reported in this study due to its reliable use on SCDOT pavement design. The FWD modulus data was used to develop correlations with the laboratory resilient modulus data.

3.5.4 Laboratory Resilient Modulus Tests

Resilient modulus tests were performed on 3 in. diameter by 6 in. long specimens obtained from the Shelby tube samples collected at each site. The Shelby tubes were tightly sealed and stored in the SCDOT concrete curing room (maintain 100% humidity) before being brought to USC for resilient modulus testing. Each Shelby tube was cut into a 6 in. long section (Figure 3.10(d)), and the soil was extruded and inserted into a rubber membrane (Figure 3.10(e)). M_R tests were performed on the samples by a repeated load triaxial test per AASHTO T 307 (1999) using a GDS Advanced Dynamic Triaxial Testing System (DYNTTS) housed in the Advanced Geotechnical Laboratory at the University of South Carolina (Figure 3.10(f)). To perform a test, a repeated axial cyclic stress of fixed magnitude, load duration, and cycle duration was applied to each 3 in. x 6 in. cylindrical specimen. During testing, the specimen is subjected to a dynamic cyclic stress and a static-

confining pressure provided by means of a triaxial pressure chamber. The total resilient or recoverable axial deformation response of the specimen was measured and used to calculate the M_R per the methodology of AASHTO (2003).

Samples are handled in such way that there is minimum disturbance. Shelby tube samples (3 in. diameter) are inserted into the 0.012 in. thick rubber membrane. During the extrusion process, the rubber membrane is placed inside a 3 in. diameter mold and is kept air-tight using a continuous vacuum pressure. Then, it is placed in the open end of Shelby tube and the soil sample is extruded slowly. To avoid any disturbance of the coarse grained soil, a 3 in. diameter cylindrical rod is also placed in the open end and is moving backward with the same rate of soil extrusion. Soil samples of 6 in. height are obtained by cutting perpendicularly during extrusion. A total of 3-5 samples are collected from each Shelby tube for testing.

Each sample is placed on the GDS machine base plate and the top cap is placed on the top of the sample. A single filter paper is placed between each end of the specimen and the top and bottom caps. Vacuum grease is used to make the connection between the sample and the top cap and base plate air-tight. Four O-rings are placed on each end of the sample to secure the membrane to the bottom and top caps. The cell cover is then placed on top of the sample and connected by making all the screws tight. The top cap is then connected with a rubber sleeve to the load piston.

The top of the specimen is connected to the back pressure and the base of the specimen is connected to the pore pressure transducer. Both these line are kept open because the resilient modulus is a drained test. The cell is completely filled with water and then the required cell pressure is applied. The required contact stress and cyclic stress is

provided using a haversine loop discussed earlier (Section 3.3.1). The axial ram is attached to a thrust-cylinder. The thrust cylinder is connected to the axial ram which passes through the balanced ram arrangement and then through the base of the cell. The base pedestal is connected to the ram. The cell base houses all of the hydraulic connections to the cell. These are: back pressure, pore pressure, cell pressure and cell fill/empty connections. The cell top is removable to allow the test specimen to be put in place. The cell top also contains the exchangeable load-cell attached to the ram which passes through the top of the cell. The deformation transducer is located in the base plate.

According to the test protocol in AASHTO T 307, a dynamic loading is repeatedly applied on top of a cylindrical specimen under confining pressure. The total load cycle duration is 1 second, which includes a 0.1 second load duration and a 0.9 second rest period. After the initial conditioning is completed; each of the 15 main test sequences are applied in 100 load repetitions and the average recoverable deformation for the last five cycles of each sequence is recorded. The maximum cyclic deviator stress, the contact stress and the total recoverable strain are used to calculate resilient modulus. For each of the three confining pressures (41.4 kPa, 27.6 kPa, 13.8 kPa) , five different cyclic stresses (12.4 kPa, 24.8 kPa, 37.3 kPa, 49.7 kPa, 62.0 kPa) are applied to the sample (see Table 3.1). Therefore, a total of 15 different resilient modulus values are found from each test. The GDS system only shows the stress and strain information. Therefore, the resilient modulus is calculated manually after the test. At the end of the resilient modulus test, a quick shear test is performed without any cell pressure according to AASHTO T 307. After the quick shear test, the entire specimen is kept in the oven overnight for determining moisture content (AASHTO T 265).

3.6 RESULTS AND ANALYSIS

3.6.1 Index Test Results

Properties of the investigated soils are shown in Table 3.3. The particle size distribution curves for samples from US-321 (Orangeburg), US-521 (Georgetown) and SC-93 (Pickens) are shown in Figure 3.11(a), (b), and (c), respectively. Orangeburg soils were classified as A-2-4 (silty or clayey sand) according to AASHTO M 145 or SC (clayey sand), SM (silty sand), and SC-SM (sandy silty clay) according to ASTM D 2488. Georgetown soils were classified as A-1-b and A-3 (non-plastic fine sand) and SP (poorly graded sand). Pickens soils were classified as A-7-6 (mostly clayey soils) and A-4 (mostly silty soils), and SC (clayey sand) and SM (silt) and ML (silt).

3.6.2 Resilient Modulus Results

A total of 82 M_R tests were performed on Shelby tube samples from 25 boring locations of 3 different pavement sections. Sample description and summary test results are shown in Table 3.4. Variation of soil type along section is shown in Table 3.5(a), Table 3.5(b), and Table 3.5 (c) for Orangeburg, Georgetown, and Pickens respectively. Cut and fill information was collected from SCDOT pavement design files for the mid zone of the Shelby tube location. SCDOT Pavement design files had the original and finished cross section after construction for each selected pavement section. If the finished pavement surface is above the original ground surface it was considered as fill section and vice versa. Relative compaction was the ratio of the average field dry density of the collected in-situ samples and the maximum dry density of the standard proctor test using the bulk soils collected from the same borehole location. Average resilient modulus was determined by taking the mean resilient modulus of all Shelby-tube samples collected from the same

borehole location. For Orangeburg, soil samples were collected from both the fill sections and cut sections (Table 3.5 (a)). Cut sections have shown higher average resilient modulus (55 MPa) than that of the fill sections (48 MPa). For Georgetown, most of the boreholes were made on fill sections except Borehole No. 7 (Table 3.5(b)). The average resilient modulus for cut and fill sections were found 42 MPa and 52 MPa, respectively. Table 3.5(c) indicates that all of the boreholes for Pickens were made on fill sections and the average resilient modulus is 40 MPa.

Typical test results for each of the three sites are shown in Figure 3.12. Figure 3.12(a) shows M_R versus cyclic stress at three different confining pressures for Sample No. 313 from Orangeburg; M_R increases with increasing cyclic stress and a higher M_R is found for higher confining pressure. These results are indicative of granular materials and were as expected for this soil that was classified as A-2-4 and SC. Figure 3.12(d) shows M_R results for Sample No. 611 from Georgetown. This particular sample shows greater effects of confining pressure on M_R than the Orangeburg sample in Figure 3.12(a). These results are indicative of granular materials as expected for this soil that was classified as A-3 and SP. Figure 3.12(g) shows M_R results for Sample No. 211 from Pickens. Unlike the previous two samples, M_R decreases with increasing cyclic stress for this sample, which is indicative of soils with higher fines content. This soil was classified as A-7-6 and SM.

The effect of bulk stress on the M_R for these three samples is shown in Figure 3.12(b), Figure 3.12(e) and Figure 3.12(h). Similar relations were obtained for each of the 37 samples for US-321 (Orangeburg), 19 samples for US-521 (Georgetown) and 26 samples for SC-93 (Pickens). The results from all of the tests for each of the three sites were combined to obtain the combined bulk stress model parameters for each site and are

shown in Figure 3.12(c), Figure 3.12(f), and Figure 3.12(i) for Orangeburg, Georgetown, and Pickens, respectively. Bulk stress models for Orangeburg, Georgetown, and Pickens soils are shown in Equation 3.9, Equation 3.10, and Equation 3.11, respectively. The coefficient of determination (R^2) values for both Orangeburg (=0.42) and Georgetown (=0.30) are low and indicate a large variation in M_R found for each of the boring locations along the length of each pavement section. The coefficient of determination (R^2) for Pickens (=0.06) is even lower.

$$M_R = 1.936\theta^{0.650} \quad (3.9)$$

$$M_R = 3.885\theta^{0.503} \quad (3.10)$$

$$M_R = 7.519\theta^{0.314} \quad (3.11)$$

Model parameters were also obtained using the generalized constitutive resilient modulus model, which can be used directly as inputs to MEPDG for local calibration. Model parameters of AASHTO M-E Pavement Design Models can be used directly as inputs to MEPDG for local calibrations which are shown in Table 3.6. Most of the test results shows good coefficient of determination ($R^2 > 0.80$). Similar to the bulk stress model, the model parameters for the generalized constitutive resilient modulus model were combined for each of the three sites and are presented in Eq. 3.12, Eq. 3.13, and Eq. 3.14 for Orangeburg, Georgetown, and Pickens, respectively.

$$M_R = 359.65P_a \left[\frac{\sigma_b}{P_a}\right]^{0.6076} \left[\frac{\tau_{oct}}{P_a} + 1\right]^{0.4504} \quad (3.12)$$

$$M_R = 356.03P_a \left[\frac{\sigma_b}{P_a}\right]^{0.4419} \left[\frac{\tau_{oct}}{P_a} + 1\right]^{0.6197} \quad (3.13)$$

$$M_R = 395.53P_a \left[\frac{\sigma_b}{P_a}\right]^{0.4965} \left[\frac{\tau_{oct}}{P_a} + 1\right]^{-1.4214} \quad (3.14)$$

At a representative bulk stress of 154.64 kPa and octahedral stress 13 kPa (per layer elastic analysis for South Carolina pavements using Weslea (v 3.0)), M_R was found as 50 MPa, 47 MPa, and 42 MPa for Orangeburg, Georgetown, and Pickens, respectively. Relatively higher bulk stress and octahedral stress were obtained for South Carolina subgrade soil conditions due to relatively lower average thickness of asphalt layer (4.3 in.), base layer (6.5 in.), and compacted subgrade layer (6.0 in.) for the selected pavement sections. At these representative stresses, higher M_R was found for pavements in the Coastal Plain and Sediment Region than Blue Ridge and Piedmont Region. The coefficient of variation for M_R was found to be 24%, 27%, and 42% for Orangeburg, Georgetown, and Pickens, respectively. If the variability of test results exceeds a coefficient of variation of 25%, then additional resilient modulus tests should be performed (i.e., more than two or three resilient modulus tests along a project per Von Quintus and Killingsworth, 1997). Although, multiple tests were performed for each borehole locations, high coefficient of variance (COV > 25%) for each site in this study suggests that the variation of M_R along each of the three pavement sections must be taken into account when selecting design M_R input to MEPDG.

Effects of soil type, moisture content, and unit weight were also investigated for the three soils. M_R versus moisture content and M_R versus dry unit weight for the three soils are shown in Figure 3.13. This includes 82 test results from the three sites. As shown in Figure 3.13(a), there is no clear relation between moisture content and the M_R obtained for the undisturbed samples; whereas, previous studies on laboratory remolded samples have shown M_R decreases with increasing moisture content (Drumm et al., 1997; Butalia et al., 2003; Fredlund et al., 1977; and Heydinger, 2003). These results represent the

inherent variation in the natural soil samples, and, because samples were tested at natural water content, the results for each soil type do not represent a range of water contents on both the dry and wet side of the optimum moisture content (i.e., for the A-7-6 and A-4 soils, M_R was measured mostly on wet side of optimum, see Table 3.3 for w_{opt}). The results for dry unit weight versus M_R shown in Figure 3.13(b) show an increasing trend as has been observed in other studies (Drumm et al., 1997; Chou et al. 1976; and Seed et al., 1962). Resilient moduli versus moisture content at different degree of saturation are shown in Figure 3.14(a), Figure 3.14(b) and Figure 3.14(c) for the three selected routes. Figure 3.15(a) shows the combined results from all 82 test samples of all three routes, and Figure 3.15(b) shows the combined results taking the average resilient modulus value of all 25 boring locations. Result shows that at a specific degree of saturation resilient modulus decreases with increasing moisture content. Figure 3.16 shows the effect of degree of saturation on resilient modulus for different moisture content. It was observed that, resilient modulus did not decrease with degree of saturations at a specific moisture content range for some instances. Figure 3.17 shows that resilient modulus increases with dry unit weight at a specific degree of saturation range.

3.7 CORRELATION OF MODEL PARAMETERS WITH SOIL INDEX PROPERTIES

The generalized constitutive resilient modulus model parameters ($k_1, k_2, and\ k_3$) were correlated with the soil index properties using multiple linear regression techniques. Soil properties which were considered in the statistical analysis include field dry density (γ_d), field moisture content (w), maximum dry density ($\gamma_{d,max}$), optimum moisture content (w_{opt}), percent passing through No. 4 (P_4), No. 40 (P_{40}), and No. 200 sieve (P_{200}), D_{60},

D_{50}, D_{30}, D_{10}, uniformity coefficient (C_u), coefficient of curvature (C_c), liquid limit (LL), plastic limit (PL), plasticity index (PI), liquidity index (LI), specific gravity (G_s), percent sand, silt, and clay. Statistical models were developed for two different types of soils based on the AASHTO M 145: granular materials (P_{200}<35%), and silt-clay materials (P_{200}>35%). For Orangeburg and Georgetown, a combined model was developed as they are both classified as granular materials (A-1-b, A-2-4, A-3), and for Pickens a separate model was developed as it is classified as silt-clay materials (A-4, A-7-6).

First, a bivariate analysis was used to examine the Pearson intercorrelation among different response variables ($k_1, k_2, and\ k_3$) and the predictor variables (different soil properties). Multicollinearity of the predictor variables was assessed. Next, a multiple regression analysis was conducted to predict the values of the response variable based on the value of predictor variables. All analyses were performed in IBM SPSS Statistics software (v 12). Table 3.7 shows the coefficients for the developed models for both granular and silt-clay materials. Low coefficients of determination (R^2) were found for most of the models. Recall, model parameters were obtained from M_R tests on undisturbed samples of natural soils, not laboratory prepared specimens, and are indicative of the natural variation of the soils. There may be other factors involved in the resilient behavior of in-situ soils such as pavement age and precipitation. Moreover, data sample size was limited to 50 soil samples for granular materials and 25 soil samples for silt-clay materials. Table 3.7 also shows the significance of different soil properties on coefficients and overall model significance using p-value, where p < 0.001 indicates a statistically highly significant effect. p < 0.01 and p < 0.001 indicate statistically moderate and low significant effects, respectively. For granular materials, percent passing No. 4 sieve and percent sand

showed statistically significant effect on k_1. Percent silt showed statistically significant effect on k_2, and percent passing No. 4 showed statistically significant effect on k_3. Unlike granular materials, silt-clay materials showed significant effect of liquidity index and plasticity index, plastic limit, and in-situ water content and dry density on k_1 and k_2.

The developed constitutive models were used to determine M_R for a representative bulk stress 154.64 kPa and octahedral stress of 13 kPa and defined as predicted M_R. The predicted M_R using the constitutive model was then compared to the laboratory measured M_R, which is shown in Figure 3.18(a) for granular materials and Figure 3.18(b) for silt-clay materials. Most of the data points from both models are observed close to the line of equity. Universal LTPP models (for sand) of laboratory prepared soils are validated for the South Carolina condition and compared in Figure 3.18(c) and Figure 3.18(d). LTPP models for silt and LTPP models for clay were also studied; however, LTPP models for sand showed better results when compared to the measured M_R for both the granular materials and silt-clay materials studied herein. The locally developed constitutive models quantified the improvement in prediction of the M_R more accurately than the universal LTPP models for undisturbed soil samples of South Carolina in terms of lower bias (e.g. 2.07 vs. 11.64 in Figure 3.18(a) and Figure 3.18(c)) and standard error (e.g. 11.52 vs. 13.60 in Figure 3.18(a) and Figure 3.18(c)). Bias was estimated by taking the difference between the mean values of the measured and predicted M_R, and the standard error was estimated by taking the standard deviation of the residual error of measured and predicted M_R.

3.8 CORRELATION OF RESILIENT MODULUS WITH FWD MODULUS

FWD is a nondestructive test which can be used to back calculate elastic modulus from pavement deflections, and is a widely used alternative to predict pavement stiffness (Zhou, 2000; Meshkani et al., 2003). The AASHTO design guide (AASHTO, 1993) recognizes that the laboratory modulus and the in situ FWD back-calculated modulus are not equal and suggests that the subgrade modulus determined from FWD be adjusted by a factor of 0.33. There are several possible reasons for these results (Kim et al., 2010):

- The samples collected from the field for laboratory triaxial tests are all disturbed samples, and therefore do not represent the actual conditions of the subgrade in the field (Ping et al., 2002; Rahim and George. 2003; Daleiden et al., 1995; Lee et al., 1988; and Hossain et al., 2000).
- The confining pressure on the sample is usually applied through compressed air, which does not perfectly replicate the original condition of self-induced passive earth pressure in the field (Ping et al., 2002; Rahim and George, 2003).
- There are significant differences in the volumes of samples which are tested in the laboratory and in the field (Rahim and George, 2003).
- The FWD back-calculation program is not a unique method and is based on the linear elastic theory of multiple layer pavement structure, but pavement is not elastic (Ping et al., 2002).
- Greater variations in the difference between the laboratory modulus and the FWD modulus are seen at sites where extensive cracking is found (Lee et al, 1988).

- Resilient modulus value varies significantly due to seasonal changes (Heydinger, 2003). Resilient modulus of subgrade is typically 12 to 4 times higher in the coldest months (December to February) as compared to the rest of the year, mainly because of stiffness increase caused by the freezing of the moisture in the subgrade (Jong et al., 1998).
- Temperature of the asphalt concrete layer affects the stiffness of the asphalt layer and also affects the deflection data of the FWD test because the asphalt layer acts as a buffer between subgrade and the FWD load (Hossain et al., 2000).

Different ratios between the laboratory modulus and the in situ FWD back-calculated modulus have been documented in previous studies. Ali and Khosla (1987) found the ratio to be 0.18-2.44 for NC subgrade soils, Newcomb (1995) found the range of 0.8-1.3 for the state of Washington, and Von Quintus and Killingsworth (1997) found the range of 0.35-0.75 (with coefficient of variation of 13% to 49%) based on data obtained from LTPP database. Ping et al. (2002) reported that the ratio of laboratory modulus and FWD back-calculated modulus were about 0.625 for granular materials with relatively lower R^2 value (0.30). Therefore, as suggested by Rahim and George (2003), the adjustment factor needs to be reevaluated.

For this study, FWD tests were performed at a total of 43 locations as indicated in Table 3.2 for the three selected pavement sections. At 25 of these locations, asphalt coring and soil boring were performed at the same location immediately following the FWD test. The FWD test equipment used by SCDOT is shown in Figure 3.19. The FWD elastic modulus has been estimated using the SCDOT program (Baus and Johnson, 1992).

Modulus probability charts for US-321, US-521, and SC-93 are presented on Figure 3.20(a), Figure 3.20(b), and Figure 3.20(c) respectively. A modulus probability chart shows the subgrade modulus for the tested section at different percentile. 85th percentile test values are also shown in the figures. Results showed that US-321 and US-521 have 85th percentile elastic modulus values of 22,145 psi and 21,005 psi, respectively. That means, 85% of the test values are lower than 22,145 psi or 21,005 psi. However, SC-93 showed very low FWD modulus of 85th percentile value of around 6500 psi. Usually, 85th percentile elastic modulus from the modulus probability charts are used by the SCDOT when they do overlay design for pavement rehabilitation.

For the three pavement sections studied herein, the correlation between the FWD back-calculated modulus and the laboratory M_R is shown in Figure 3.21. Due to the limited number of boreholes, the results of the three different pavement locations are combined. The developed FWD model with different conversion coefficients and coefficient of determination is shown in Figure 3.21 (a). There is good correlation (R^2= 0.49) for the conversion coefficient of 0.27. Whereas, some other studies reported lower coefficient of determination (R^2= 0.30) which is shown in Figure 3.21 (b) for studies by Ping et al., 2002 and Von Quintus and Killingsworth, 1997. It was found that the ratio of laboratory modulus and FWD back-calculated modulus ranged from minimum 0.16 to maximum 0.57 for South Carolina soils. Orangeburg, Georgetown, and the Pickens soil showed the range of 0.16-0.43, 0.20-0.34, 0.23-0.57 respectively. Based on this data, the following model was developed to relate FWD modulus to laboratory M_R and can be used to estimate Level 3 M_R inputs for MEPDG in South Carolina.

$$M_R(Lab) = 0.27 \times M_R(FWD) \quad (3.15)$$

3.9 EFFECTS OF RESILIENT MODULUS OF SOIL ON SUBGRADE RUTTING

The approach used in the MEPDG to calculate total rut depth (i.e., the pavement surface depression in the wheel paths caused by the permanent deformation of the Hot Mix Asphalt (HMA), unbound layers, and foundation soil, and originating from the lateral movement of pavement material due to cumulative traffic loading) is based upon calculating incremental distortion or rutting within each sub-layer. The study by Orobio and Zaniewski (2011) examined each of the pavement material characteristics and determined the sampling based sensitivity analysis of the MEPDG applied to material input. They found that the M_R of subgrade had the largest effect on the rutting predicted from MEPDG.

In the current study, the effect of M_R on subgrade rutting using the MEPDG was studied for four different resilient modulus input types: M_R obtained from repeated load triaxial tests (AASHTO T 307), the constitutive model developed from index properties for South Carolina (Table 3.7), FWD model (Equation 3.15), and LTPP model for sand (*7*) for a representative bulk stress of 154.64 kPa and octahedral stress of 13 kPa. The analysis was performed using AASHTOWare (v. 2.2.4). Preliminary local calibration coefficients ($\beta_{GB} = 2.979, \beta_{SG} = 0.393$) were used. The Orangeburg (US-321), Georgetown (US-521), and Pickens (SC-93) pavements are asphalt concrete pavements having different type of bases (Gassman and Rahman, 2016): Orangeburg has a graded aggregate base, Georgetown has a cement treated base, and Pickens has an asphalt aggregate base. Site-specific climate, traffic, and subgrade properties were used as Level 1 MEPDG inputs; whereas, asphalt and base properties were not available, thus MEPDG default values were used. The dates of construction for Orangeburg, Georgetown, and Pickens pavement

sections are 2004, 2004 and 2001, respectively; therefore, MEPDG analysis was run for 12 years for Orangeburg and Georgetown, and 15 years for Pickens.

As shown in Figure 3.22, the four M_R input types produced different results for subgrade rutting. The results using the M_R from the constitutive model based on index properties and the M_R from the direct measurement in the laboratory (AASHTO T 307) were in closest agreement. These results were also in good agreement with the results using the M_R from the FWD model for Orangeburg and Georgetown, but not for Pickens. For Georgetown, the LTPP sand model was in good agreement with the first two models; however, for Orangeburg the LTPP sand model over predicted the rutting and for Pickens under predicted the rutting. These results show that the LTPP model for sands is in good agreement with the two models developed herein for Georgetown (A-1-b, A-3, SP); whereas, it is not in agreement with the models developed for Orangeburg (A-2-4, SM, SC-SM and SC) and Pickens (A-7-6, A-4, SM, SC). Recall, LTPP models for silt and clay were also studied for the Orangeburg and Pickens soils, however, the LTPP sand models showed better results (Figure 3.18). This means that none of the LTPP models are appropriate for the Orangeburg and Pickens soils and site-specific models are required. Results also indicate that in MEPDG, when keeping all other subgrade material properties constant, subgrade M_R values from different models have significant differences in subgrade rutting over the life of the pavement (i.e., in Figure 3.22(a), the difference between M_R from constitutive model and LTPP sand model is 19 MPa, which showed the differences in subgrade rutting at the construction year of 0.017 in. However, it showed relatively large difference in the subgrade rutting at the end of year 15 (0.038 in.)).

Therefore, pavement engineers should be cautious when selecting resilient modulus values for design.

3.10 CONCLUSIONS

The following conclusions are drawn from this study:

- Even for a relatively short pavement section (1.34 miles long in Pickens), resilient modulus can have a wide range of values (COV = 42%) which must be considered when selecting input values for MEPDG.
- Resilient modulus found for undisturbed soil samples did not show a distinct pattern with the in-situ moisture content as has been shown for laboratory prepared samples.
- For granular materials, percent passing No. 4 sieve and percent sand showed statistically significant effect on k_1. Percent silt showed statistically significant effect on k_2, and percent passing No. 4 showed statistically significant effect on k_3. For silt-clay materials, liquidity index, plasticity index in-situ water content and dry density showed a significant effect of on k_1 and k_2.
- Developed constitutive models predicted the resilient modulus more accurately (standard error was 11.52 and 18.63 for granular and silt-clay materials, respectively) than the universal LTPP models (standard error was 13.60 and -21.14 for granular and silt-clay materials, respectively).
- Good correlation was obtained between laboratory resilient modulus and the FWD modulus and can be used to estimate M_R as a Level 3 input.

- Subgrade rutting predicted by the developed constitutive model was in closer agreement to the rutting predicted by the laboratory measured resilient modulus than the FWD model or LTPP model.
- It is recommended to perform resilient modulus tests for laboratory prepared samples for a range of water contents on both the wet and dry side of the optimum moisture content to compare with the undisturbed soil samples to properly compare the behavioral change of dynamic properties of soil due to disturbance.

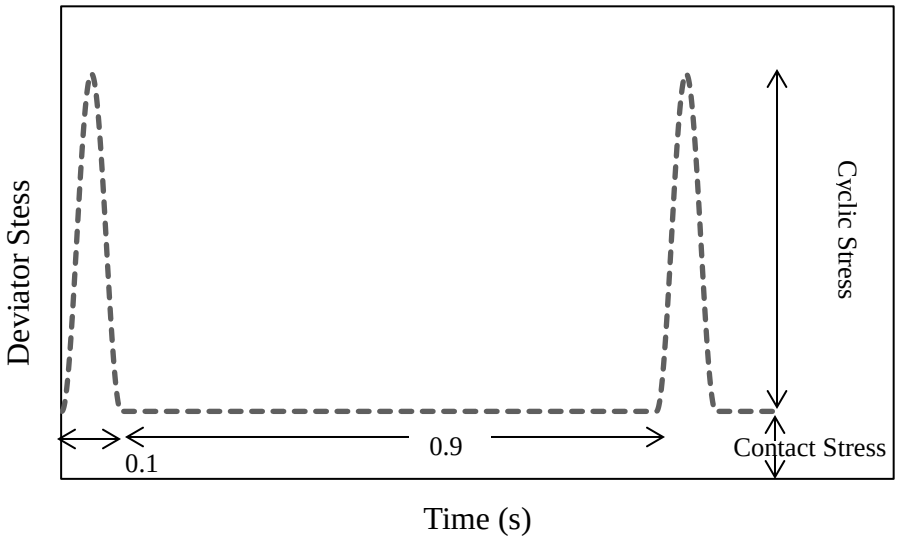

Figure 3.1 Shapes and Duration of Repeated Load

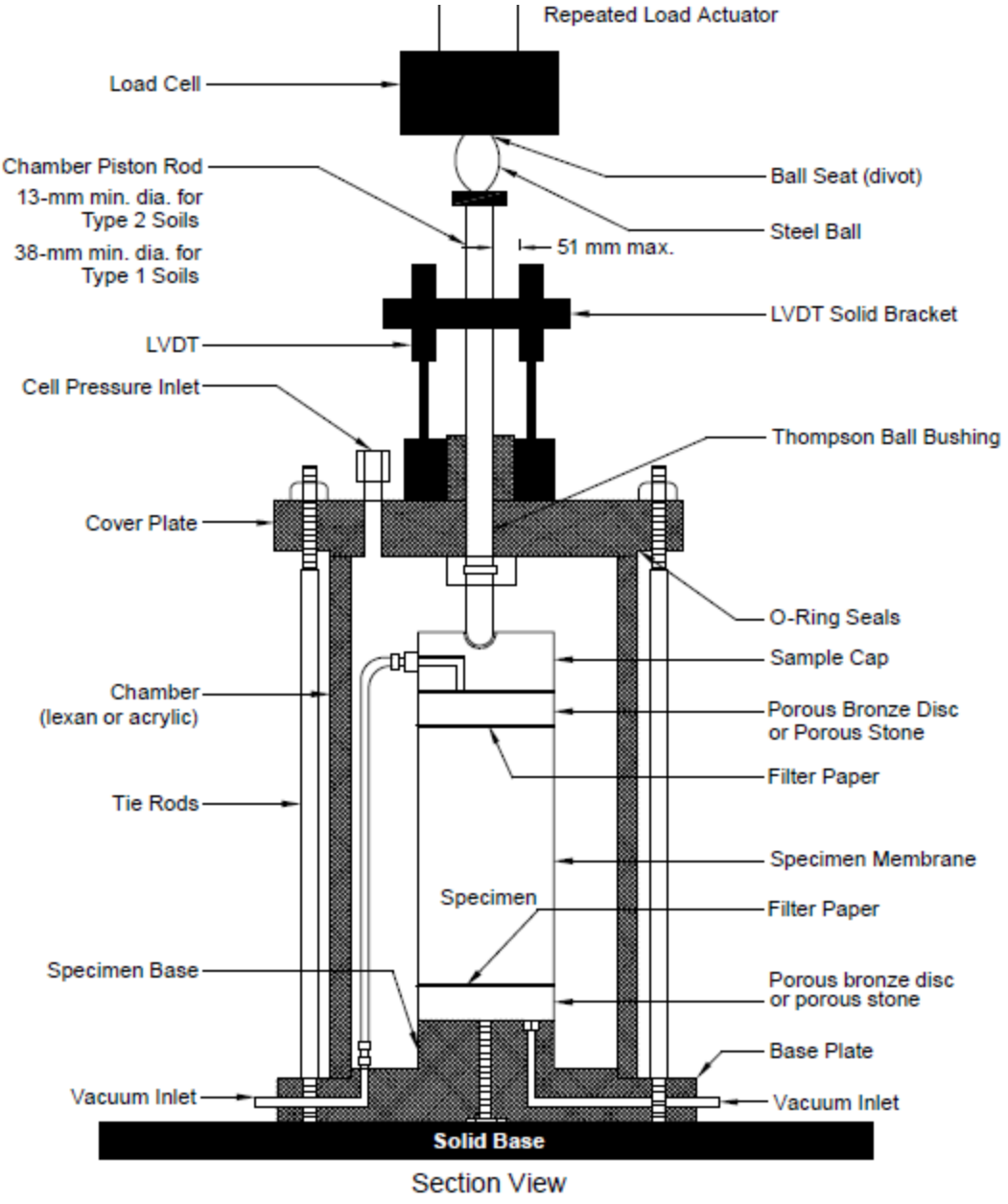

Figure 3.2 Schematic of Soil Specimen in a Triaxial Chamber (AASHTO T 307)

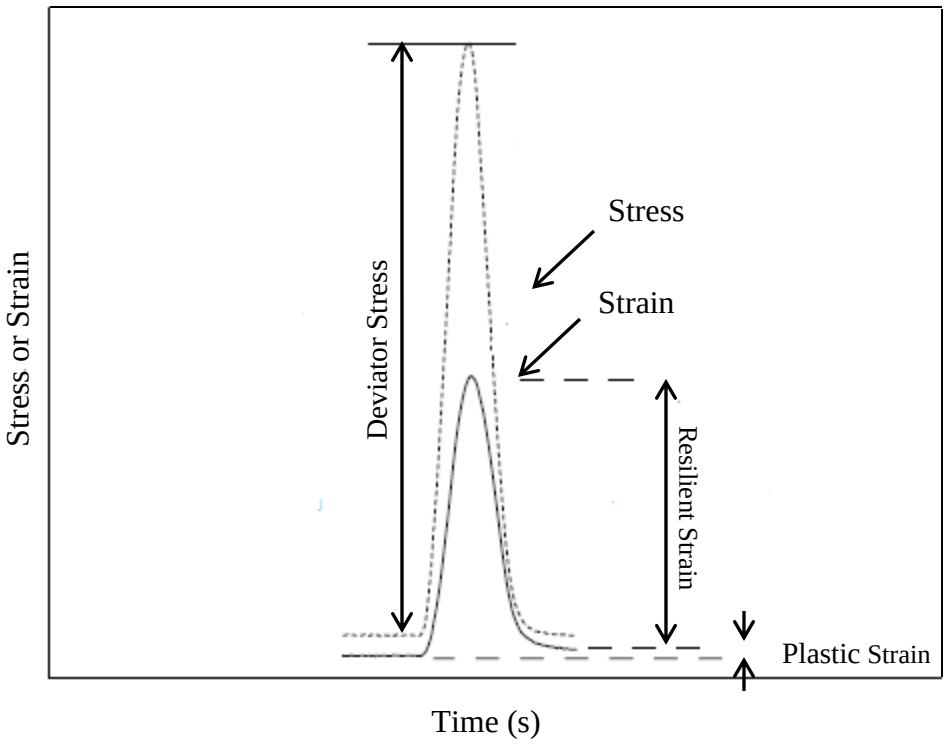

(a) Stress and Strain of One Load Cycle

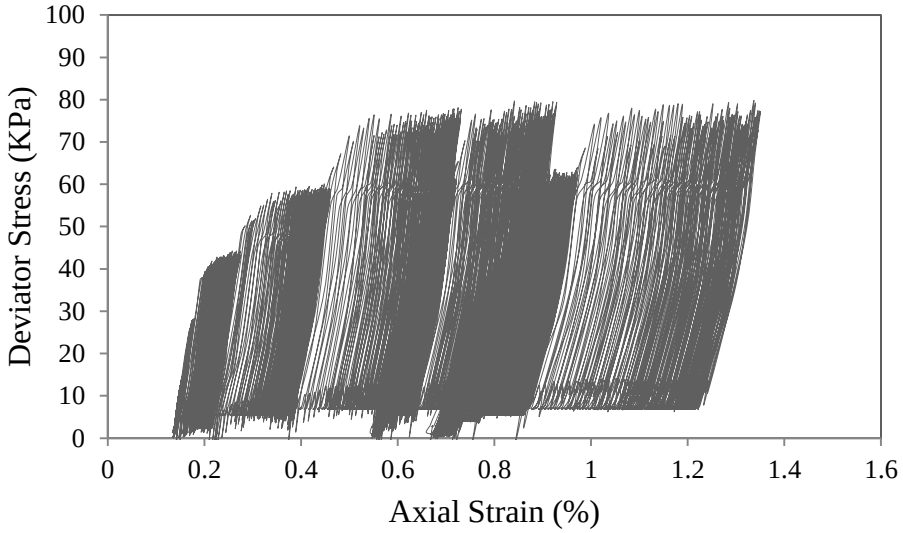

(b) Stress versus Strain for 1500 Load Cycle

Figure 3.3 Stress Strain Behavior on Resilient Modulus Tests

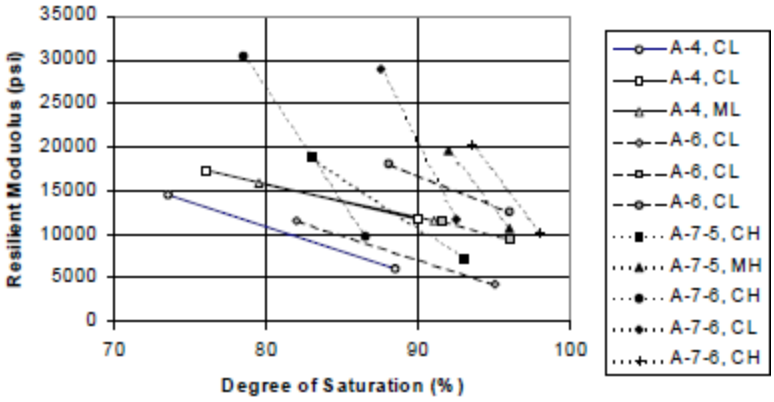

Figure 3.4 Effect of Degree of Saturation on Resilient Modulus (Drumm et al., 1997)

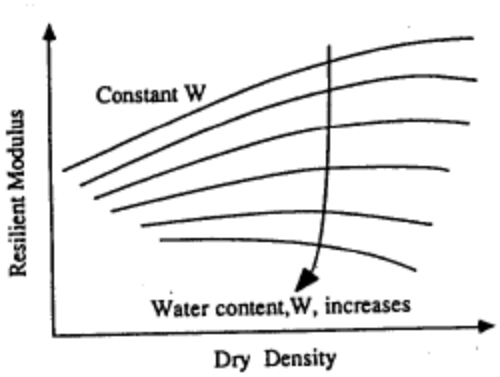

Figure 3.5 Effect of Dry Density on Resilient Modulus (Seed et al., 1962)

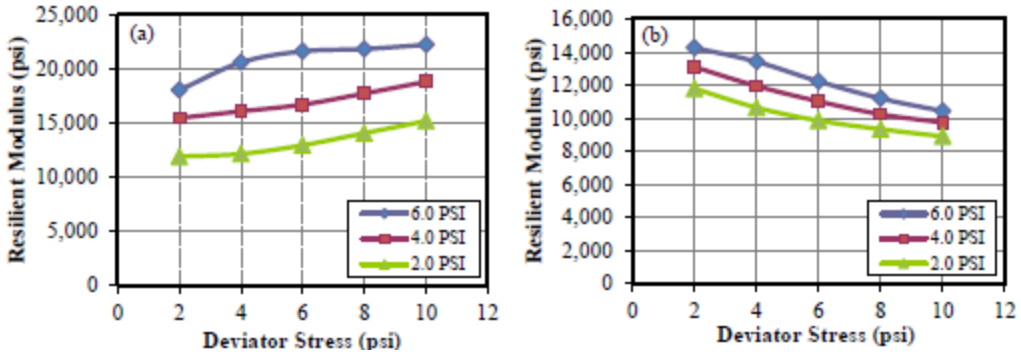

(a) Coarse Grained (b) Fine Grained

Figure 3.6 Effect of Deviator Stress and Confining Pressure on M_R (Ng et al., 2015)

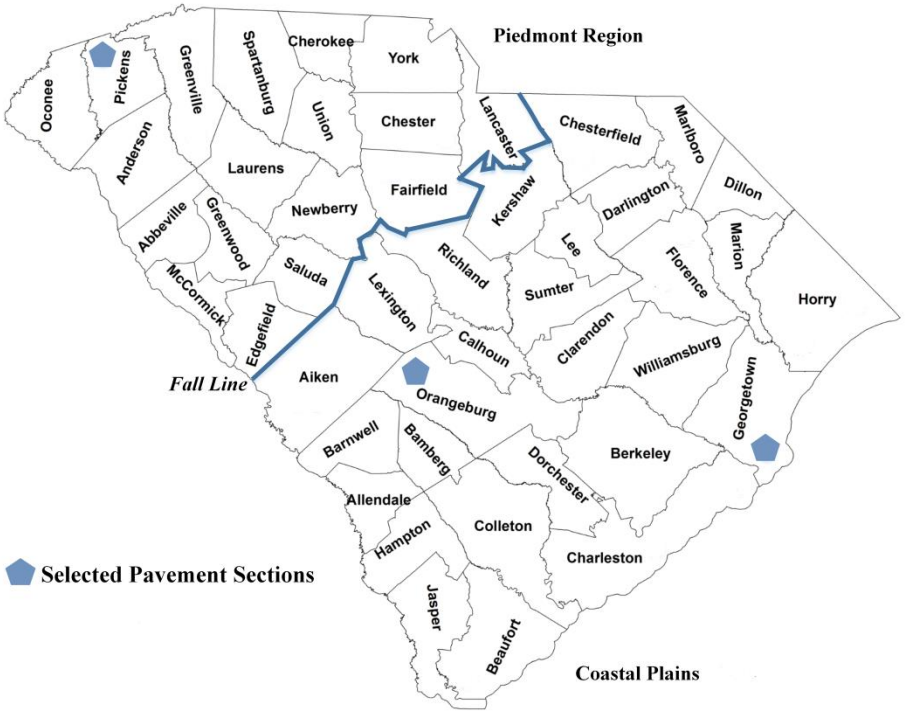

Figure 3.7 Selected Sections for Pavement Coring

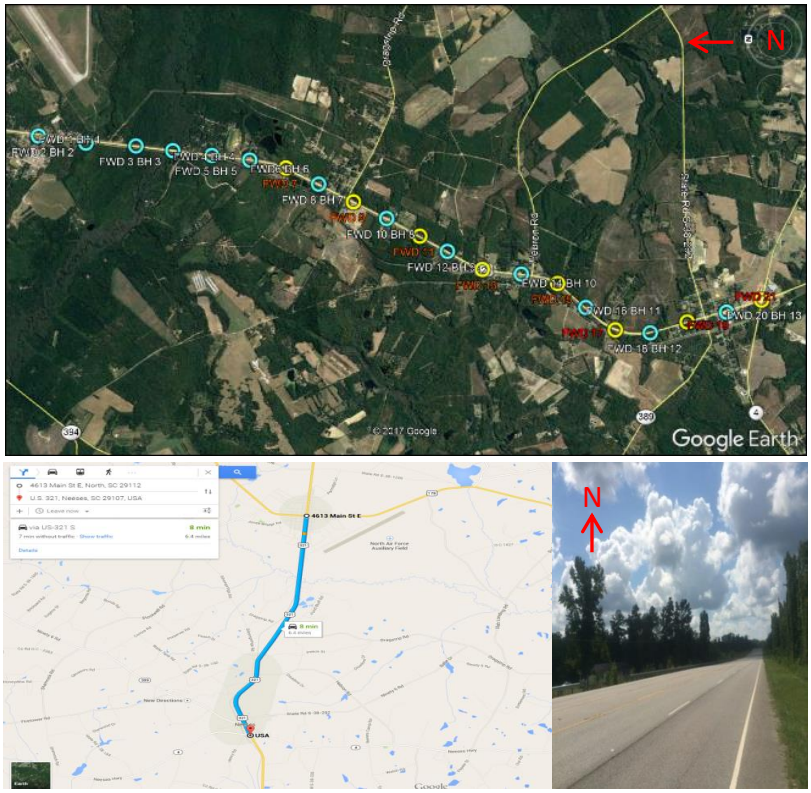
N
FWD 1 BH 1
FWD 2 BH 2
FWD 3 BH 3
FWD 5 BH 5
FWD 8 BH 7
FWD 10 BH 8
FWD 12 BH 9
FWD 16 BH 11
FWD 18 BH 12
FWD 20 BH 13
© 2017 Google
Google Earth
4613 Main St E
N

(a)

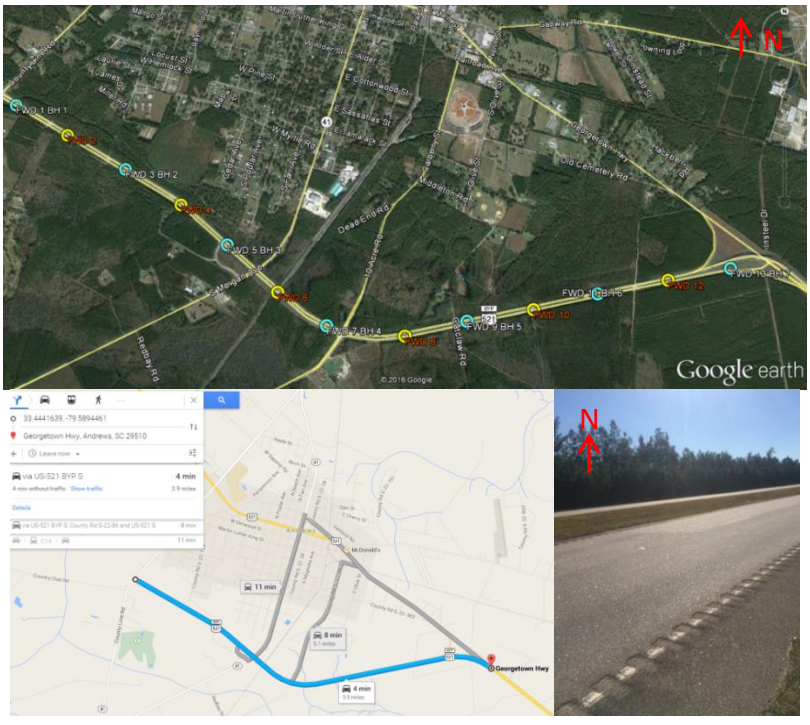
N
FWD 1 BH 1
FWD 3 BH 2
FWD 5 BH 3
FWD 7 BH 4
FWD 9 BH 5
FWD 12
FWD 10
© 2016 Google
Google earth
Georgetown Hwy, Andrews, SC 29510
N

(b)

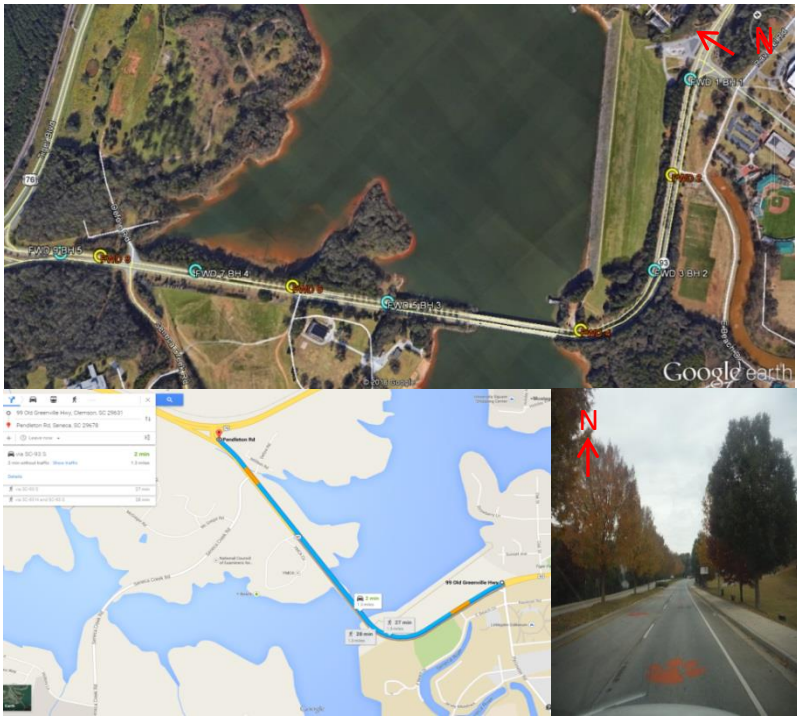

(c)

Figure 3.8 FWD Testing and Borehole Locations for (a) Orangeburg, (b) Georgetown, and (c) Pickens

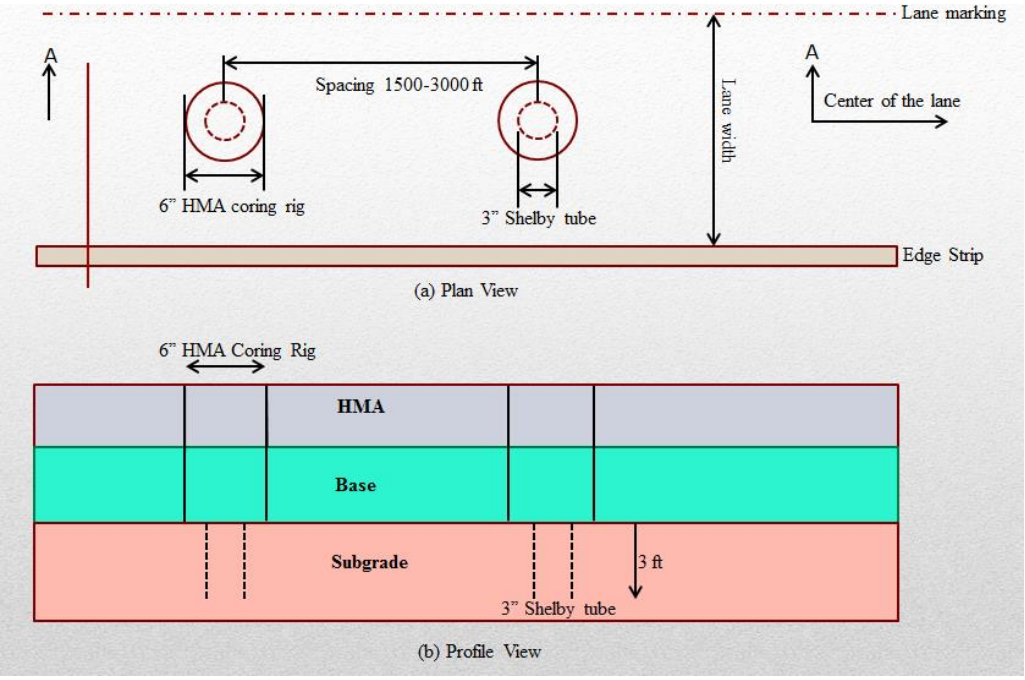

Figure 3.9 Plan and Profile View for Subgrade Sampling

(a) Asphalt Coring

(b) Shelby Tube Sample

(c) Bulk Soil Collection

(d) Cutting Shelby Tube

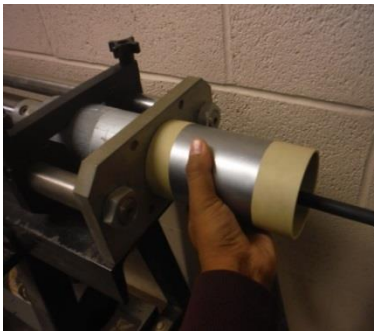

(e) Soil Extrusion

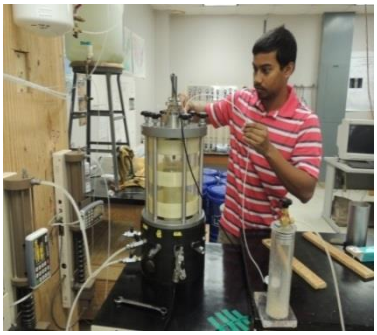

(f) M_R Testing

Figure 3.10 Field Sample Collection and Laboratory Testing

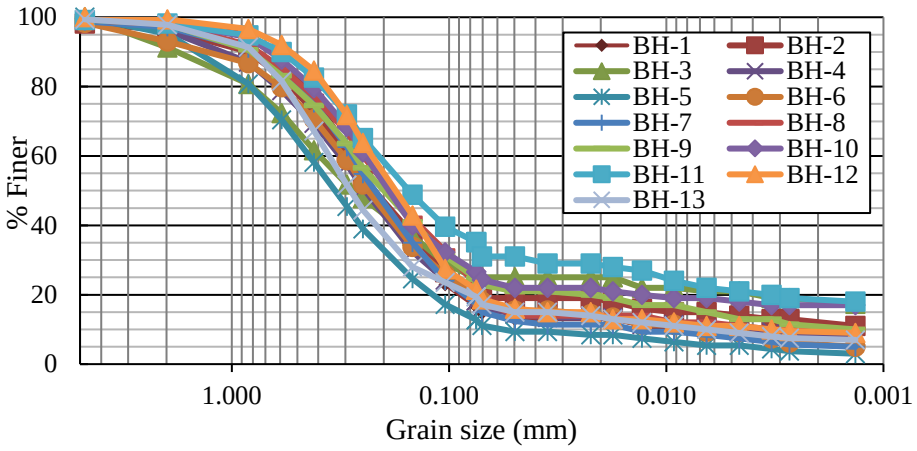

(a)

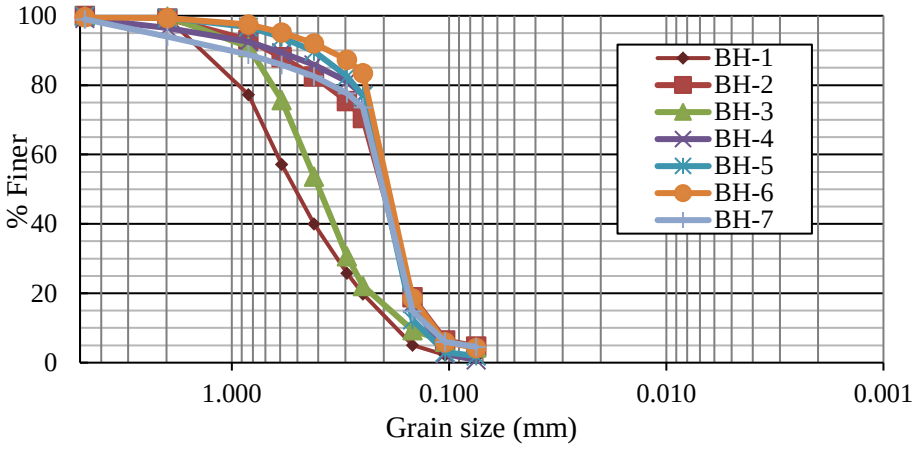

(b)

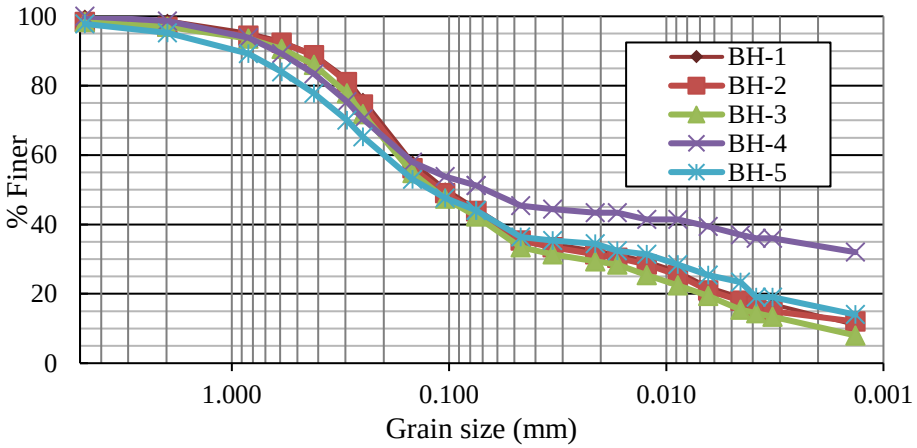

(c)

Figure 3.11 Particle Size Distributions for (a) Orangeburg, (b) Georgetown, and (c) Pickens

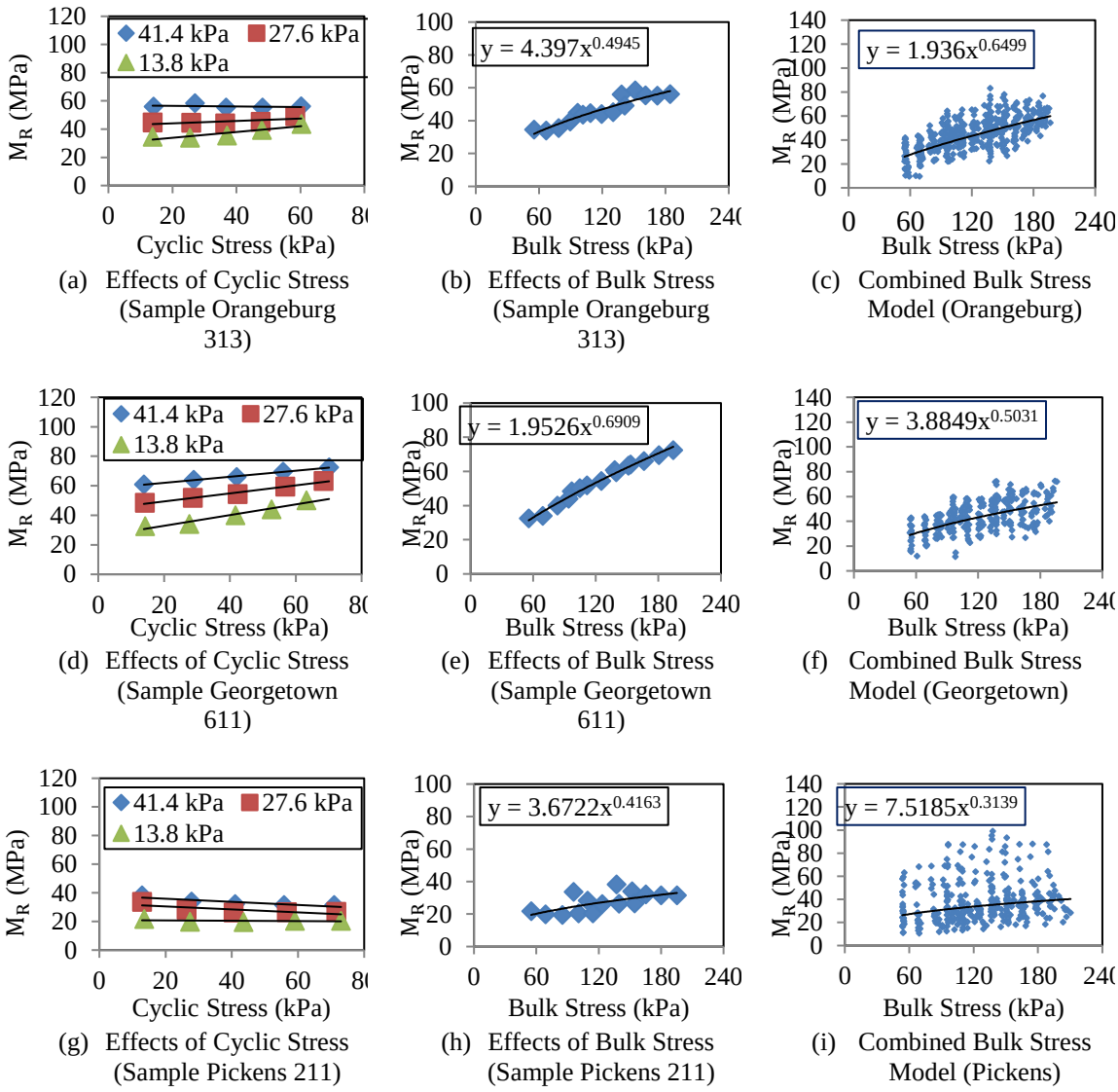

(a) Effects of Cyclic Stress (Sample Orangeburg 313)

(b) Effects of Bulk Stress (Sample Orangeburg 313)

(c) Combined Bulk Stress Model (Orangeburg)

(d) Effects of Cyclic Stress (Sample Georgetown 611)

(e) Effects of Bulk Stress (Sample Georgetown 611)

(f) Combined Bulk Stress Model (Georgetown)

(g) Effects of Cyclic Stress (Sample Pickens 211)

(h) Effects of Bulk Stress (Sample Pickens 211)

(i) Combined Bulk Stress Model (Pickens)

Figure 3.12 Resilient Modulus Test Results

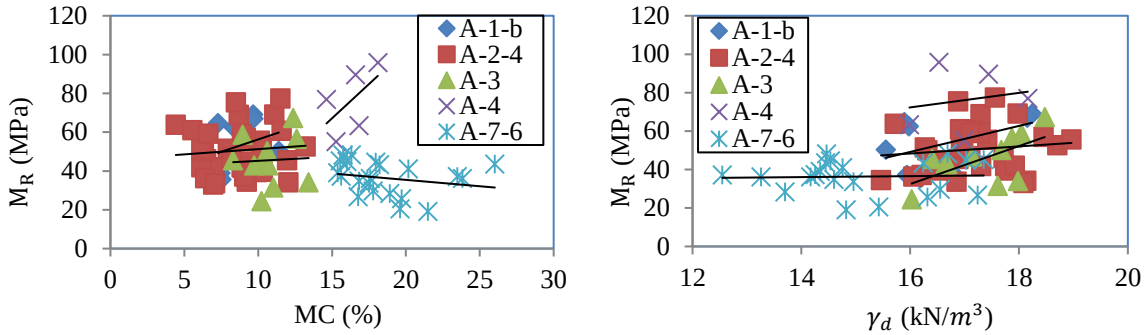

(a) Effects of Moisture Content (b) Effects of Dry Unit Weight

Figure 3.13 Effect of Moisture Content and Dry Unit Weight on M_R

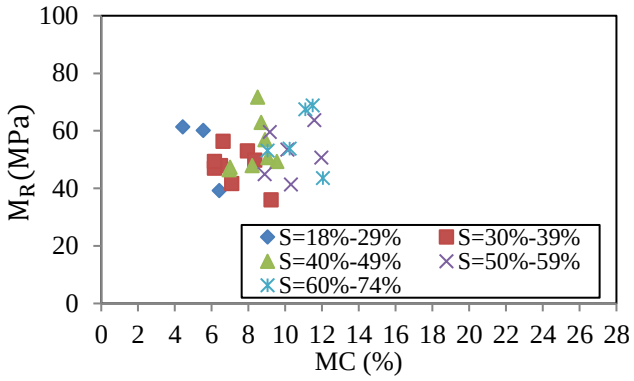

(a) Resilient Modulus versus Moisture Content (Orangeburg)

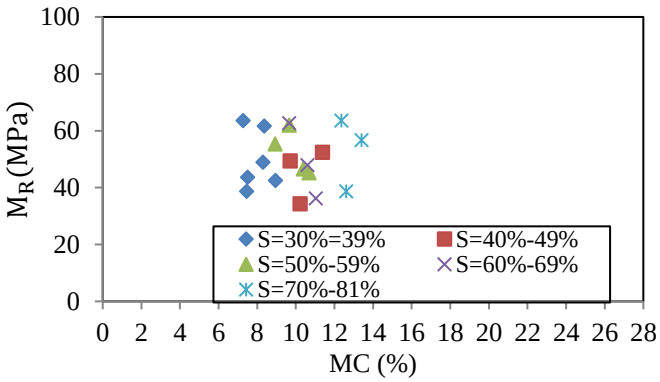

(b) Resilient Modulus versus Moisture Content (Georgetown)

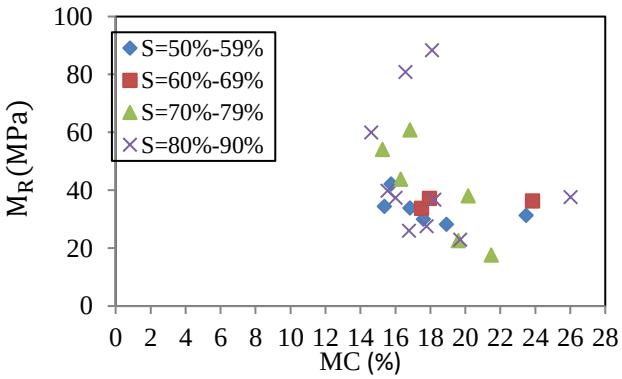

(c) Resilient Modulus versus Moisture Content (Pickens)

Figure 3.14 Effect of Moisture Content for Each Site

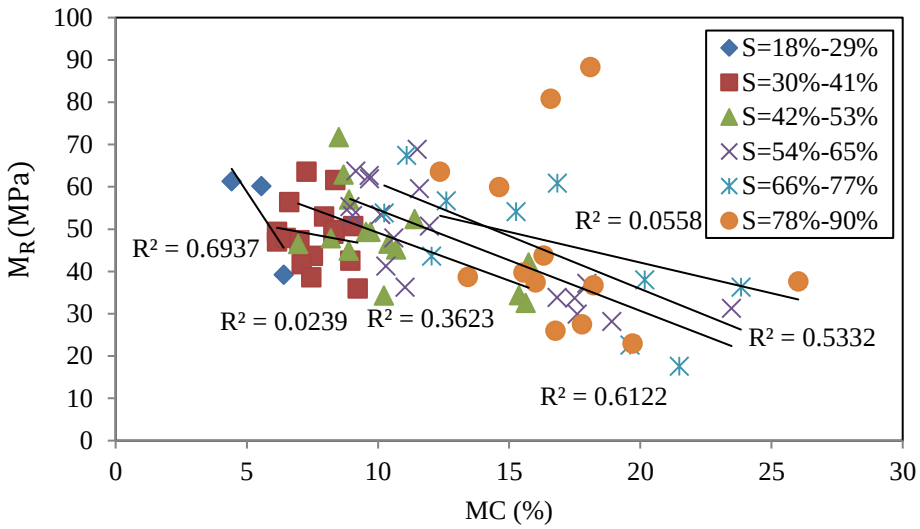

(a) Resilient Modulus versus Moisture Content (All Samples)

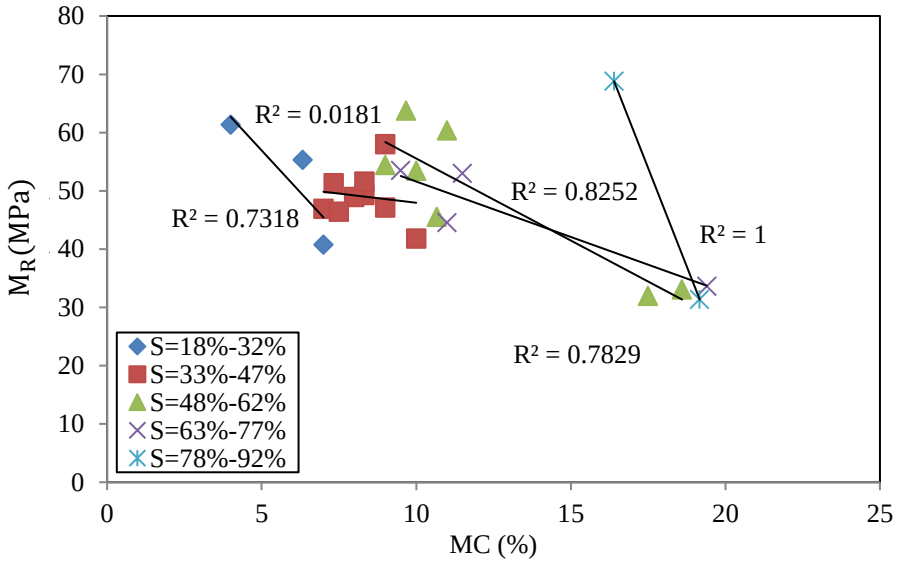

(b) Resilient Modulus versus Moisture Content (Boring Locations)

Figure 3.15 Effect of Moisture Content on M_R (All Sites Combined)

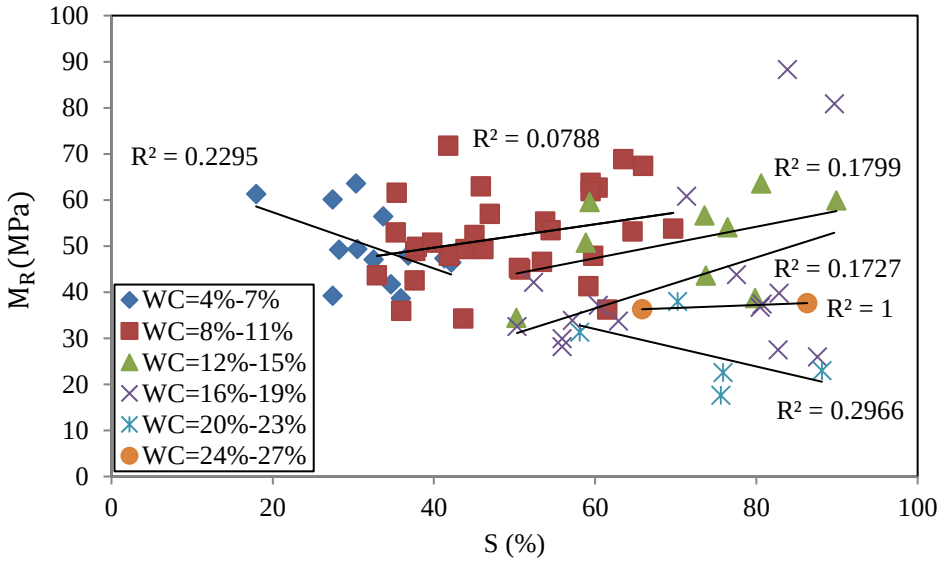

(a) Resilient Modulus versus Degree of Saturation (All Samples)

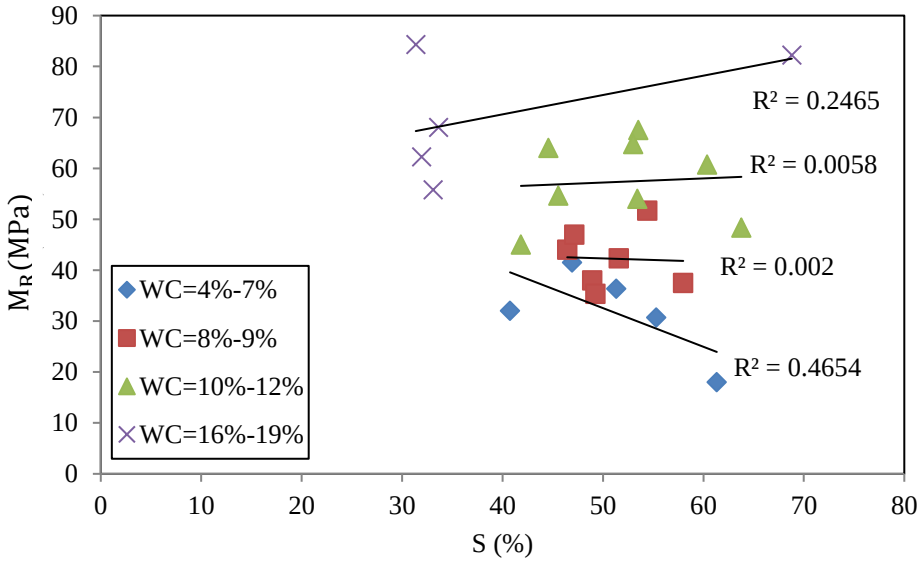

(b) Resilient Modulus versus Degree of Saturation (Boring Locations)

Figure 3.16 Effect of Degree of Saturation on M_R (All Sites Combined)

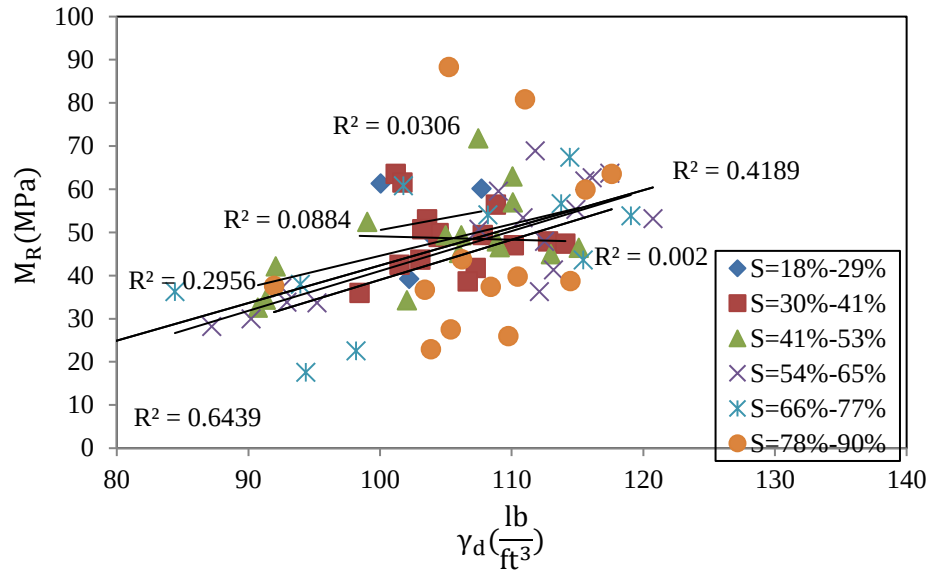

(a) Resilient Modulus versus Dry Unit Weight (All Samples)

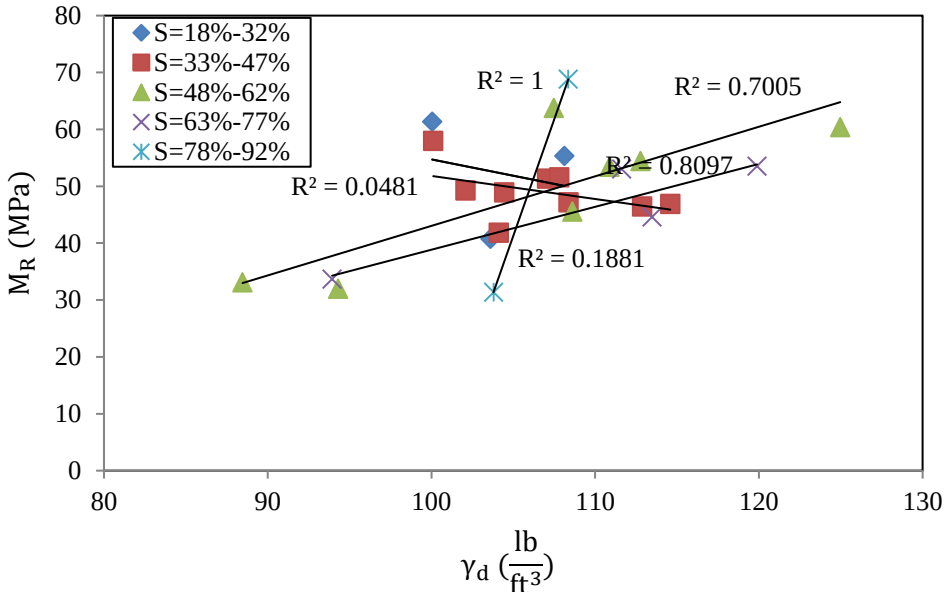

(c) Resilient Modulus versus Dry Unit Weight (Boring Locations)

Figure 3.17 Effect of Unit Weight on M_R (All Sites Combined)

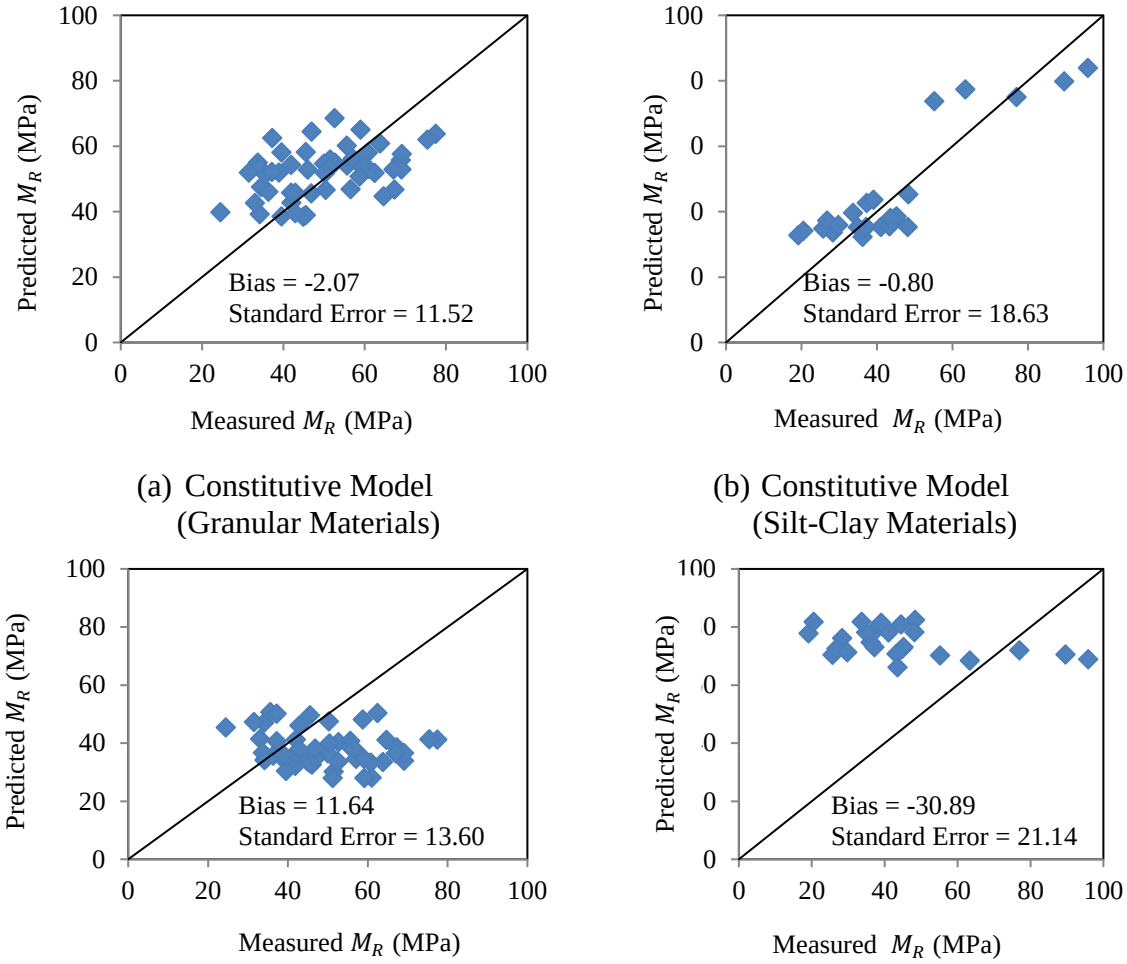

(a) Constitutive Model (Granular Materials)

(b) Constitutive Model (Silt-Clay Materials)

(c) LTPP Sand Model (Granular Materials)

(d) LTPP Sand Model (Silt-Clay Materials)

Figure 3.18 Predicted Versus Measured Resilient Modulus

Figure 3.19 Falling Weight Deflectometer (FWD) Testing Equipment

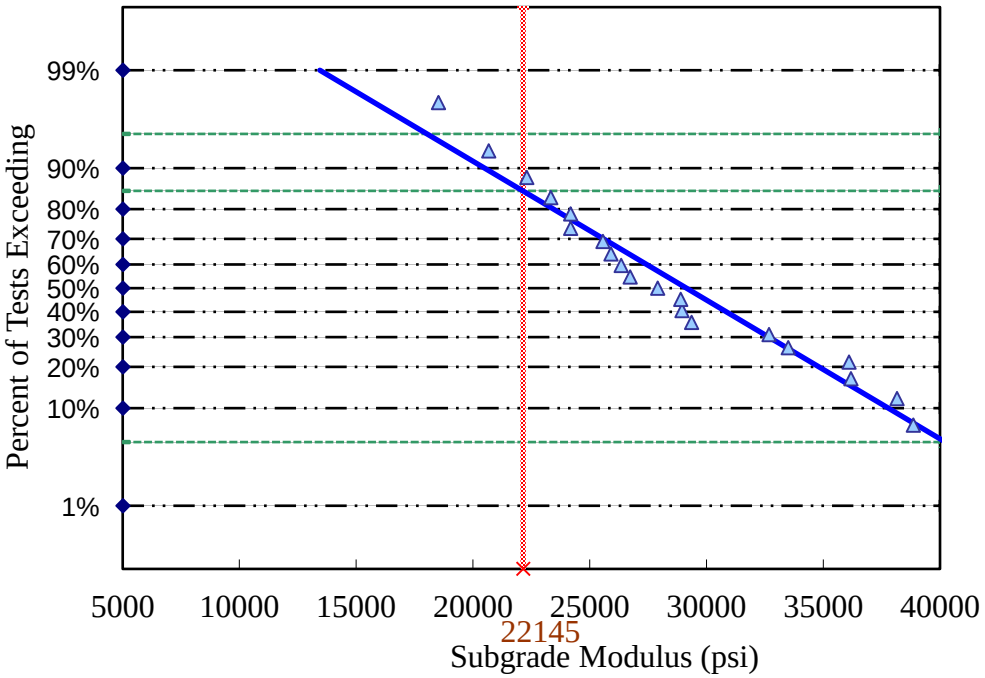

(a) Modulus Probability Chart for US-321 (Orangeburg)

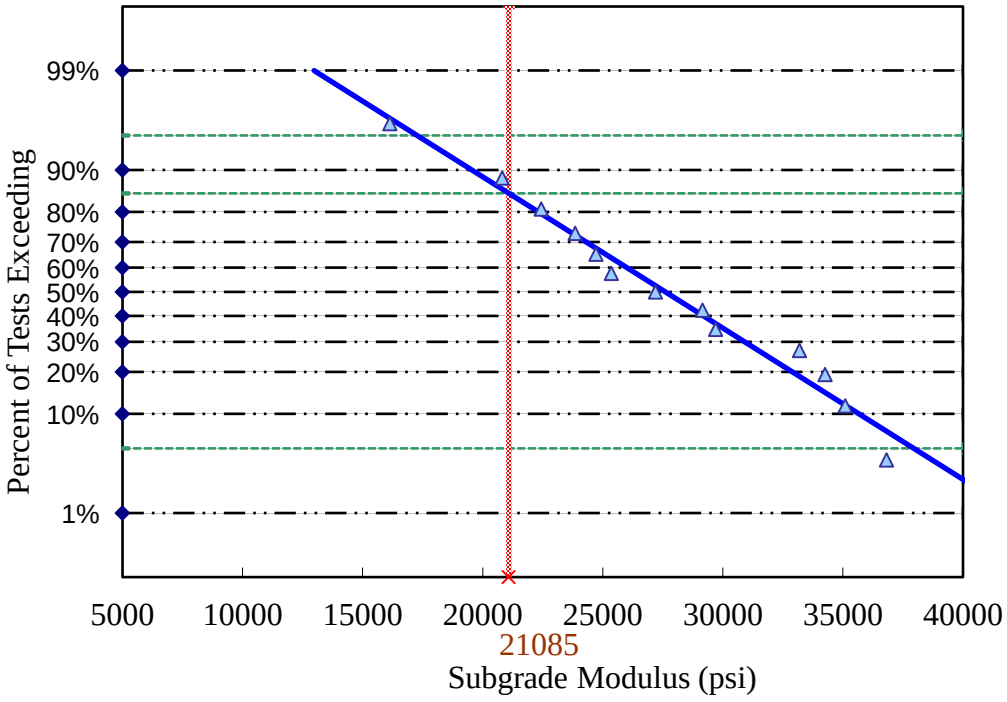

(b) Modulus Probability Chart for US-521 (Georgetown)

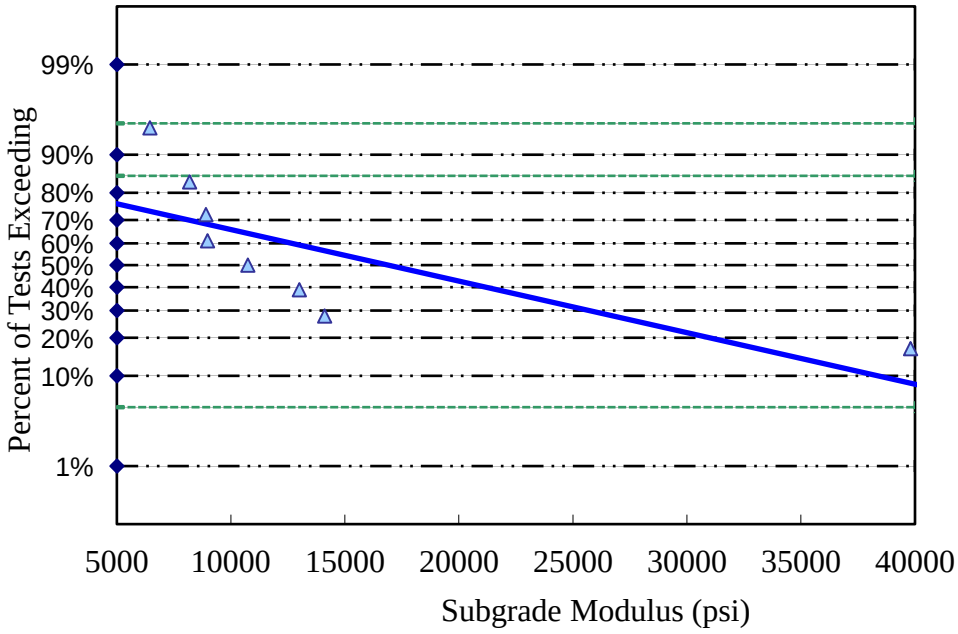

(c) Modulus Probability Chart for SC-93 (Pickens)

Figure 3.20 Modulus Probability Chart

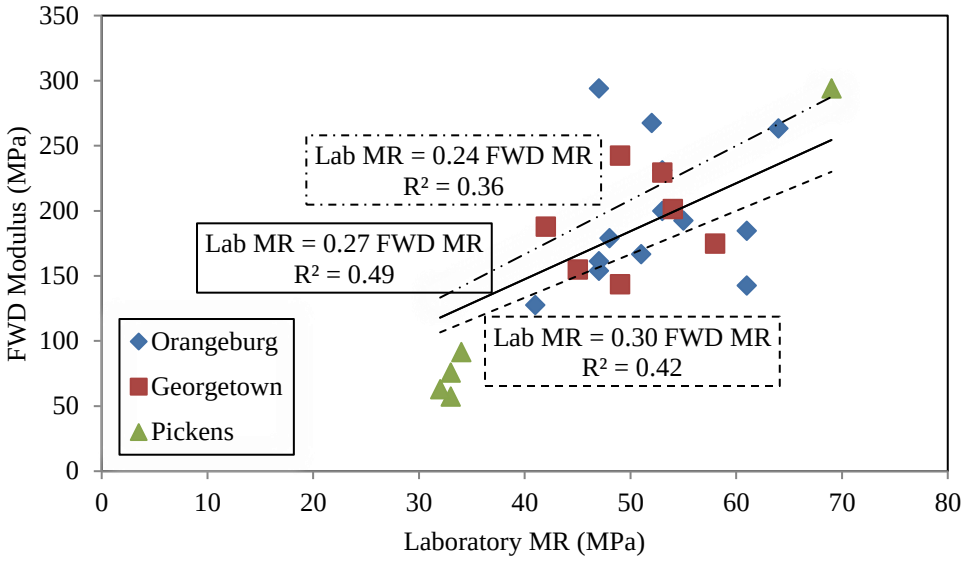

(a) Developed Model with Different Conversion Coefficients

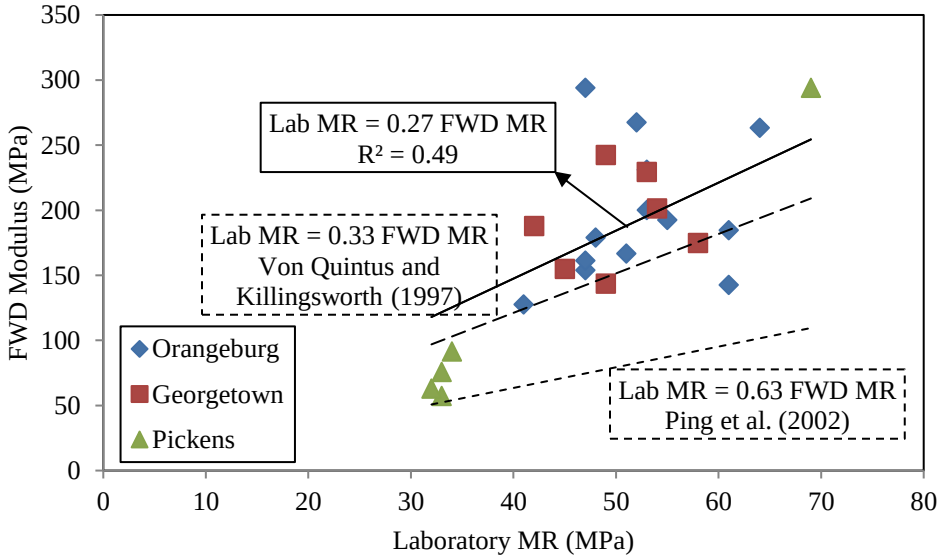

(b) Developed Model versus other Models

Figure 3.21 FWD Modulus versus Laboratory Resilient Modulus

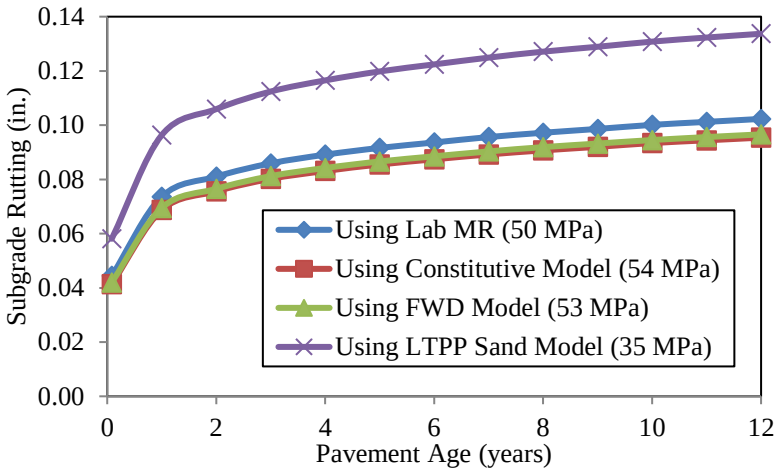

(a) Effect of Resilient Modulus (Orangeburg)

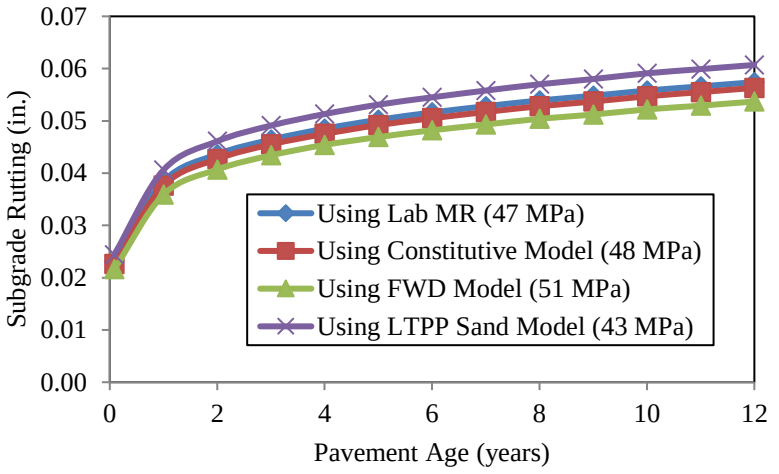

(b) Effect of Resilient Modulus (Georgetown)

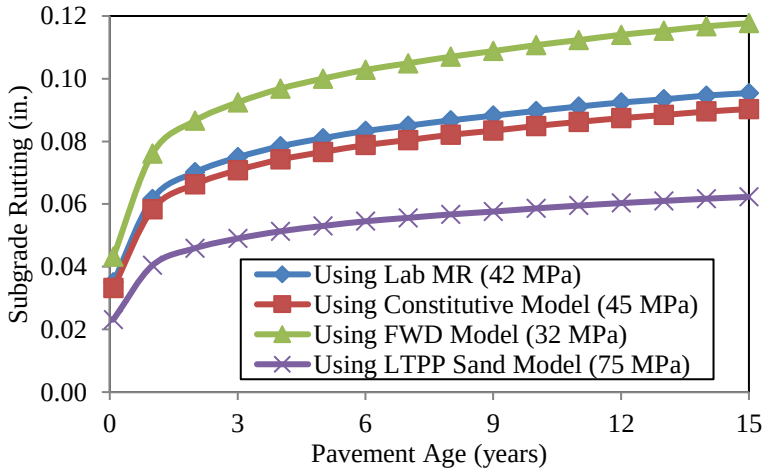

(c) Effect of Resilient Modulus (Pickens)

Figure 3.22 Effect of Resilient Modulus on Subgrade Rutting

Table 3.1 Testing Sequence for Subgrade Soil (AASHTO T 307)

Sequence No.	Confining Pressure		Max. Axial Stress		Cyclic Stress		Constant Stress		No. of Load Applications
	kPa	psi	kPa	psi	kPa	psi	kPa	psi	
0	41.4	6	27.6	4	24.8	3.6	2.8	0.4	500-1000
1	41.4	6	13.8	2	12.4	1.8	1.4	0.2	100
2	41.4	6	27.6	4	24.8	3.6	2.8	0.4	100
3	41.4	6	41.4	6	37.3	5.4	4.1	0.6	100
4	41.4	6	55.2	8	49.7	7.2	5.5	0.8	100
5	41.4	6	68.9	10	62.0	9.0	6.9	1.0	100
6	27.6	4	13.8	2	12.4	1.8	1.4	0.2	100
7	27.6	4	27.6	4	24.8	3.6	2.8	0.4	100
8	27.6	4	41.4	6	37.3	5.4	4.1	0.6	100
9	27.6	4	55.2	8	49.7	7.2	5.5	0.8	100
10	27.6	4	68.9	10	62.0	9.0	6.9	1.0	100
11	13.8	2	13.8	2	12.4	1.8	1.4	0.2	100
12	13.8	2	27.6	4	24.8	3.6	2.8	0.4	100
13	13.8	2	41.4	6	37.3	5.4	4.1	0.6	100
14	13.8	2	55.2	8	49.7	7.2	5.5	0.8	100
15	13.8	2	68.9	10	62.0	9.0	6.9	1.0	100

Note: Load sequences 14 and 15 are not to be used for material designed as Type 1

Table 3.2 Summary of Sample Collection

Site	County	Length (mi)	Boring Spacing (feet)	No. of Bore-holes	No. of Shelby Tube Samples	Bags of Bulk Soils	No. of Asphalt Cores	No. of FWD Tests
US 321	Orangeburg	6.17	1500-3000	13	37	13	13	21
US 521	Georgetown	4.07	3000	7	19	7	7	13
SC 93	Pickens	1.34	3000	5	26	5	5	9

Table 3.3 Properties of Investigated Soils

Site	No.	Passing No. 200 Sieve (%)	LL (%)	PL (%)	PI (%)	G_s	w_{opt} (%)	$\gamma_{d,max}$ (kN/ m^3)	Soil Classification	
									USCS	AASHTO
Orangeburg	1	16.5	14	13	1	2.65	9.7	18.6	SM	A-2-4
	2	21.1	18	12	6	2.61	10.3	19.9	SC-SM	A-2-4
	3	24.7	26	17	9	2.66	10.1	19.8	SC	A-2-4
	4	18.2	14	13	1	2.64	9.6	19.4	SM	A-2-4
	5	12.8	15	13	2	2.63	7.3	18.8	SM	A-2-4
	6	20.6	18	17	1	2.39	10.7	19.4	SM	A-2-4
	7	17.6	17	14	3	2.65	9.8	18.7	SM	A-2-4
	8	22.8	20	16	4	2.6	10.6	19.5	SC-SM	A-2-4
	9	24.6	22	14	8	2.61	10.2	20	SC	A-2-4
	10	26.6	24	23	1	2.66	9.9	19.6	SM	A-2-4
	11	35	26	15	11	2.61	11.8	19.2	SC	A-2-4
	12	21.4	17	13	4	2.69	9.6	19	SC-SM	A-2-4
	13	19.4	15	13	2	2.72	7.6	19.9	SM	A-2-4
Georgetown	1	1.5	NA	NA	NA	2.65	9.3	19.5	SP	A-1-b
	2	4.7	NA	NA	NA	2.68	11.9	17.7	SP	A-3
	3	4.4	NA	NA	NA	2.58	10.3	19.8	SP	A-3
	4	0.8	NA	NA	NA	2.71	12.2	17	SP	A-3
	5	1.9	NA	NA	NA	2.7	12.6	17.1	SP	A-3
	6	4.3	NA	NA	NA	2.65	10.8	17.1	SP	A-3
	7	4.5	NA	NA	NA	2.68	12.5	17.7	SP	A-3
Pickens	1	44.6	43	25	18	2.56	14	17.8	SC	A-7-6
	2	43.8	45	29	16	2.55	15.1	17.6	SM	A-7-6
	3	43.4	44	23	21	2.54	14.7	17.6	SC	A-7-6
	4	51.2	36	26	10	2.52	16.3	17.7	ML	A-4
	5	44	42	28	14	2.51	13.8	18.5	SC	A-7-6

Note: LL = liquid limit, PL = plastic limit, PI = plasticity index, G_s= specific gravity of soil, w_{opt}= optimum moisture content, $\gamma_{d,max}$= maximum dry unit weight, NA = not available.

Table 3.4 (a) Sample Description and Summary Test Results (Orangeburg)

County	Sample	H (mm)	D (mm)	H/D	γ_{Moist} (lb/ft^3)	MC (%)	M_R, BS=154.64kPa
Orangeburg	111	142	74	1.92	120	13	*
	223	157	74	2.13	129	12	44
	222	169	74	2.28	*	*	*
	221	152	74	2.07	116	10	*
	211	159	73	2.18	115	10	49
	121	154	77	1.99	104	4	61
	513	139	75	1.85	121	9	*
	512	148	75	1.96	112	8	53
	511	150	73	2.04	125	10	41
	412	156	74	2.10	120	6	48
	411	164	74	2.22	123	9	45
	313	164	73	2.23	132	9	53
	312	135	74	1.83	131	10	54
	613	161	75	2.16	123	7	46
	612	147	73	2.01	122	7	47
	713	156	76	2.06	109	6	39
	712	150	74	2.03	117	6	47
	711	148	73	2.02	108	9	36
	822	149	74	2.01	120	9	63
	821	135	74	1.82	115	10	*
	912	154	75	2.06	122	10	53
	911	162	75	2.16	122	12	*
	811	154	74	2.08	115	7	42
	812	145	76	1.92	110	6	49
	1014	170	73	2.32	122	12	60
	1013	159	73	2.17	120	12	51
	1012	157	73	2.14	127	11	67
	1011	166	73	2.27	128	9	64
	1123	157	73	2.16	117	9	72
	1122	151	72	2.09	125	11	69
	1121	142	75	1.89	122	13	*
	1111	164	72	2.29	113	9	51
	1221	128	76	1.68	113	8	50
	1212	129	75	1.71	118	8	48
	1211	139	75	1.86	120	9	57
	1312	135	75	1.80	114	6	60
	1321	147	74	1.99	116	7	56
	1311	145	75	1.94	114	6	49

Note: *Sample was broken before testing

Table 3.4 (b) Sample Description and Summary Test Results (Georgetown)

County	Sample	H (mm)	D (mm)	H/D	γ_{Moist} (lb/ft^3)	MC (%)	M_R, BS=154.64kPa
Georgetown	114	164	73	2.24	132	12	64
	113	156	73	2.12	128	13	57
	112	145	76	1.92	117	11	45
	111	142	74	1.92	120	10	47
	223	150	74	2.02	124	11	36
	222	155	74	2.10	125	9	55
	221	150	73	2.04	124	11	48
	211	151	73	2.07	130	13	39
	322	132	73	1.81	115	7	39
	321	138	73	1.88	127	10	62
	311	158	73	2.15	127	10	63
	421	143	76	1.88	118	22	*
	411	141	74	1.89	113	8	49
	513	145	77	1.89	111	9	43
	512	137	77	1.78	110	8	62
	511	142	76	1.86	111	8	44
	613	143	76	1.88	110	11	52
	611	131	75	1.74	109	7	64
	722	149	74	2.03	112	10	34
	721	150	73	2.04	116	10	49

Note: *Sample was broken before testing

Table 3.4 (c) Sample Description and Summary Test Results (Pickens)

County	Sample	H (mm)	D (mm)	H/D	γ_{Moist} (lb/ft^3)	MC (%)	M_R, BS=154.64kPa
Pickens	311	163	73	2.23	112	17	34
	312	161	73	2.20	117	20	23
	313	167	73	2.28	109	18	37
	314	169	73	2.31	105	15	34
	215	164	73	2.24	107	16	42
	214	154	74	2.07	99	23	31
	213	164	73	2.25	109	17	34
	212	161	73	2.20	104	19	28
	211	164	73	2.24	106	18	30
	115	165	73	2.26	124	16	44
	114	162	73	2.21	115	21	18
	113	165	73	2.25	105	24	36
	112	158	73	2.16	113	20	38
	111	163	74	2.21	105	16	33
	512	135	73	1.84	128	16	40
	511	152	73	2.07	126	16	37
	525	161	73	2.20	116	26	38
	524	163	73	2.22	122	18	37
	523	163	73	2.25	124	18	27
	522	160	73	2.18	128	17	26
	521	151	73	2.05	124	20	23
	415	166	73	2.28	133	15	60
	414	159	73	2.17	125	15	54
	413	162	74	2.20	119	17	61
	412	160	73	2.19	124	18	88
	411	169	73	2.31	129	17	81

Table 3.5 (a) Variation of Soil Type Along Section (Orangeburg)

Borehole No.	Cut/ Fill	Soil Type	Average M_R (MPa)	Relative Compaction (%)
1	Cut	SM (A-2-4)	61	88
2	Fill	SC-SM (A-2-4)	47	85
3	Cut	SC (A-2-4)	54	95
4	Cut	SM (A-2-4)	47	92
5	Fill	SM (A-2-4)	47	91
6	Cut	SM (A-2-4)	47	93
7	Fill	SM (A-2-4)	41	88
8	Fill	SC-SM (A-2-4)	51	86
9	Fill	SC (A-2-4)	53	87
10	Cut	SM (A-2-4)	61	90
11	Cut	SC (A-2-4)	64	89
12	Cut	SC-SM (A-2-4)	52	89
13	Cut	SM (A-2-4)	55	85

Table 3.5 (b) Variation of Soil Type Along Section (Georgetown)

Borehole No.	Cut/ Fill	Soil Type	Average M_R (MPa)	Relative Compaction (%)
1	Fill	SP (A-1-b)	53	90
2	Fill	SP (A-3)	45	100
3	Fill	SP (A-3)	55	89
4	Fill	SP (A-3)	49	93
5	Fill	SP (A-3)	50	94
6	Fill	SP (A-3)	58	92
7	Cut	SP (A-3)	42	92

Table 3.5 (c) Variation of Soil Type Along Section (Pickens)

Borehole No.	Cut/ Fill	Soil Type	Average M_R (MPa)	Relative Compaction (%)
1	Fill	SC (A-7-6)	34	83
2	Fill	SM (A-7-6)	33	79
3	Fill	SC (A-7-6)	32	84
4	Fill	ML (A-4)	69	96
5	Fill	SC (A-7-6)	33	89

Table 3.6 (a) Model Parameters for US-321 (Orangeburg)

County	Sample	k_1	k_2	k_3	R^2
Orangeburg	121	521	0.5815	-0.4697	0.99
	211	366	0.0153	1.5230	0.39
	221	228	0.7665	1.7602	0.68
	223	210	0.3742	2.6134	0.88
	312	423	0.3983	0.3155	0.69
	313	474	0.5545	-0.7247	0.95
	411	301	0.4231	1.1437	0.83
	412	295	0.8643	0.5415	0.93
	511	226	1.0940	0.6946	0.87
	512	374	0.5943	0.4530	0.84
	612	239	0.7979	1.7598	0.87
	613	169	0.2916	4.4158	0.91
	711	214	0.9368	0.5674	0.94
	712	288	0.4356	1.4698	0.88
	713	203	1.0389	1.0715	0.82
	811	188	0.4284	3.2315	0.83
	812	332	0.9900	-0.1844	0.94
	822	599	0.6676	-1.2901	0.99
	912	437	0.7035	-0.5806	0.97
	1011	414	0.2389	1.7091	0.64
	1012	539	0.6703	-0.3943	0.82
	1013	341	0.2068	1.5598	0.63
	1014	430	0.8750	-0.3099	0.92
	1111	263	0.8419	-0.1828	0.82
	1122	704	0.7032	-1.7826	0.98
	1123	624	0.6117	-0.6808	0.95
	1211	458	0.6821	-0.4018	0.99
	1212	383	0.3870	0.2243	0.93
	1221	402	0.8087	-0.7142	0.97
	1311	377	0.8294	-0.4701	0.99
	1312	501	0.4811	-0.1593	0.99
	1321	491	0.5862	-0.6179	0.99

Table 3.6 (b) Model Parameters for US-521 (Georgetown)

County	Sample	k_1	k_2	k_3	R^2
Georgetown	111	392	0.4136	-0.0870	0.79
	112	337	0.3222	0.7625	0.79
	113	487	0.3113	0.0333	0.53
	114	543	0.6788	-0.7112	0.93
	211	256	0.1433	1.7622	0.86
	221	391	0.7856	-0.7849	0.90
	222	553	0.3476	-0.8293	0.86
	223	183	0.7132	1.8977	0.74
	311	635	0.5696	-1.4083	0.98
	321	618	0.4955	-1.1701	0.96
	322	319	0.4635	-0.0896	0.80
	411	353	0.2666	1.0594	0.49
	511	208	0.4990	2.5897	0.79
	512	446	0.8075	-0.1503	0.99
	513	247	0.4523	1.6902	0.77
	611	484	0.7143	-0.2119	0.99
	613	413	0.2853	0.5394	0.68
	721	332	0.0425	1.8625	0.87
	722	129	0.1933	4.5193	0.76

Table 3.6 (c) Model Parameters for SC-93 (Pickens)

County	Sample	k_1	k_2	k_3	R^2
Pickens	111	323	0.7742	-1.6326	0.98
	112	386	0.3598	-0.8676	0.54
	113	313	0.2994	0.0406	0.43
	114	162	0.6043	-0.8476	0.80
	115	417	0.6279	-1.0916	0.86
	211	349	0.6788	-2.1792	0.94
	212	232	0.4578	-0.0576	0.75
	213	300	0.4220	-0.3387	0.60
	214	344	0.7413	-2.0678	0.96
	215	444	0.6306	-1.6429	0.95
	311	295	0.2736	0.0263	0.51
	312	145	0.5578	0.8150	0.81
	313	403	0.7879	-2.0498	0.93
	314	338	0.7418	-1.5104	0.94
	411	825	0.5795	-1.4574	0.82
	412	911	0.4199	-1.1576	0.95
	413	623	0.1779	-0.5906	0.37
	414	567	-0.0271	-0.2383	0.05
	415	886	0.4912	-2.9989	0.96
	511	395	0.7726	-1.7618	0.87
	512	474	0.2371	-1.3406	0.53
	521	227	0.5753	-1.0861	0.79
	522	222	0.4876	-0.2695	0.58
	523	278	0.3417	-0.7560	0.45
	524	427	0.4721	-1.6531	0.78
	525	434	0.3985	-1.4768	0.67

Table 3.7 Developed Constitutive Models of Coefficients for South Carolina

AASHTO Soil Type	Models	R^2	F Value
Granular	$k_1 = -12181.026^{***} + 130.194{P_4}^{***} - 4.322Sand^{*} - 2.096w_{opt} - 8.443(\frac{w}{w_{opt}} \times \frac{\gamma_d}{\gamma_{d,max}})$	0.23	3.49*
	$k_2 = -11.581 + 0.123P_4 + .023Silt^{**} - 0.014w_{opt} - 0.078(\frac{w}{w_{opt}} \times \frac{\gamma_d}{\gamma_{d,max}})$	0.21	3.05*
	$k_3 = 116.825^{***} - 1.176{P_4}^{***} + 0.242w_{opt} - 0.141\gamma_d + 0.783(\frac{w}{w_{opt}} \times \frac{\gamma_d}{\gamma_{d,max}})$	0.28	4.41**
Silt-Clay	$k_1 = 2016.479^{***} - 77.095PI^{***} + 938.699LI^{***} + 1593.47\left(\frac{\gamma_d}{\gamma_{d,max}}\right)^{***} - 1160.430(\frac{w}{w_{opt}} \times \frac{\gamma_d}{\gamma_{d,max}})^{***}$	0.81	21.95***
	$k_2 = -0.563 + 0.073PL^{*} + 1.024LI^{**} - 0.075(w - w_{opt})^{*}$	0.33	3.55*
	$k_3 = 6.726 - 0.158PL - 1.046LI - 0.264\gamma_{d,max}$-$0.140(w - w_{opt})$	0.11	0.63

*$p < 0.05$; **$p < 0.01$; ***$p < 0.001$

CHAPTER 4

EFFECT OF SUBGRADE SOIL MOISTURE CONTENT ON RESILIENT MODULUS AND PAVEMENT RUTTING[1]

[1]Adapted from Rahman, M. M., and S. L. Gassman. Submitted to *Transportation Research Record: Journal of Transportation Research Board*

4.1 GENERAL

Pavement rutting depends largely on subgrade soil stiffness, which is a function of the in-situ moisture content and soil index properties. The subgrade soil moisture content may vary from the specified condition due to variations in the compaction procedure during construction and fluctuations in the ground water table from seasonal changes. The resilient modulus (M_R) is used to define the subgrade soil stiffness, and is one of the most important material inputs for the Mechanistic-Empirical (M-E) pavement design method. M_R is typically determined by conducting cyclic triaxial tests. These tests can be complex and time consuming to perform; therefore, correlations between M_R and other stiffness parameters and index properties that are easier to obtain are often utilized. In this study, California Bearing Ratio (CBR) tests and laboratory M_R tests were performed on remolded samples of soils collected from different regions in South Carolina. The samples were prepared at moisture contents above and below the optimum moisture content (w_{opt}). Correlations between the results from the two tests were developed as a function of moisture content and statistical models were developed to correlate generalized constitutive M_R model parameters with soil index properties. Furthermore, pavement rutting was studied using the resilient modulus determined for the subgrade soils compacted at w_{opt} and $\pm 2\% w_{opt}$. Statistical analysis showed that soil moisture content and density played an important role for the subgrade soil M_R. A slight change in moisture content during compaction has a significant effect on pavement rutting. The peak value of both CBR and M_R was found on the dry side of optimum and at a dry density less than the maximum. It is also found that the subgrade soil moisture condition has a significant influence on subgrade rutting if graded aggregate base is used. However, if a higher

strength base layer is used (i.e., cement stabilized base or asphalt treated aggregate base), the effect of the moisture content is less significant.

4.2 INTRODUCTION

Rutting is categorized as a structural distress that affects the riding quality and structural health of flexible pavements. It is considered to be a major failure mode that can cause structural failure of the pavement. Traffic conditions (Zaghloul et al., 2006; Jadoun and Kim, 2012), climate conditions (Zaghloul et al., 2006; Johanneck and Kazanovich, 2010; Zapata et al. 2007) and the pavement and subgrade materials (Singh et al., 2011; Saxena et al., 2010; Xu et al., 2013; Hossain et al., 2011; Wu et al., 2012; Graves and Mahboub 2006) all have a significant influence on the structural life of a pavement.

The Mechanistic Empirical Pavement Design Guide (MEDPG) (AASHTO, 2008) is the latest pavement design method which accounts for material behavior, in-situ materials, new materials, climate, and changing load types. MEPDG makes forecasts of various distresses (i.e., pavement rutting, roughness) over the design life of the pavement based on the proposed pavement structure, material characteristics, traffic inputs and climate conditions. The resilient modulus, $M_{R,}$ of subgrade soil has been found to have the largest effect on rutting predicted using MEPDG (Orobio and Zaniewski, 2011), and thus is one of the most important material inputs for the MEPDG.

The M_R of subgrade soil can be found directly in the laboratory using a cyclic triaxial test; however, the test is complex, time-consuming and expensive to perform. Therefore, correlations of M_R to other stiffness parameters and index properties that are easier to obtain are often utilized. These include correlations to the pavement resilient modulus found using the Falling Weight Deflectometer (FWD) (e.g. Nazzal and

Mohammad (2010), Flintsch et al. (2003), and Ksaibati et al. (2000)) and correlations to the dynamic cone penetrometer (Chen et al., 2001) and California Bearing Ratio (CBR) (Heukelom, 1962; George, 2004; Garg and Larkin, 2009). Correlations between soil index properties and M_R tests have been developed by Mohammad et al. (1999), Yau and Quintos (2004), Malla and Joshi (2007), Zhou et al. (2014) and Titi et al. (2015). Titi et al. (2015) developed correlations between soil physical properties and M_R constitutive model parameters for fine-grained soils using a regression analysis technique and Baig and Nazarian (1995) determined subgrade M_R using bender elements in the laboratory.

All of the previous studies correlated the subgrade M_R to other test results for a specified subgrade condition (i.e., optimum moisture condition and maximum dry density), rather than for a range of moisture conditions and dry densities with exception of the studies by Mohammad et al. (1999) and Zhou et al. (2014). Mohammad et al. (1999) developed correlations between the resilient modulus model parameters with soil properties and CBR for a range of moisture contents for eight different soils of Louisiana. However, they have not studied the effects of subgrade moisture variations on pavement performance. Zhou et al. (2014) on the other hand, studied soil resilient modulus and the effect of seasonal variation on pavement rutting for MEPDG. In that study, the M_R coefficients were obtained at different post-compaction water contents, to allow the estimation of pavement response under seasonal moisture variation of subgrade. However, the soil type they considered for their study was AASHTO silt-clay materials (more than 35% passing no. 200). Therefore, it is important to study on correlation of subgrade M_R with alternate test results (i.e., CBR) and soil index properties for a range of moisture content for both silt-clay materials and granular materials (35% or less passing no. 200).

Moisture variation and soil index properties play an important role on subgrade soil stiffness (e.g. Khoury and Zaman, 2004; Yau and Quintos, 2004; and Titi et al. 2015). Due to variations during construction, and fluctuations in the ground water table due to seasonal changes, the subgrade soil moisture content might vary from the specified condition. Khoury and Zaman (2004) evaluated the variation of M_R with post-compaction moisture content and suction and found that moisture content has significant influence on subgrade M_R. Correlations between physical properties and repeated load resilient modulus tests have been developed for unbound materials and soils within the Long-Term Pavement Performance (LTPP) program by Yau and Quintus (2004). In addition, Titi et al. (2015) developed correlations between soil index properties and M_R constitutive model parameters using regression analysis techniques.

Pavement material characteristics for different pavement layers are prone to change with different temperature and moisture content; therefore, several studies have been performed to determine the seasonal variation of the subgrade M_R (Ceratti, 2004; Khoury and Zaman, 2004; Heydinger, 2003; and Guan et al., 1998). In South Carolina, limited data on the seasonal variation of subgrade strength was obtained by Chu (1972). In that study, field tests were performed at select sites in South Carolina to examine subgrade moisture variations under existing pavements. The study recommended a complete moisture variation study below South Carolina pavements in connection with pavement performance and design. Ceratti (2004) performed both laboratory tests and in situ tests to determine the seasonal variation of subgrade soil M_R in Southern Brazil. Laboratory testing was carried out to establish the relationship between water content and soil suction. They quantified the effects of moisture content and soil suction on resilient modulus and found

an increase in moisture content above optimum results in decreasing resilient modulus. However, the resilient modulus results obtained for specimens submitted to a dry side were close to those of specimens tested at w_{opt}. A relation between M_R, moisture variation and soil suction for subgrade soils was developed by Khoury and Zaman (2004). Their study concluded that changes in M_R values due to drying are influenced by the initial moisture content of specimen. For given water content, the M_R values are higher for a drying cycle than for a wetting cycle. Heydinger (1998) evaluated the seasonal variation of subgrade soil for Ohio as part of LTPP instrumentation project seasonal monitoring program (SMP). They found that the subgrade M_R varies seasonally because of changes in moisture content. Resilient modulus decreases with increases in moisture content.

The effects of moisture variation of subgrade resilient modulus on pavement performance for MEPDG were studied on few previous literatures. Soil resilient modulus regressed from physical properties and influence of seasonal variation on pavement performance was studied by Zhou et al. (2014). Rutting and roughness of two typical pavement sections were analyzed to investigate the effect of the seasonal variation of soil resilient modulus on pavement performance. Results showed that moisture variation has a significant influence on subgrade resilient modulus and, subsequently, on pavement performance. They observed when the moisture in subgrade is higher than the optimum through a whole year, the seasonal variation of subgrade M_R due to the moisture change increased the longitudinal tensile strain at the bottom of the asphalt layers and comprehensive strain on the subgrade surface, resulting in increased rutting depth in the subgrade and decreased fatigue life of flexible pavements. The influence of compaction moisture content applied on the measured permanent deformation was addressed by

Puppala et al. (2009). They also performed validation studies to address the adequacy of the formulated model to predict rutting or permanent strains in soils. They found soil samples compacted on the wet side of w_{opt} experienced higher permanent strain potentials than those compacted dry side of w_{opt} and at w_{opt}.

Above literatures indicate that limited studies have been performed to develop correlations between resilient modulus and soil index properties and alternate stiffness test parameters (i.e., CBR) for a range of moisture contents. Furthermore, only a few studies have been performed to study the effects of moisture variation of subgrade resilient modulus on pavement rutting. Therefore, the purpose of this study is to perform repeated load laboratory M_R tests, CBR tests, and soil index property tests on subgrade soils from different regions in South Carolina. The different test results are compared and correlations are developed to predict resilient modulus and subsequent pavement rutting for moisture content at, above and below the w_{opt} using MEPDG.

4.3 BACKGROUND

4.3.1 Laboratory Resilient Modulus

Resilient modulus represents the stiffness of the pavement unbound layer subjected to repeated traffic loading. Resilient modulus is defined as the ratio of the repeated maximum axial cyclic stress to the resultant recoverable or resilient axial strain.

$$M_r = \frac{\sigma_{cyclic}}{\varepsilon_r} \qquad 4.1$$

where, σ_{cyclic} is the maximum axial cyclic stress and ε_r is the recoverable strain due to σ_{cyclic}.

In the laboratory, resilient modulus is determined by performing a repeated load triaxial compression test. In the test, a repeated axial cyclic stress of fixed magnitude, load

duration, and cycle duration is applied to a cylindrical test specimen. During testing, the specimen is subjected to a dynamic cyclic stress and a static-confining pressure provided by means of a triaxial pressure chamber. The total resilient or recoverable axial deformation response of the specimen is measured and used to calculate the resilient modulus (AASHTO, 2003). The current protocol to determine the resilient modulus of soil and aggregate material is AASHTO T 307. According to this test protocol, a haversine-shaped loading waveform is repeatedly applied on top of a cylindrical specimen under confining pressure.

Different models were developed to correlate resilient modulus with stresses and fundamental soil properties. The generalized constitutive resilient modulus model is the most widely used M_R model, which can also be used for all types of subgrade materials. The general constitutive resilient modulus model selected for implementation in the MEPDG was developed through the National Cooperative Highway Research Program (NCHRP) project 1-28A as follows.

$$M_R = k_1 P_a \left[\frac{\sigma_b}{P_a}\right]^{k_2} \left[\frac{\tau_{oct}}{P_a} + 1\right]^{k_3} \quad 4.2$$

where P_a is atmospheric pressure (101.325 kPa), σ_b is the bulk stress = $\sigma_1 + \sigma_2 + \sigma_3$, σ_1 is the major principal stress, σ_2 is the intermediate principal stress and is equal to σ_3 for axisymmetric conditions (i.e., triaxial test), σ_3 is the minor principal stress (or confining pressure in the repeated load triaxial test), τ_{oct} is the octahedral shear stress, and k_1, k_2 and k_3 are the model parameters/material constants.

4.3.2 Laboratory Resilient Modulus with California Bearing Ratio

California Bearing Ratio (CBR) is a penetration test used for the evaluation of mechanical strength of unbound pavement layers. The test is performed by penetrating a standardized piston at a standard rate into a compacted soil specimen confined in a cylindrical mold. The general function between CBR and M_R proposed by the AASHTO design guide for fine-grained soils is (AASHTO, 2008):

$$M_R = 1500 \times CBR \qquad 4.3$$

The data used for developing this equation ranged from 750 to 3000 times CBR (Heukelom 1962). This correlation appears to be effective for CBR values less than 20 which restricts the use of this equation for designing pavement (Coleri 2007). However, this equation has been extensively used by design agencies and researchers for fine grained soils with a soaked CBR of 10 or less (George, 2004).

The Georgia Department of Transportation developed the following relation between resilient modulus and CBR value for cohesionless soil (Webb and Campbell, 1986):

$$M_R(psi) = 3116 \times CBR^a \qquad 4.4$$

where a = 0.4779707

Garg and Larkin (2009) summarized a comparative subgrade evaluation using CBR, vane shear, light weight deflectometer, and resilient modulus tests. They studied only low CBR (less than 15) values and one soil type (a CH soil known as DuPont Clay). They recommended more testing on different soil types (clays, silts, and sands) for reaching significant conclusions.

The model used in the MEPDG for estimating M_R from CBR for all types of soil is

$$M_R(psi) = 2555 \times CBR^{0.64} \quad (4.5)$$

For indirect relationships, the material property is first related to CBR and then CBR is related to M_R (AASHTO, 2008). Note that the studies by Coleri (2007) on the estimation of M_R from CBR test results showed that the reliability of prediction models are not statistically satisfactory which is due to the structural differences and stress states between these two tests.

4.3.3 Resilient Modulus with Subgrade Rutting

Rutting is the pavement surface depression in the wheel paths and is caused by the permanent deformation of the asphalt layers, unbound layers, and foundation soil. It originates from the lateral movement of pavement material due to repeated traffic loading. The approach used in the MEPDG to calculate total rut depth is based upon calculating cumulative distortion or rutting within each sub-layer. MEPDG (AASHTO 2008) uses the following equation to calculate total rutting:

$$RD = \sum_{i=1}^{n} \varepsilon_{p(i)} h_i \quad (4.6)$$

where RD = total rut depth, i = sub-layer number, n = total number of sub-layers, $\varepsilon_{p(i)}$ = plastic strain in sub-layer i, and h_i = thickness of sub-layer i. The MEPDG permanent deformation model for unbound base and subgrade layers is

$$\Delta_{p(soil)} = \beta_{s_1} k_{s_1} \varepsilon_v h_{soil} \left(\frac{\varepsilon_0}{\varepsilon_r}\right) \left(e^{-\left(\frac{\rho}{N}\right)^{\beta}}\right) \quad (4.7)$$

where $\Delta_{p(soil)}$ = Permanent or plastic deformation for the unbound layer, in.,

N = Number of axle-load repetitions,

ε_0 = Intercept determined from laboratory repeated load permanents deformation test, in./in.

ε_r = Resilient strain imposed in laboratory test to obtain material properties ε_0, ε, and ρ, in./in.,

ε_v = Average vertical strain, in./in.,

h_{soil} = Thickness of the unbound layer, in.,

k_{s_1} = Global calibration coefficients; $k_{s_1} = 1.673$ for granular materials and 1.35 for fine grained materials, and

β_{s_1} = Local calibration constant for the rutting in the unbound layers ($\beta_{s_1} = \beta_B$ for unbound base; and $\beta_{s_1} = \beta_{SG}$ for subgrade material).

$$Log\beta = -0.61119 - 0.017638(W_c)$$

$$\rho = 10^9\left(\frac{C_0}{(1-(10^9)^{\beta})}\right)^{\frac{1}{\beta}}$$

$$C_0 = ln\left(\frac{a_1 M_r^{b_1}}{a_9 M_r^{b_9}}\right)=0.0075$$

Where, $a_{1,9}$, $b_{1,9}$= regression constants, M_r= resilient modulus of the unbound layer, psi, and W_c = water content, %.

4.4 RESEARCH OBJECTIVE

The objectives of the current study are to:

- Perform CBR tests on soils collected from different regions of South Carolina (US-321 from Orangeburg County, US-521 from Georgetown County, and SC-93 from Pickens County) remolded at different moisture contents and densities.
- Perform laboratory cyclic triaxial tests to determine the resilient modulus of the subgrade soils at different moisture contents above and below the w_{opt} and develop relations between CBR and resilient modulus.

- Establish model parameters for the generalized constitutive resilient modulus model for South Carolina to use in MEPDG. Develop statistical models between soil index properties and the resilient modulus model parameters for remolded soil.
- Study the effect of subgrade soil moisture content on pavement rutting using MEPDG.

4.5 METHODOLOGY

Three pavement sections were selected to represent different soil regions above and below the fall line as shown in Figure 4.1. The selected pavement sections are a 6.17 mi pavement section on US-321 in Orangeburg County (Coastal Plain, near the fall line), a 4.07 mi pavement section on US-521 in Georgetown County (Coastal Plain), and a 1.34 mi pavement section on SC-93 in Pickens County (Upstate Area). Photographs of the field sample collection and laboratory testing are shown in Figure 4.2. Asphalt cores that were 6 in. diameter and spaced at intervals of 1500 to 3000 ft were made at the center of the right lane (Figure 4.2(a)). Bulk samples of the subgrade soil were collected from adjacent holes (Figure 4.2(b)). There were 13 boreholes along US-321, 7 boreholes on US-521 and 5 boreholes on SC-93. Around 50 lbs of bulk soil was collected from each borehole for laboratory index tests, CBR tests, and M_R tests.

The laboratory index tests included grain size analysis (ASTM D 6913/AASHTO T 311), Atterberg Limits (ASTM D 4318/AASHTO T 90), specific gravity (ASTM D 854/ AASHTO T 100), maximum dry density and optimum moisture content (w_{opt}) (ASTM D 698/AASHTO T 99), and moisture content tests (ASTM D 2216/AASHTO T 265). Soils were classified according to USCS (ASTM D 2488) and AASHTO (AASHTO M 145).

Relationships between density and moisture content were developed by compacting the soil in a standard Proctor mold (4 in. diameter and 4.584 in. height of the sample, compacted in 3 layers, 25 blows per layer) per ASTM D 698/AASHTO T 99 and also by compacting the soil in a CBR mold (6 in. diameter and 5 in. height of the sample, compacted in 3 layers, 56 blows per layer). A standard Proctor hammer was used to compact the soil in both molds (ASTM D 698/AASHTO T 99).

CBR tests were performed in accordance with AASHTO T 193 (AASHTO, 2003). Specimens were prepared at moisture contents of w_{opt}, ±4%w_{opt}, ±2%w_{opt}, and others as needed to define the relation between CBR and MC. The soil was compacted in a 6 in. by 5 in. CBR mold using three layers, 56 blows per layer, and the standard Proctor hammer. CBR values were calculated as the ratio of load needed for 0.1 in. penetration of a circular spindle of 3 in^2 in area to 3000 lb load or for 0.2 in. penetration to 4500 lb load. The CBR is generally selected at 0.10 in. penetration; however, if the ratio at 0.2 in. penetration is greater, the test shall be rerun. If the check test shows similar result, the ratio at 0.20 in. penetration shall be used (AASHTO T 193). Figure 4.2(c) and Figure 4.2(d) show the specimen preparation and CBR tests respectively.

M_R tests were performed in accordance with AASHTO T 307 using a GDS Advanced Dynamic Triaxial Testing System (Figure 4.2(f)). Specimens were fabricated by compacting the soil in a CBR mold (6 in. diameter and 7 in. height (without the disk spacer), compacted in 4 layers, 65 blows per layer) at moisture contents of ±2% w_{opt} and w_{opt}. Once the soil was compacted in the CBR mold, a 3 in. diameter Shelby tube was pushed into the soil (Figure 4.2(e)) to collect a 3 in. x 6 in. cylindrical specimen. The specimen was then extruded and inserted into a rubber membrane. Directly following

specimen preparation, the specimen was subjected to a static confining pressure, and a repeated axial cyclic stress of fixed magnitude, load duration, and cycle duration was applied. The total recoverable axial deformation response of the specimen was measured and used to calculate the M_R.

4.6 RESULTS AND ANALYSIS

4.6.1 Index Test Results

The properties of the investigated soils are shown in Table 4.1. The samples listed represent one sample for each of the 8 different soil classifications (considering both USCS and AASHTO) found at the pavement sites. Orangeburg soils were classified as A-2-4 (silty or clayey sand) according to AASHTO M 145 and SC (clayey sand), SM (silty sand), and SC-SM (sandy silty clay) according to ASTM D 2488. Georgetown soils were classified as A-1-b and A-3 (non-plastic fine sand) and SP (poorly graded sand). Pickens soils were classified as A-7-6 (mostly clayey soils) and A-4 (mostly silty soils), and SC (clayey sand) and SM (silt) and ML (silt).

4.6.2 Moisture Density Relations

Prior to performing the CBR tests, the maximum dry density ($\gamma_{d,max}$) and optimum moisture content (w_{opt}) were determined for each soil in accordance with ASTM D 698 and AASHTO T 99, respectively (see Table 4.1). Relationships between density and moisture content developed for specimens compacted in a standard Proctor mold and a CBR mold are shown in Figure 4.3.

Figure 4.3(a), Figure 4.3(b), and Figure 4.3(c) show the results for Orangeburg B-3 (SC/A-2-4), Orangeburg B-6 (SM/A-2-4), and Orangeburg B-8 (SC-SM/A-2-4) respectively. It is found that samples compacted in the CBR molds showed a maximum

dry density around 125 lb/ft^3 at an w_{opt} around 10.1%-10.7% for all three samples which is close to the maximum dry density for samples compacted in the Proctor mold. The similar moisture density relations for all three Orangeburg borehole locations were expected because the soils were all classified according to AASHTO as A-2-4 and had similar USCS classifications (SC, SM and SC-SM). SC (B-3), SC-SM (B-8), and SM (B-6) soils showed w_{opt} of 10.1%, 10.6%, and 10.7% respectively.

Figure 4.3(d) and Figure 4.3(e) show the results for Georgetown B-1 (SP/A-1-b) and Georgetown B-4 (SP/A-3), respectively. Like the Orangeburg soil, the Georgetown samples compacted in the CBR molds had a maximum dry density close to that of the samples compacted in the Proctor mold. The maximum dry density was found to be around 125 lb/ft^3 at a w_{opt} around 9.3% for B-1 and 110 lb/ft^3 at an w_{opt} around 12.2% for B-4. Note that although both soils are classified as SP or poorly graded sand (USCS), the A-3 soil (AASHTO) (B-4) in Figure 4.3(e) showed less response to water (a flatter moisture density curve) compared to the A-1-b soil (B-1) in Figure 4.3(d).

Figure 4.3(f), Figure 4.3(g), and Figure 4.3(h) show the results for Pickens B-2 (SM/A-7-6), Pickens B-4 (ML/A-4), and Pickens B-5 (SC/A-7-6), respectively. For each of these 3 boreholes, the maximum dry density was found to be 112 lb/ft^3, 105 lb/ft^3, and 117 lb/ft^3, at w_{opt} of 15%, 16%, and 14%, respectively for both the CBR and Proctor molds.

Shelby tube samples collected from the field were used to measure the field moisture content and dry density. These results are also shown in Figure 4.3. The water contents of the field samples were found within a 1.5% to 5% range on both the dry and wet sides of w_{opt} (i.e., MC = 9.0% to 10.2%, w_{opt} = 10.1% for Orangeburg B-3 (Fig 4.3a) and MC = 15.5% to 19.7%, w_{opt} = 13.8% for Pickens B-5 (Fig 4.3h)). The dry unit weights

for the field samples were 3% to 22% less than the standard Proctor dry density, except for the Pickens B-4 (ML/A-4) field samples which were 4% lower to 9% higher than the maximum dry density obtained from the standard Proctor test.

4.6.3 CBR Test Results

The CBR results found for penetration depths of 0.1 in. and 0.2 in. over a range of moisture contents for the 8 different soil types are shown in Figure 4.4. For all 8 soils, the relationships between CBR and moisture content show a distinct peak similar to the moisture-density relation found from a standard Proctor compaction test (i.e., Figure 4.3). For a penetration of 0.1 in., the peak CBR values were found to be 25, 18, and 28 for Orangeburg B-3, B-6, and B-8, respectively; 31 and 17 for Georgetown B-1 and B-4, respectively; and 16, 18, and 21 for Pickens B-2, B-4, and B-5, respectively. The peak CBR for a penetration of 0.20 in. was found to be 8% to 25% higher than the peak CBR for a penetration of 0.10 in. for the Orangeburg soils, 11% to 83% higher than the peak CBR for Georgetown soils; and about the same (16, 18, 21) for the Pickens soils. Note that the peak value of CBR does not coincide with the w_{opt}. Rather, it is on the dry side of optimum (0.5% to 5% dry side for the different soil types).

4.6.3 Resilient Modulus Results

M_R test results for Orangeburg B-6, Georgetown B-1 and Pickens B-4 are shown in Figure 4.5 to illustrate example results for each of the three sites. M_R versus cyclic stress at three different confining pressures is shown for specimens prepared at -2%w_{opt}, w_{opt} and +2%w_{opt}. For the two granular soils (Orangeburg in Figs 4.5(a)-(c) and Georgetown in Figs 4.5(d)-(f)), M_R increases with increasing cyclic stress and a higher M_R is found for higher confining pressure; whereas, for the finer grained soil (Pickens in Figs 4.5 (g)-(i)), M_R decreases with increasing cyclic stress for this soil. The trend in these results agree with published literature (i.e., Maher et al., 2000; Ng. et al., 2015, Rahman and Tarefder, 2015).

The effect of moisture content on M_R is shown by comparing the results of $-2\%w_{opt}$ to w_{opt} to +2%w_{opt}. As the moisture content increases from 2%w_{opt} to w_{opt} to +2%w_{opt}, the resilient modulus decreases for each cyclic stress and confining pressure. Hence, tests performed on specimens compacted on the dry side of optimum showed higher M_R compared to those compacted at $w_{opt,}$ and those compacted on the wet side of optimum showed lower M_R than those compacted at w_{opt}. Moreover, M_R for the specimens compacted on the wet side of optimum are less sensitive to the confining pressure at higher cyclic stress (i.e., M_R is independent of confining stress at a cyclic stress of about 50 kPa).

4.6.4 Resilient Modulus Model Parameters and the Effects of Moisture Content

Model parameters were obtained for the generalized constitutive resilient modulus model used in the AASHTO M-E Pavement Design Guide (Equation 4.2) which is shown in Table 4.2 for three states (dry, optimum, wet) for all 8 soils. Most of the test results show good coefficient of determination ($R^2 > 0.80$). The M_R values in Table 4.2 are representative of a bulk stress of 154.64 kPa and octahedral stress 13 kPa (per layer elastic

analysis for South Carolina pavements using Weslea (v 3.0)). Results indicate that for the 8 soil types, specimens prepared on the dry side of optimum have a higher M_R than those prepared at w_{opt}, and those prepared at w_{opt} have a higher M_R than those prepared on the wet side of optimum.

The effects of soil type, moisture content, and unit weight were also investigated for the 8 soil types. As shown in Figure 4.6(a), M_R decreases with increasing moisture content, as observed by others (e.g., Drumm et al., 1997; Butalia et al., 2003; Fredlund et al., 1977; and Heydinger, 2003). The results for dry unit weight versus M_R shown in Figure 4.6(b) show no distinct pattern. For most cases, the densities of the specimens compacted at w_{opt} are close to those compacted at $\pm 2\% w_{opt}$ (see Table 4.2), Thus, for small changes in density (i.e., 123.2 lb/ft^3 and 124.6 lb/ft^3 for specimens compacted at $-2\% w_{opt}$ and w_{opt} respectively for Orangeburg B-3) there is no clear trend in M_R.

4.7 CORRELATION OF RESILIENT MODULUS WITH CBR VALUES

As shown in Figure 4.7, both CBR and M_R decrease with increasing moisture content for the 8 soils tested. The highest CBR and M_R values were found on the dry side of w_{opt} and the lowest CBR and M_R values were found on the wet side of w_{opt}. Correlations between resilient modulus and CBR are shown in Figure 4.8. Figure 4.8(a) shows the correlation between resilient modulus of remolded soil samples and laboratory CBR for both 0.1 in. and 0.2 in. penetration and indicates that CBR increases with increasing M_R for both penetrations, with the M_R for 0.1 in. penetration being about 6% higher than 0.2 in. penetration. The correlation equations have a coefficient of determination of 0.40 and 0.48 for 0.1 in. penetration and 0.2 in. penetration, respectively. Figure 4.8(b) shows the correlation between resilient modulus and CBR as a function of different soil types and

indicates that CBR increases with increasing M_R for all of the soils tested herein. The following correlation equation between M_R and CBR was developed for South Carolina using the CBR data for all 8 soils at 0.10 in. penetration:

$$M_R(psi) = 5182 \times CBR^{0.35} \quad (4.8)$$

Resilient modulus tests were also performed for Shelby tube samples collected from 8 different boreholes. CBR tests were then performed with the same moisture content and density to correlate resilient modulus of undisturbed soil samples with CBR. Figure 4.8(c) shows the correlation between resilient modulus of undisturbed soil samples and laboratory CBR for both 0.1 in. and 0.2 in. penetration and indicates that CBR increases with increasing M_R for both penetrations, with the M_R for 0.1 in. penetration being almost same values with the 0.2 in. penetration. The correlation equations have a coefficient of determination of 0.64 and 0.63 for 0.1 in. penetration and 0.2 in. penetration, respectively. Figure 4.8(d) shows the correlation between resilient modulus and CBR as a function of different soil types and indicates that CBR increases with increasing M_R for all of the soils tested herein. The following correlation equation between the M_R for undisturbed samples and CBR was developed for South Carolina using the CBR data for all 8 soils at 0.10 in. penetration:

$$M_R(psi) = 4457 \times CBR^{0.22} \quad (4.9)$$

Using the developed CBR correlation equations, for the same moisture content and density, M_R found using the undisturbed samples for the 8 borehole locations were compared with the M_R found for the laboratory remolded specimens. Figure 4.8(e) shows the relation between remolded M_R and undisturbed M_R. It indicates that remolded M_R is 1.5 times higher than that of the undisturbed soil samples for the same CBR with good

coefficient of determination (R^2 = 0.65). To compare with the CBR, for both undisturbed and remolded soil samples resilient modulus, CBR tests have been performed for the same moisture content and density found in undisturbed/remolded samples. It signifies the aging of pavement may have effects on lower resilient modulus for undisturbed soil samples as the selected pavement sections are at least 10 years old.

4.8 CORRELATION OF MODEL PARAMETERS WITH SOIL INDEX PROPERTIES

Using multiple liner regression techniques, the generalized constitutive resilient modulus model parameters ($k_1, k_2, and\ k_3$) for remolded soils were correlated with soil index properties. The soil properties considered in the statistical analysis include the compacted soil dry density (γ_d), moisture content (w), maximum dry density ($\gamma_{d,max}$), optimum moisture content (w_{opt}), percent passing through No. 4 (P_4), No. 40 (P_{40}), and No. 200 sieve (P_{200}), D_{60}, D_{50}, D_{30}, D_{10}, uniformity coefficient (C_u), coefficient of curvature (C_c), liquid limit (LL), plastic limit (PL), plasticity index (PI), liquidity index (LI), specific gravity (G_s), and the percent sand, silt, and clay. Combined statistical models were developed using the results for the 8 soils. All of the soils are classified as coarse grained soils (P_{200}>50%) except for Pickens B-4, based on ASTM D 2488. Table 4.3 shows the coefficients for the developed models. Coefficients of determination (R^2) of 0.43, 0.61 and 0.71 were found for k_1, k_2, and k_3 respectively. Data sample size was limited to 30 soil samples for the 8 borehole locations. These developed models would be considered as representative statistical models for South Carolina as the soil samples are collected from three different locations of two different geographic regions. However, It is recommended

to increase the sample size and to develop two separate models for Type A and Type B soils of South Carolina to improve these models.

Table 4.3 shows the significance of different soil properties on the coefficients and overall model significance using p-value, where $p < 0.001$ indicates a statistically highly significant effect. $p < 0.01$ and $p < 0.001$ indicate statistically moderate and low significant effects, respectively. For the 8 soils tested, the percent passing No. 4 sieve, liquidity index, optimum moisture content, and maximum dry density showed a statistically significant effect on all three model coefficients (k_1, k_2 and k_1). The moisture content and dry density showed a statistically significant effect on k_1, and moisture content, dry density, and G_s showed statistically significant effect on k_2. The other soil index properties (i.e., P_{40}, P_{200}, D_{60}, D_{50}, D_{30} , D_{10} , C_u, C_c, LL, PL, PI, and the percent sand, silt, and clay) did not show a statistically significant effect on any of the model parameters).

Predicted and measured k_1, k_2, k_3 are shown in Figure 4.9(a), 4.9(b), and 4.9(c) respectively. Model coefficients k_1, k_2, and k_3 are the regression constants of Equation 4.2, and therefore, these were measured from the applied bulk stresses, and octahedral shear stresses, and the resultant resilient modulus values obtained from 15 different test sequences for each test using regression analysis. Most of the data points for all three models are observed close to the line of equity.

The developed constitutive models of coefficients in Table 4.3 were used to determine M_R from Equation 4.2 for a representative bulk stress 154.64 kPa and octahedral stress of 13 kPa and defined as the predicted M_R. The laboratory measured M_R is compared to the predicted M_R in Figure 4.10(a) and to the LTPP sand model in Figure 4.10(b). As shown, the predicted M_R (from the locally developed constitutive model) more accurately

predicted M_R than the LTPP sand model in terms of lower bias (e.g. -2.07 vs. 37.40 in Figure 4.10(a) and Figure 4.10(b)) and standard error (e.g. 21.56 vs. 34.59 in Figure 4.10(a) and Figure 4.10(b)). LTPP model for silts and LTPP model for clay were also studied. However, LTPP model for sand showed better results when compared to the measured M_R for the soils studied herein. Figure 4.10 demonstrates the importance of performing local calibration studies to find the constitutive model parameters for use in the MEPDG, rather than using the universal constitutive model parameters (i.e., for the Universal LTPP model for sand) that were found within the LTPP program (Yau and Quintus, 2004) from studies on soils and unbound pavement materials from all over the United States.

4.9 MOISTURE EFFECT OF SUBGRADE RESILIENT MODULUS ON PAVEMENT RUTTING

The effect of M_R on pavement rutting using the MEPDG was studied for three different resilient modulus input types for each location: M_R obtained from 2% dry side of w_{opt}, w_{opt}, and 2% wet side of w_{opt}. A summary of the MEPDG inputs is shown in Table 4.4. The Orangeburg (US-321), Georgetown (US-521), and Pickens (SC-93) pavements are asphalt concrete pavements having different type of bases (Gassman and Rahman, 2016): Orangeburg has a graded aggregate base, Georgetown has a cement stabilized base, and Pickens has an asphalt aggregate base. The dates of construction for Orangeburg, Georgetown, and Pickens pavement sections are 2004, 2003 and 2001, respectively; therefore, MEPDG analysis was run for 12 years for Orangeburg, 13 years for Georgetown, and 15 years for Pickens.

Figure 4.11 shows the cumulative rutting of different layers for each of the three pavement sections. Rutting for the AC layer only, rutting for the AC and base layer, and

the total rutting (AC + base + subgrade rutting) are shown. Total rutting is shown for three different subgrade M_R inputs (wet, w_{opt}, dry) to show the effect of subgrade moisture content on the total rutting. For all three sites, the highest total rutting was obtained using a M_R wet of optimum as the input for the subgrade soil and the lowest total rutting is obtained using a M_R dry of optimum as the input.

As observed for Orangeburg in Figure 4.11(a), using a wet of optimum M_R as the input for the subgrade soil showed subgrade rutting (total rutting – AC and base rutting) that is more than twice the subgrade rutting using a dry of optimum M_R for a pavement age of 12 years (0.11 in. versus 0.04 in. subgrade rutting). Using the M_R found at w_{opt} produced rutting that was in between these values (0.07 in.). Georgetown (Figure 4.11(c)) showed subgrade rutting of 0.04, 0.035, and 0.03 in. respectively for wet side of optimum, w_{opt}, and dry side of optimum, respectively for a pavement age of 13 years. Pickens showed largest subgrade rutting (0.09 in.) for the M_R at wet of optimum (Figure 4.11 (e)).

Even though Orangeburg has a higher subgrade M_R value for the wet side of optimum (6527 psi) than that of Pickens (5512 psi), higher subgrade rutting (0.11 in. in Orangeburg) was observed (0.09 in. in Pickens). This is because subgrade rutting is affected by the rutting of the layers above it (i.e., base layer rutting and AC rutting). These three sites were modeled with the same AC layer but a different type of base layer: Orangeburg has a 6 in. thick graded aggregate base (GAB), Georgetown has 7.7 in thick cement stabilized aggregate base (CSB), and Pickens has a 5.8 in. thick asphalt treated aggregate base (AAB).

The GAB has a lower modulus (E = 20,000 psi) than CSB and AAB (E = 1,000,000 psi); therefore, the largest subgrade rutting (and total rutting) was observed for all three M_R

inputs (wet, w_{opt}, dry) for the Orangeburg site with GAB as the base course (see Figure 4.11a) when compared to the Georgetown and Pickens sections with CSB and AAB as the base courses (see Figures 4.11b and 4.11c), respectively. This indicates that the effect of moisture variation on the M_R for a subgrade layer, and the resulting rutting predicted in MEDPG, is more important when an untreated unbound layer (i.e. GAB) is present than when a stabilized layer (i.e., cement stabilized aggregate base layer or asphalt aggregate base layer) is present.

4.10 CONCLUSIONS

The following conclusions can be made based on this study:

- The peak value of both CBR and resilient modulus was not found at the optimum moisture content and maximum dry density, rather they were found on the dry side of the optimum water content and at a dry density less than the maximum.
- For coarse grained soils, specimens compacted at 2% dry side of w_{opt} showed higher resilient modulus than specimens compacted at w_{opt}. Specimens compacted at 2% wet side of w_{opt} showed lower resilient modulus than specimens compacted at w_{opt}.
- Resilient modulus for the specimens compacted on the wet side of w_{opt} are less sensitive to the confining pressure at higher cyclic stress.
- Resilient modulus decreased as the moisture content increased for the 8 soil types tested herein.

- Good correlation was made between soil resilient modulus and CBR (R^2 = 0.40). Resilient modulus increases with increasing CBR for different types of soils.
- For remolded soils, the percent passing the No. 4 sieve, liquidity index, optimum moisture content, and maximum dry density showed a statistically significant effect on all three model coefficients (k_1, k_2, and k_1).
- The locally developed constitutive models predicted M_R more accurately than the universal LTPP models in terms of lower bias (e.g. -2.07 vs. 37.40) and standard error (e.g. 21.56 vs. 34.59).
- The subgrade soil moisture condition has a significant influence on the subgrade resilient modulus and the resulting subgrade rutting if graded aggregate base is used. However, if a higher stiffness base layer is used (i.e., cement stabilized base or asphalt treated aggregate base), the moisture effect is less significant.

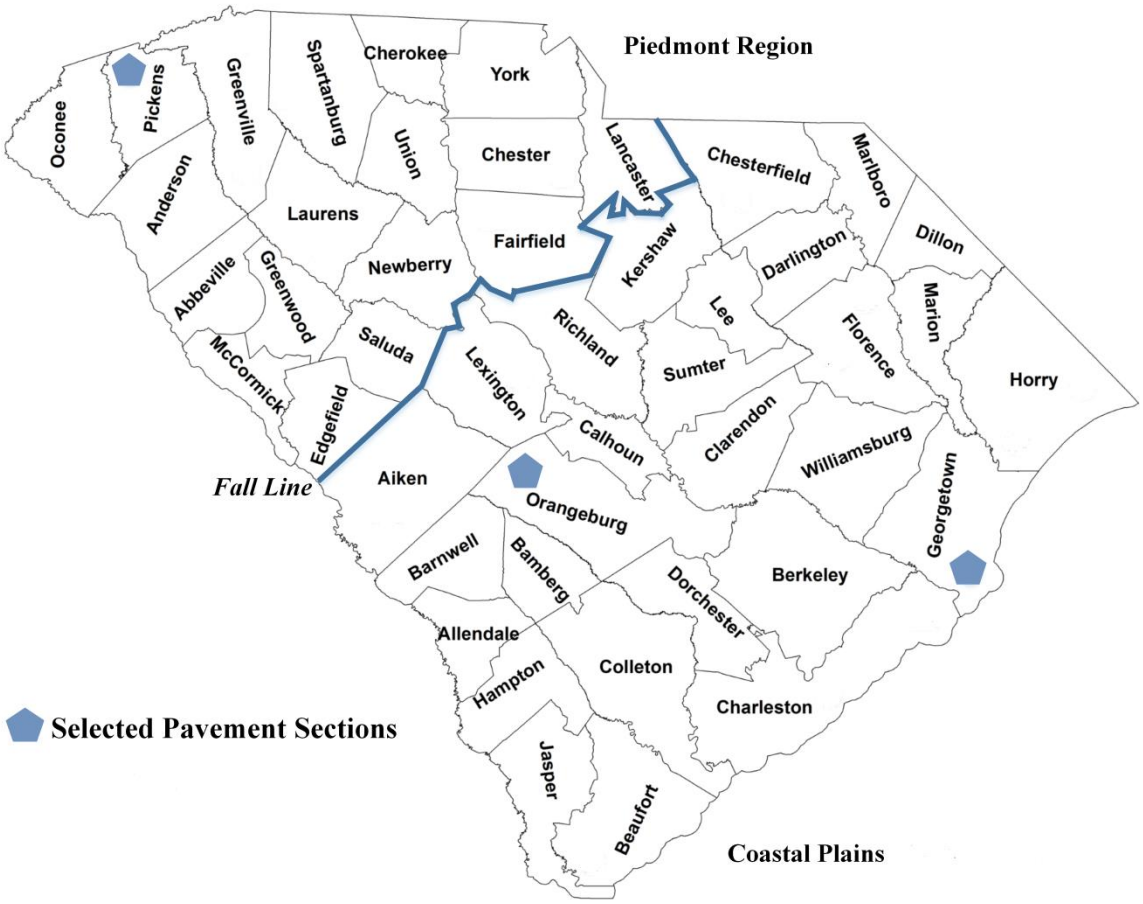

Figure 4.1 Selected Pavement Sections

(d) Asphalt Coring

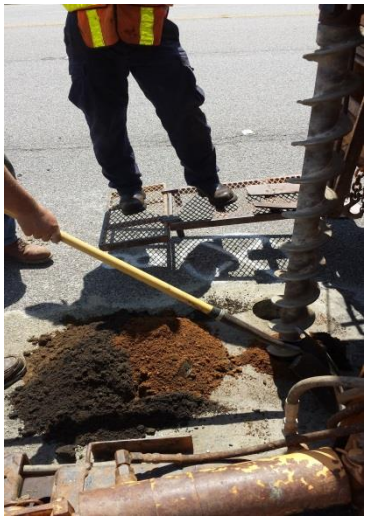

(e) Bulk Soil Collection

(f) Sample Preparation

(d) CBR Testing

(g) Specimen Collection

(h) M_R Testing

Figure 4.2 Field Sample Collection and Laboratory Testing

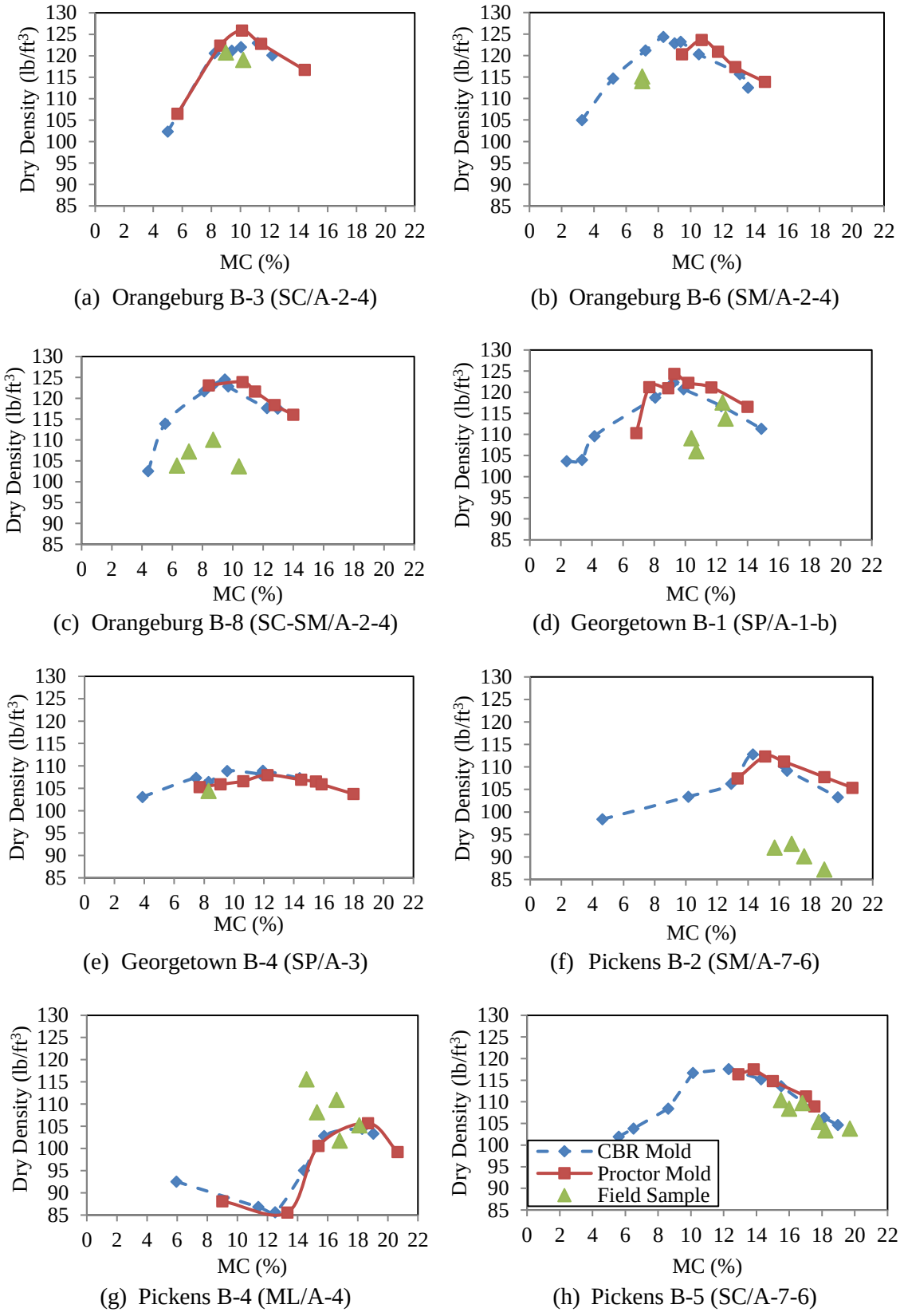

(a) Orangeburg B-3 (SC/A-2-4)

(b) Orangeburg B-6 (SM/A-2-4)

(c) Orangeburg B-8 (SC-SM/A-2-4)

(d) Georgetown B-1 (SP/A-1-b)

(e) Georgetown B-4 (SP/A-3)

(f) Pickens B-2 (SM/A-7-6)

(g) Pickens B-4 (ML/A-4)

(h) Pickens B-5 (SC/A-7-6)

Figure 4.3 Relationships Between Density and Moisture Content

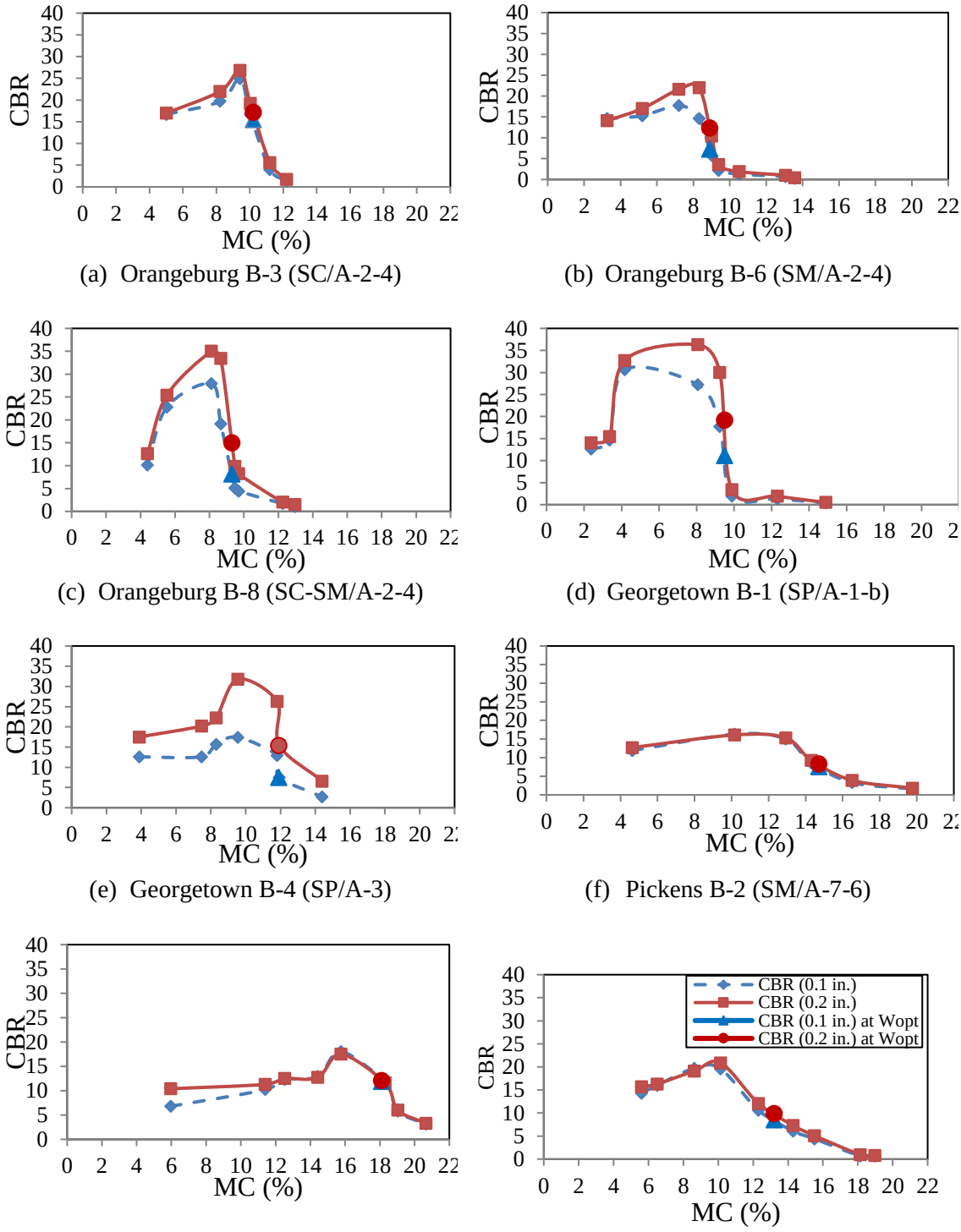

(a) Orangeburg B-3 (SC/A-2-4)

(b) Orangeburg B-6 (SM/A-2-4)

(c) Orangeburg B-8 (SC-SM/A-2-4)

(d) Georgetown B-1 (SP/A-1-b)

(e) Georgetown B-4 (SP/A-3)

(f) Pickens B-2 (SM/A-7-6)

(g) Pickens B-4 (ML/A-4)

(h) Pickens B-5 (SC/A-7-6)

Figure 4.4 CBR Test Results

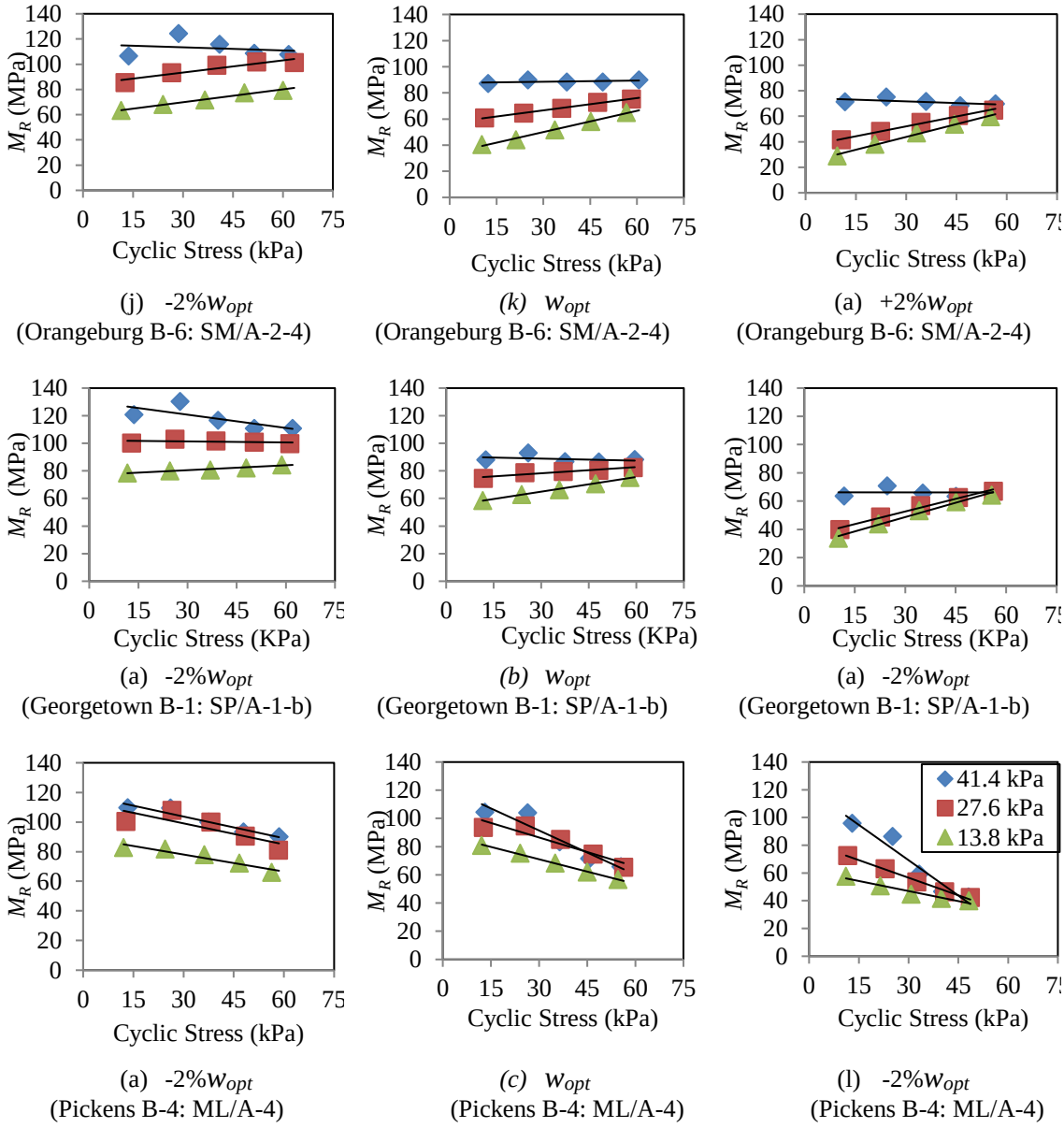

(j) -2%w_{opt} (Orangeburg B-6: SM/A-2-4)

(k) w_{opt} (Orangeburg B-6: SM/A-2-4)

(a) +2%w_{opt} (Orangeburg B-6: SM/A-2-4)

(a) -2%w_{opt} (Georgetown B-1: SP/A-1-b)

(b) w_{opt} (Georgetown B-1: SP/A-1-b)

(a) -2%w_{opt} (Georgetown B-1: SP/A-1-b)

(a) -2%w_{opt} (Pickens B-4: ML/A-4)

(c) w_{opt} (Pickens B-4: ML/A-4)

(l) -2%w_{opt} (Pickens B-4: ML/A-4)

Figure 4.5 Resilient Modulus Test Results

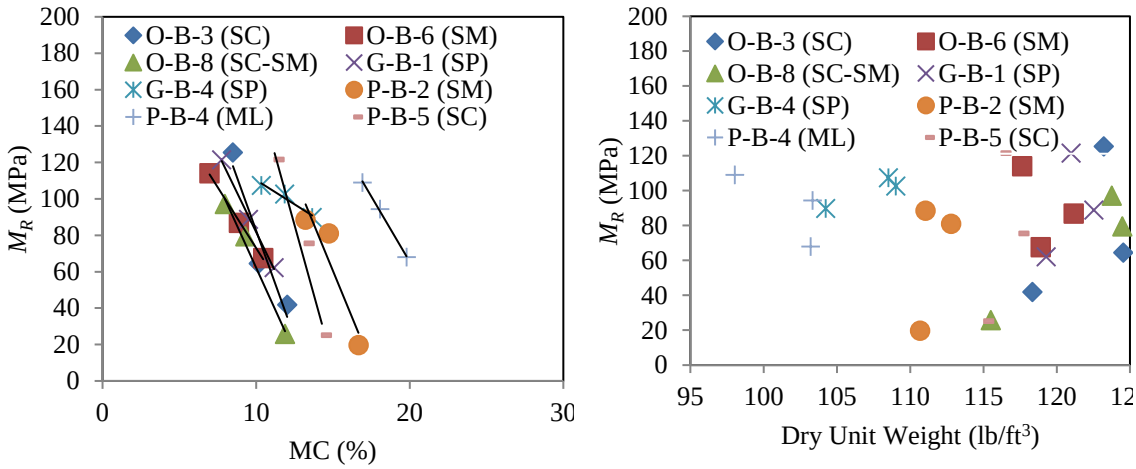

(a) (b)

Figure 4.6 Effects of a) Moisture Content and b) Dry Unit Weight on Resilient Modulus

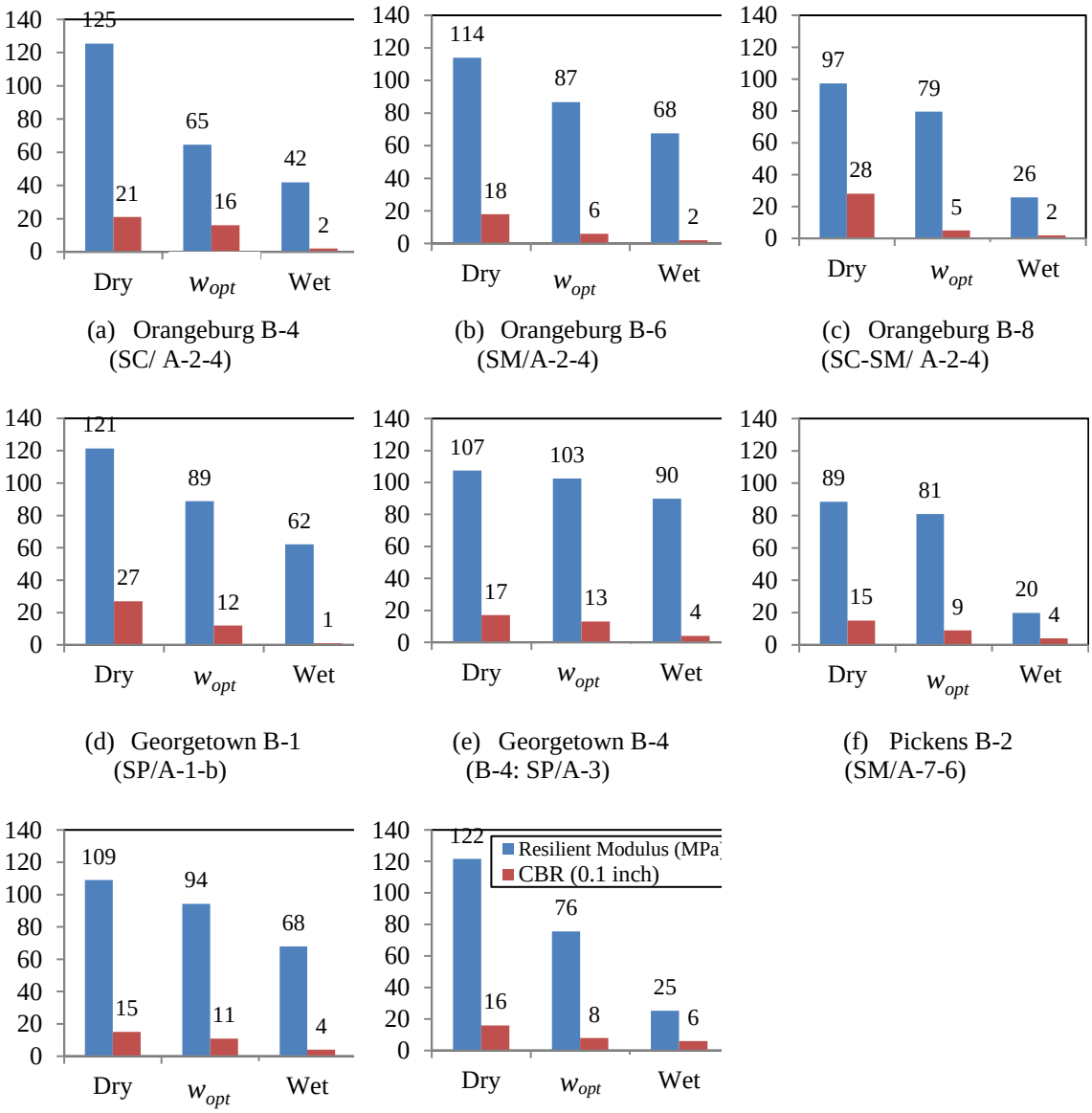

(a) Orangeburg B-4 (SC/ A-2-4)

(b) Orangeburg B-6 (SM/A-2-4)

(c) Orangeburg B-8 (SC-SM/ A-2-4)

(d) Georgetown B-1 (SP/A-1-b)

(e) Georgetown B-4 (B-4: SP/A-3)

(f) Pickens B-2 (SM/A-7-6)

(g) Pickens B-4 (ML/A-4)

(h) Pickens B-5 (SC/A-7-6)

Figure 4.7 Resilient Modulus with CBR

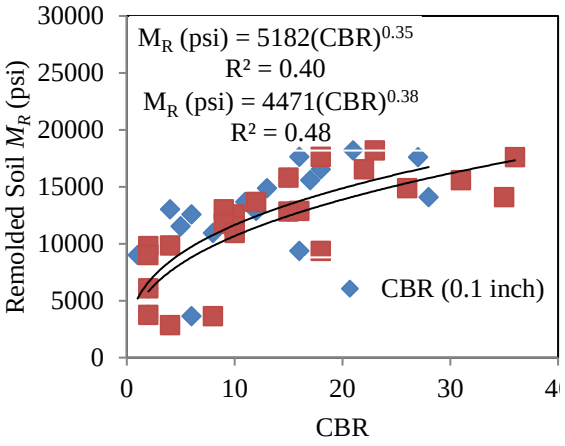

(a) For Laboratory Resilient Modulus

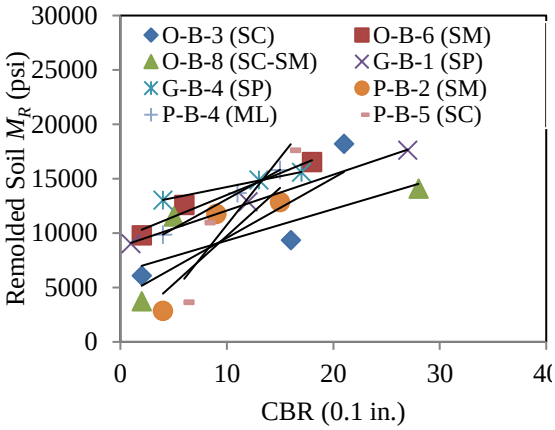

(b) For Different Soil Types

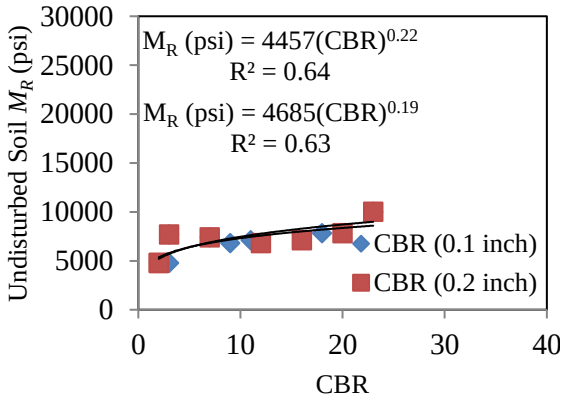

(c) For Field Resilient Modulus

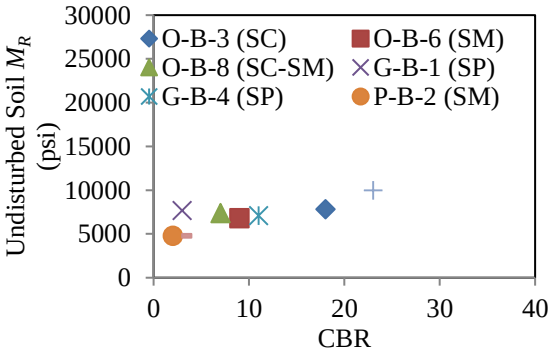

(d) For Different Soil Types

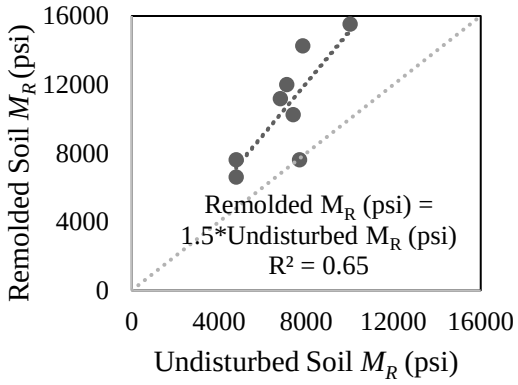

(e) Remolded and Undisturbed Soil M_R

Figure 4.8 Resilient Modulus and CBR Correlation

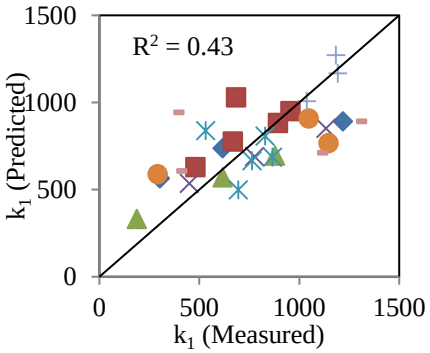

(a) Model Coefficient: k_1

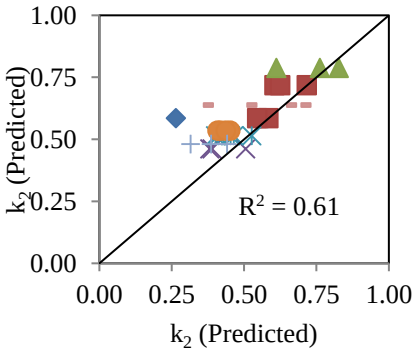

(b) Model Coefficient: k_2

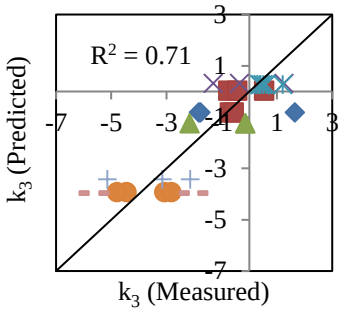

(c) Model Coefficient: k_3

Figure 4.9 Predicted Versus Measured Model Coefficients

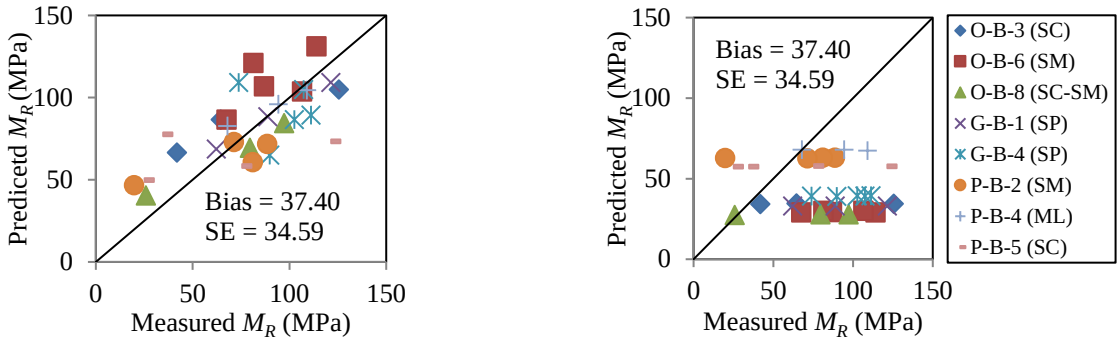

(a) Remolded Constitutive Model

(b) LTPP Sand Model

Figure 4.10 Comparison of Different Models

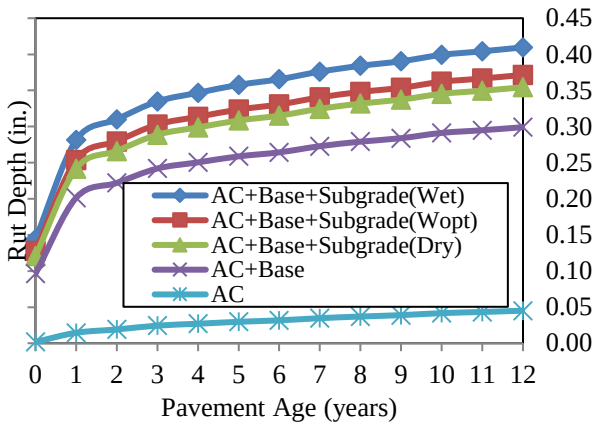

(a) Orangeburg Rutting

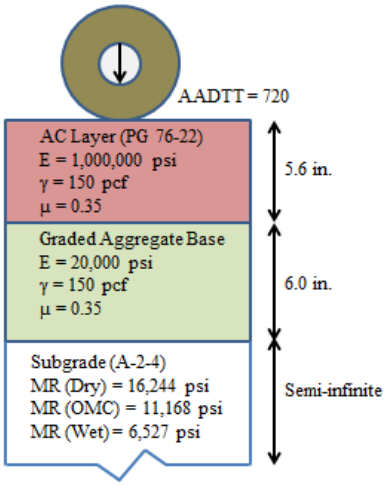

(b) Orangeburg Cross Section

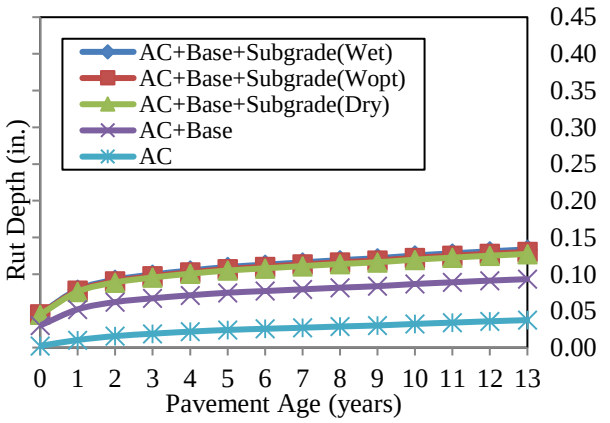

(c) Georgetown Rutting

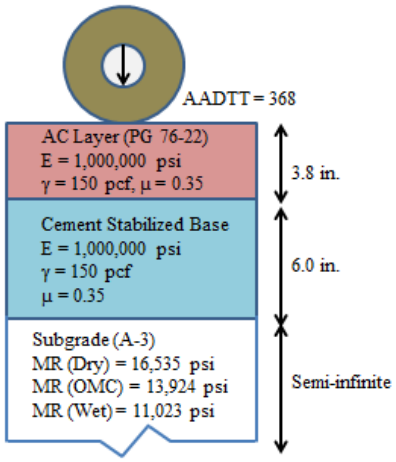

(d) Georgetown Cross Section

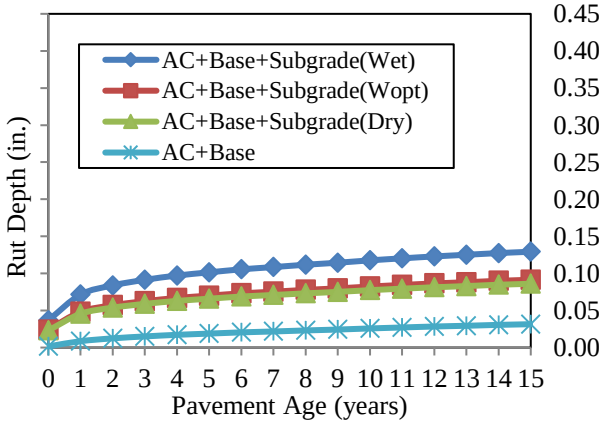

(e) Pickens Rutting

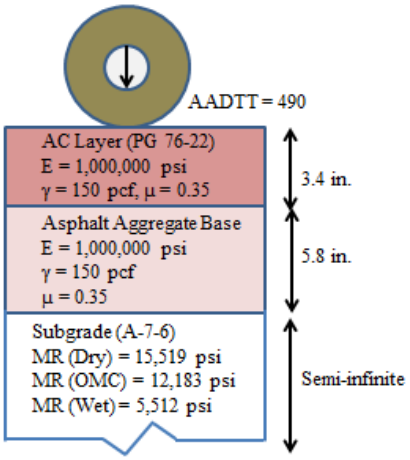

(f) Pickens Cross Section

Figure 4.11 Effect of Moisture Content on Subgrade Rutting

Table 4.1 Properties of Investigated Soils

Site	Bore-hole No.	Passing No. 200 Sieve (%)	LL (%)	PL (%)	PI (%)	G_s	w_{opt} (%)	$\gamma_{d,max}$ (kN/m^3)	Soil Classification	
									USCS	AASHTO
Orangeburg	B-3	24.7	26	17	9	2.66	10.1	19.8	SC	A-2-4
	B-6	20.6	18	17	1	2.39	10.7	19.4	SM	A-2-4
	B-8	22.8	20	16	4	2.6	10.6	19.5	SC-SM	A-2-4
Georgetown	B-1	1.5	NA	NA	NA	2.65	9.3	19.5	SP	A-1-b
	B-4	0.8	NA	NA	NA	2.71	12.2	17	SP	A-3
Pickens	B-2	43.8	45	29	16	2.55	15.1	17.6	SM	A-7-6
	B-4	51.2	36	26	10	2.52	16.3	17.7	ML	A-4
	B-5	44	42	28	14	2.51	13.8	18.5	SC	A-7-6

Note: LL = liquid limit, PL = plastic limit, PI = plasticity index, G_s= specific gravity of soil, w_{opt}= optimum moisture content, $\gamma_{d,max}$= maximum dry unit weight, NA = not available.

Table 4.2 Resilient Modulus Model Parameters

Site	Soil	State	γ_d (lb/ft^3)	MC (%)	k_1	k_2	k_3	R^2	M_R (MPa)
Orangeburg	B-3 (SC/ A-2-4)	Dry	123.2	8.5	1219	0.5585	-1.8260	0.92	125
		w_{opt}	124.6	10.2	617	0.5820	-1.7710	0.70	65
		Wet	118.4	12.0	303	0.2642	1.6491	0.63	42
	B-6 (SM/ A-2-4)	Dry	117.7	7.0	955	0.6050	-0.7623	0.96	114
		w_{opt}	121.2	8.9	667	0.7167	-0.4379	0.97	87
		Wet	118.9	10.5	480	0.6250	0.5291	0.86	68
	B-8 (SC-SM/ A-2-4)	Dry	123.8	8.0	879	0.8272	-2.1703	0.96	97
		w_{opt}	124.5	9.3	617	0.6108	-0.1492	0.82	79
		Wet	115.5	11.9	188	0.7616	-0.1470	0.81	26
Georgetown	B-1 (SP/ A-1-b)	Dry	121.0	7.8	1134	0.5054	-1.3099	0.97	121
		w_{opt}	122.6	9.5	777	0.3886	-0.3628	0.96	89
		Wet	119.3	11.2	449	0.3814	1.2511	0.79	62
	B-4 (SP/ A-3)	Dry	108.5	10.3	830	0.4098	0.5921	0.99	107
		w_{opt}	109.0	11.9	763	0.5265	0.4989	0.99	103
		Wet	104.2	13.7	694	0.4645	0.4067	0.99	90
Pickens	B-2 (SM/ A-7-6)	Dry	111.1	13.2	1047	0.4518	-3.0797	0.95	89
		w_{opt}	112.8	14.7	1147	0.4173	-4.4504	0.94	81
		Wet	110.7	16.7	292	0.4084	-4.7921	0.67	20
	B-4 (ML/ A-4)	Dry	98.0	16.9	1183	0.3862	-2.1402	0.87	109
		w_{opt}	103.4	18.1	1192	0.3151	-3.1520	0.90	94
		Wet	103.2	19.8	1037	0.4409	-5.1491	0.90	68
	B-5 (SC/ A-7-6)	Dry	116.2	11.2	1288	0.3607	-1.8520	0.85	122
		w_{opt}	117.5	13.2	1093	0.6480	-5.4391	0.94	76
		Wet	115.1	14.3	389	0.6976	-6.1519	0.87	25

Table 4.3 Developed Constitutive Models of Coefficients for South Carolina

Models	R^2	F Value
$k_1 = -25340.939^{**} + 238.99{P_4}^{**} - 43.411LI + 12.77\left(w_{opt}\times\gamma_{d,max}\right)^{***} -92.557(\gamma_{d,max})^{**} + 559.692(\frac{w}{w_{opt}}\times\frac{\gamma_d}{\gamma_{d,max}})$	0.43	3.58*
$k_2 = +9.958^{**} - 0.075{P_4}^{*} + 0.037LI^{***} - 0.002\left(w_{opt}\times\gamma_{d,max}\right)^{**} - 0.635(\frac{w}{w_{opt}}\times\frac{\gamma_d}{\gamma_{d,max}})^{***} - 0.613(G_s)^{*} + 0.839(\frac{\gamma_d}{\gamma_{d,max}})^{*} -0.078$	0.61	6.06***
$k_3 = -63.2 + 0.682{P_4}^{*} - 0.235LI^{**} - 0.03\left(w_{opt}\times\gamma_{d,max}\right)^{***}$	0.71	21.01***

*$p < 0.05$; **$p < 0.01$; ***$p < 0.001$

Table 4.4 Summary of MEPDG Inputs

County	Orangeburg	Georgetown	Pickens
Roadway	US-321	US-521	SC-93
Base Year	2004	2003	2001
Base Year AADTT	720	368	490
Design Life (years)	12	13	15
AC Layer and Thickness (in.)	PG 76-22 (5.6)	PG 76-22 (3.8)	PG 76-22 (3.4)
Effective Binder Content (%) (IL)	11.6 (2)	11.6 (2)	11.6 (2)
Air Void (%) (IL)	7 (2)	7 (2)	7 (2)
Base Layer and Thickness (in.)	Graded Aggregate (6.0)	Cement Stabilized (6.0)	Asphalt Aggregate (5.8)
Elastic Modulus (psi) (IL)	20,000 (3)	1,000,000 (3)	1,000,000 (3)
Subgrade Layer and Thickness (in.)	A-2-4 (semi-infinite)	A-3 (semi-infinite)	A-7-6 (semi-infinite)
Resilient Modulus at Dry State (psi) (IL)	16,244 (1)	16,535 (1)	15,519 (1)
Resilient Modulus at w_{opt} State (psi) (IL)	11,168 (1)	13,924 (1)	12,183 (1)
Resilient Modulus at Wet State (psi) (IL)	6,527 (1)	11,023 (1)	5,512 (1)

Note: IL = Input Level (3 = National, 2 = State Specific, 1 = Project Specific)
The, following preliminary local calibration factors were used for rutting: $\beta_{s_1} = \beta_{GB}$ = 2.979 for unbound untreated/stabilized granular base; $\beta_{s_1} = \beta_{SG} = 0.393$ for subgrade material;$\beta_{r_1} = 0.24$, $\beta_{r_2} = 1$, $\beta_{r_3} = 1$ for asphalt concrete layer. These are the required local calibration factors described by MEPDG guide (AASHTO, 2008) and these factors for South Carolina were determined by Gassman and Rahman (2016). Studies are ongoing to develop the final local calibration coefficients for South Carolina.

CHAPTER 5

CONCLUSIONS

5.1 SUMMARY

Resilient modulus is used to characterize the stress-strain behavior of subgrade soil and is one of the most important material inputs in the Mechanistic-Empirical Pavement Design Guide (MEPDG). This study examined the effect of subgrade resilient modulus of both undisturbed and remolded soil samples on pavement rutting using MEPDG.

Firstly, a preliminary study was performed to examine the effect of different traffic, climate, and materials inputs on pavement performance. By performing statistical analysis, pavement performance evaluation models were developed using data from primary and interstate highway systems in the state of South Carolina. Twenty pavement sections were selected from across the state, and historical pavement performance data of those sections were collected. A total of 9 models were developed based on regression techniques, which include 5 for Asphalt Concrete (AC) pavements and 4 for Jointed Plain Concrete Pavements (JPCP). Five different performance indicators were considered as response variables in the statistical analysis: Present Serviceability Index (PSI), Pavement Distress Index (PDI), Pavement Quality Index (PQI), International Roughness Index (IRI), and AC pavement rutting. Annual Average Daily Traffic (AADT), Free Flow Speed (FFS), precipitation, temperature, and soil type (soil Type A from Blue Ridge and Piedmont Region, and soil Type B from Coastal Plain and Sediment Region) were considered as predictor variables. Using the developed models, local transportation

agencies could estimate future corrective actions, such as maintenance and rehabilitation, as well as future pavement performances.

As the preliminary study showed the soil type has a statistically significant effect on pavement rutting, resilient modulus (M_R) of subgrade soils for different geographic regions in South Carolina was examined next. Shelby tube samples of subgrade soils were collected from existing pavements in different regions: SC-93 in Pickens county (Upstate Area), US-521 in Georgetown county (Coastal Plain), and US-321 in Orangeburg county (Coastal Plain, near the fall line). Resilient modulus model parameters were obtained using both the bulk stress model and the generalized constitutive resilient modulus model. Statistical analysis was performed to develop M_R estimation models for undisturbed soils using soils index properties. A correlation between laboratory measured M_R with the modulus from Falling Weight Deflectometer tests was also developed. Finally, the effects of M_R on subgrade rutting were studied using MEPDG.

Moisture variation along with different soil index properties plays an important role in subgrade stiffness. Due to variability during construction, subgrade soil moisture content might vary from the specified condition. Therefore, studying the effect of subgrade soil moisture variation on pavement rutting is of great importance. Resilient modulus is typically determined by conducting cyclic triaxial tests, which is complex and time consuming to perform. Therefore, correlations of resilient modulus with other stiffness parameters and index properties that are easier to obtain are often developed. In this study, California Bearing Ratio (CBR) tests were performed on remolded samples for a range of moisture contents. The samples were collected from three different regions in South Carolina. Laboratory M_R tests were performed on soil samples compacted at optimum

moisture content (w_{opt}), and $\pm$2% of w_{opt}. The M_R results were compared and correlations were made with CBR values for different moisture contents. Statistical models were developed to correlate generalized constitutive M_R model parameters with soil index properties for South Carolina. Finally, pavement rutting was studied for three different locations of South Carolina for resilient modulus determined for subgrade soil compacted at w_{opt}, and $\pm$2% of w_{opt}. Statistical analysis showed that soil moisture content and density played an important role for the subgrade soil M_R. MEPDG analysis showed that a slight change in moisture content during compaction has a significant effect on pavement rutting.

5.2 CONCLUSIONS

From the analyses and discussions presented in the preceding chapters, the following conclusions can be drawn:

5.2.1 Conclusions Based on Pavement Performance Evaluation Models

Pavement performance evaluation models were developed using data from primary and interstate highway systems in the state of South Carolina. A total of 9 models were developed based on regression techniques, which include 5 for AC pavements and 4 for JPCP pavements. Regarding the study of pavement performance evaluation models, the following conclusions are made:

- For the IRI models developed for AC and JPCP, AADT, FFS and precipitation showed statistically significant effects on IRI ($p < 0.01$). AADT and precipitation have positive effects on IRI, whereas FFS has negative effects on IRI for both AC and JPCP. That means IRI increases with increasing AADT and increasing precipitation. However, IRI decreases with increasing FFS. AC Rutting models showed very low coefficient of determination (R^2 = 0.179) and AADT had no

significant influence ($p > 0.05$). South Carolina soil type A produced statistically higher rutting ($p < 0.001$).

- For the PSI models developed for AC and JPCP, AADT, FFS and precipitation showed statistically significant effects on PSI ($p < 0.01$). AADT and precipitation have negative effects on PSI, whereas FFS has positive effects on PSI for both AC and JPCP. That means PSI decreases with increasing AADT and increasing precipitation. However, PSI increases with increasing FFS. As PSI is a function of only IRI, different models for these two dependent variables showed similar results.
- Temperature does not show any significant effect on IRI or PSI. Temperature showed significant effect only on AC pavement PDI and PQI ($p < 0.01$) and rutting ($p < 0.05$). Precipitation was found to be a significant predictor for PSI on both types of pavement, JPCP PDI and PQI, and AC and JPCP IRI ($p < 0.05$). Therefore, the climate input precipitation was found to be more important than temperature for predicting different pavement performance in South Carolina.
- Considering soil type, Type A soil produced statistically higher PDI, PQI ($p < 0.01$), and rutting ($p < 0.001$) compared to Type B soil on AC pavements; whereas, Type A soil produced statistically higher IRI and lower PSI ($p < 0.001$) compared to Type B soil on JPCP.
- Using the developed performance evaluation models, different local pavement performance indicators for a given climatic (temperature and precipitation), traffic (AADT) and material (soil type A or B, pavement type AC or JPCP) condition can be predicted. Additionally, developed performance evaluation models for IRI

would be a useful tool for MEPDG local calibration, to predict IRI in different climatic, traffic and material conditions.

5.2.2 Conclusions Based on Undisturbed Subgrade Soil Resilient Modulus Study

Resilient modulus of subgrade soils was characterized for different regions in South Carolina. Shelby tube samples of subgrade soils were collected from existing pavements in three different locations. Statistical analysis was performed to develop resilient modulus estimation models for undisturbed soils using soils index properties. Regarding the undisturbed subgrade soil resilient modulus study, the following conclusions are made:

- For undisturbed soil sample resilient modulus tests, even for a relatively short pavement section (1.34 miles long in Pickens), resilient modulus showed a wide range of values (COV = 42%) that must be considered when selecting input values for MEPDG.
- Resilient modulus found for undisturbed soil samples did not show a distinct pattern with the in-situ moisture content as has been shown for laboratory prepared samples. Good correlation was obtained between laboratory resilient modulus and the FWD modulus and can be used to estimate M_R as a Level 3 input.
- For granular materials, percent passing No. 4 sieve and percent sand showed statistically significant effect on k_1. Percent silt showed statistically significant effect on k_2, and percent passing No. 4 showed statistically significant effect on k_3. For silt-clay materials, liquidity index, plasticity index in-situ water content and dry density showed a significant effect of on k_1 and k_2.
- Developed constitutive models predicted the resilient modulus more accurately (standard error was 11.52 and 18.63 for granular and silt-clay materials,

respectively) than the universal LTPP models (standard error was 13.60 and -21.14 for granular and silt-clay materials, respectively).

- Subgrade rutting predicted by the developed constitutive model was in closer agreement to the rutting predicted by the laboratory measured resilient modulus than the FWD model or LTPP model.

5.2.3 Conclusions Based on Remolded Subgrade Soil Resilient Modulus Study

Correlations between the subgrade soil resilient modulus obtained for remolded samples and California Bearing Ratio (CBR) were established for a range of moisture content. Statistical models were developed to correlate generalized constitutive resilient modulus model parameters with soil index properties. The soil samples were prepared at moisture contents above and below the optimum moisture content. Pavement rutting was studied using the resilient modulus determined for the subgrade soils compacted at w_{opt} and $\pm 2\% w_{opt}$. Regarding the study of remolded subgrade soil resilient modulus, the following conclusions are made:

- The peak value of both CBR and resilient modulus was not found at the optimum moisture content and maximum dry density, rather it was found on the dry side of optimum and at a dry density less than the maximum.
- For different types of coarse grained soils, soil compacted 2% dry of optimum showed higher resilient modulus than soil compacted at the optimum moisture content Soil compacted 2% wet of optimum showed lower resilient modulus than soil compacted at the optimum moisture content.

- Resilient modulus increases with increasing cyclic stress for samples compacted 2% dry of optimum but it decreases with increasing cyclic stress for samples compacted 2% wet of optimum.
- Resilient modulus always decreases for increasing moisture content for different types of soils. However, no distinct relation between resilient modulus and soil dry density was shown.
- Good correlation was made between soil resilient modulus and CBR for both remolded soil and undisturbed soil. Resilient modulus increases with increasing CBR (for both 0.1 in. and 0.2 in. penetrations) for different types of soils. It was found that remolded M_R is 1.5 times higher than that of the undisturbed soil samples for the same CBR with good coefficient of determination ($R^2 = 0.65$).
- For remolded materials, percent passing No. 4 sieve, liquidity index, optimum moisture content, and maximum dry density showed a statistically significant effect on all three model coefficients (k_1, k_2, and k_1).
- The locally developed constitutive models quantified the improvement in prediction of the M_R more accurately than the universal LTPP models in terms of lower bias (e.g. -2.07 vs. 37.40) and standard error (e.g., 21.56 vs. 34.59).
- It was found that the subgrade soil moisture condition has a significant influence on the subgrade resilient modulus and resulting subgrade rutting if graded aggregate base is used. However, if a higher strength base layer is used (e.g., cement stabilized base or asphalt treated aggregate base), the moisture effect is less significant.

5.3. OVERALL CONCLUSIONS

In summary, the following conclusions can be made based on this study:

- Two different types of soil above and below the fall line have statistically significant effect on South Carolina pavement performance.
- Resilient modulus for both the undisturbed and remolded soil samples increases with increase in moisture content for different type of South Carolina soils. In general, w, w_{opt}, γ_d, $\gamma_{d,max}$, P_4, and LI have significant effect on three resilient modulus model parameters ($k1$, $k2$, and $k3$) for both undisturbed and remolded soil samples. The locally developed constitutive models of coefficients predicted resilient modulus more accurately than the universal LTPP models for both undisturbed and remolded soil samples.
- Resilient modulus found for undisturbed soil samples did not show a distinct pattern with the in-situ moisture content. However, resilient modulus decreases with increasing moisture content for remolded soil samples. The subgrade soil moisture condition has a significant influence on the subgrade soil resilient modulus and the resulting subgrade rutting if graded aggregate base is used.
- The locally developed constitutive models of coefficients predicted resilient modulus more accurately that the universal LTPP models for both undisturbed and remolded soil samples.
- Developed models (evaluation, index properties, FWD, CBR) can be used to estimate resilient modulus and predict pavement rutting and hence, enhance MEPDG local calibration for South Carolina.

5.4 RECOMMENDATIONS

The following recommendations are made for future studies:

1. It is recommended to use more reliable pavement distress data to evaluate and validate pavement performance models. This is because very low regression coefficients were obtained from the AC pavement PDI model (Adjusted R^2 = 0.128), AC pavement PQI model (Adjusted R^2 = 0.152), and AC pavement rutting model (Adjusted R^2 = 0.179), which were not expected. This may be a result of routine maintenance performed by the SCDOT on AC pavements which was not considered in this study and/or there might be some inconsistencies in the SCDOT's manual survey techniques for distress measurements.
2. It is recommended to develop a stress dependent and moisture sensitive resilient modulus model to use in MEPDG. Currently, MEPDG uses a single value of resilient modulus to predict different distresses. However, resilient modulus shows different values due to stress condition, soil properties, and moisture variation.
3. It is recommended to study the seasonal variation of subgrade resilient modulus on pavement rutting for South Carolina by performing both cyclic triaxial test using collected undisturbed soil samples and performing FWD test at different seasons.
4. Pavement coring and trench studies are recommended to measure rutting for the individual pavement layers (i.e., asphalt, base, subgrade) to perform comprehensive study of the effect of resilient modulus on pavement rutting using MEPDG. Moreover, it is recommend to install instrumented pavement section on one of the studied pavement sections to measure weight of traffic, stress, strain, moisture, and

temperature of pavement to better understand the effect of pavement material characteristics on pavement rutting in South Carolina.

REFERENCES

American Association of State Highway and Transportation Officials (AASHTO) (1986). *AASHTO Guide for Design of Pavement*. Washington, D. C.

American Association of State Highway and Transportation Officials (AASHTO) (1993). *Guide for Design of Pavement Structures*. Washington, D. C.

American Association of State Highway and Transportation Officials (AASHTO) (2003). *Determining the Resilient Modulus of Soils and Aggregate Materials*, T 307-99, Washington, D. C.

American Association of State Highway and Transportation Officials (AASHTO) (2003). *Standard Specifications for Transportation Materials and Methods of Sampling and Testing*, 23rd edition, Washington, D. C.

American Association of State Highway and Transportation Officials (AASHTO) (2008). *Mechanistic-Empirical Pavement Design Guide: A Manual of Practice*, Interim edition, Washington, D. C.

AASHTO M 145 (2003). *Standard Specification for Classification of Soils and Soil-Aggregate Mixtures for Highway Construction Purposes*. Washington, D. C.

AASHTO T 307 (1999). Determining the Resilient Modulus of Soils and Aggregate Materials. *Standard Specifications for Transportation Materials and Methods of Sampling and Testing*, Washington, D. C.

Ahmed, K., Abu-Lebdeh, G., and Lyles, R. W. (2006). Prediction of Pavement Distress Index with Limited Data on Causal Factors: An Auto-Regression Approach. *International Journal of Pavement Engineering*, Vol. 7, No. 1, pp. 23–35.

Ali, N.A., and Khosla, N. P. (1987). "Determination of Layer Moduli using a Falling Weight Deflectometer." *Transportation Research Record*, 1117, 1-10.

Al-Mansour, A., Sinha, K. C., and Kuczek, T. (1994). Effects of Routine Maintenance on Flexible Pavement Condition. *Journal of Transportation Engineering*, 120(1), 65–73.

ARA, Inc. (2004). *Guide for Mechanistic-Empirical Design of New and Rehabilitated Pavement Structures*, National Cooperative Highway Research Program, Report 1-37A.

Archilla, A. R., and Madanat, S. (2001). Statistical Model of Pavement Rutting in Asphalt Concrete Mixes. *Transportation Research Record: Journal of the Transportation Research Board*, 1764, 70–77.

Baig, S., and Nazarian, S. (1995). Determination of Resilient Modulus of Subgrades using Bender Elements, *Journal of Transportation Engineering*, 1504, 79-86.

Banerjee, A., Aguiar-Moya, J.P., and Prozzi, J.A. (2009). Calibration of Mechanistic-Empirical Pavement Design Guide Permanent Deformation Models, *Transportation Research Record*, 2094, 12-20.

Baus, R.L., and Hong, W. (2004). *Development of Profiler-Based Rideability Specifications for Asphalt Pavements and Asphalt Overlays*, Federal Highway Administration, Report GT04-07.

Baus, R.L., and Johnson, A.M. (1992). Flexible Pavement Overlay Design by Dynamic Deflections - Phase II, *Final Project Report*, Submitted to the South Carolina State Highway Department and the Federal Highway Administration.

Baus, R.L., Stires, and N.R. (2010). Mechanistic Empirical Pavement Design Guide Implementation, *Final Project Report*, Submitted to the South Carolina Department of Transportation and the Federal Highway Administration.

Behzadi, J.M., Ksaibati, K., Anderson-Sprecher, R., and Farrar, M.J. (1994). Factors Influencing Determination of a Subgrade Resilient Modulus Value, *Transportation Research Record*, 1462, 72-78.

Burczyk, G., and Yandell, W.O. (1996). Determination of Elastic and Plastic Subgrade Soil Parameters for Asphalt Cracking and Rutting Prediction, *Transportation Research Record*, 1540, 97-104.

Butalia, T.S., Huang, J., Kim, D. G., and Croft, F. (2003). Effect of Moisture Content and Pore Water Pressure Build on Resilient Modulus of Cohesive Soils, *Resilient Modulus Testing for Pavement Components*, ASTM STP 1437. West Conshohocken, PA.

Ceratti, J.A., Gehling, W.Y., and Nunez, W. (2004). Seasonal Variation of a Subgrade Soil Resilient Modulus in Southern Brazil. *Journal of Transportation Research Record*, 1876, 165-173.

Chan, P. K., Oppermann, M. C., and Wu, S.S. (1997). North Carolina's Experience in Development of Pavement Performance Prediction and Modeling. *Transportation Research Record: Journal of the Transportation Research Board*, 1592, 80–88.

Chang, C.-M., Baladi, G. Y., and Wolff, T. F. (2001). Using Pavement Distress Data to Assess Impact of Construction on Pavement Performance. *Transportation Research Record: Journal of the Transportation Research Board*, 1761, 15–25.

Chen, D., Wang, J., and Bilyeu, J (2001). Application of Dynamic Cone Penetrometer in Evaluation of Base and Subgrade Layers, *Transportation Research Record*, 1764, 1-10.

Chou, Y.T. (1976). Evaluation of Nonlinear Resilient Modulus of Unbound Granular Materials from Accelerated Traffic Test Data, U.S. Army Engineer Waterways Experiment Station, Vicksburg, MS, Final Technical Report.

Chu, C.Y., and Durango-Cohen, P. L. (2008). Empirical Comparison of Statistical Pavement Performance Models. *Journal of Infrastructure Systems*, 14(2), 138–149.

Chu, T.Y. (1972). Investigation of Subgrade Moisture Conditions in connection with the Design of Flexible Pavement Structures, *Final Project Report*, Submitted to the South Carolina State Highway Department and the Federal Highway Administration.

Coleri, E. (2007). Relationship between Resilient Modulus and Soil Index Properties of Unbound Materials. *Master's Thesis Submitted to The Graduate School of Natural and Applied Sciences of Middle East Technical University*.

Cooper, S.B., Elseifi, M.A., and Mohammad, L.N. (2012). Parametric Evaluation of Design Input Parameters on the Mechanistic-Empirical Pavement Design Guide Predicted Performance. *International Journal of Pavement Research and Technology*, 5(4), 218-224.

Dai, S., and Zollars, J. (2002). Resilient Modulus of Minnesota Road Research Project Subgrade Soil, *Transportation Research Record*, 1786, 20-28.

Daleiden, J.F., Killingsworth, B.M., Simpson, A.L. , and Zamora, R.A. (1995). Analysis of Procedures for Establishing In Situ Subgrade Moduli. *Journal of Transportation Research Record*, 1462, 102-107.

DeLisle, R. R., Sullo, P., and Grivas, D. A. (2003). Network-Level Pavement Performance Prediction Model Incorporating Censored Data. *Transportation Research Record: Journal of the Transportation Research Board*, 1853, 72–79.

Dowling, R., Kittelson, W., Zegeer, J., and Skabardonis, A. (1997). *Planning Techniques to Estimate Speeds and Service Volumes for Planning Applications*, National Cooperative Highway Research Program, Report 387.

Drumm, E.C., Reeves, J.S., Madgett, M.R., and Trolinger, W. D. (1997). Subgrade Resilient Modulus Correction for Saturation Effects, *Journal of Geotechnical and Geoenvironmental Engineering*, 123(7), 663-670.

ELMOD, (1985). ELMOD: Evaluation of Layer Moduli and Overlay Design, Users Manual, *Dynatest Consulting, Inc.*, Ojai, California.

El-Badawy, S., Bayomy, F., and Awed, A. (2012). Performance of MEPDG Dynamic Modulus Predictive Models for Asphalt Concrete Mixtures: Local Calibration for Idaho, *Journal of Materials in Civil Engineering*, 24(11), 1412-21.

EVERCALC, (1990). EVERCALC Version 3.0. University of Washington and Washington State Department of Transportation.

Ferreira, A., Picado-Santos, L. D., Wu, Z., and Flintsch, G. (2011). Selection of Pavement Performance Models for use in the Portuguese PMS. *International Journal of Pavement Engineering*, 12(1), 87–97.

Federal Aviation Administration (FAA) (2002). *Use of Non Destructive Testing in the Evaluation of Airport Pavements*. Federal Aviation Administration, Independence Avenue, Washington, D. C., United States.

Federal Highway Administration (FHWA) (2001). *Adequacy of the Rut Bar Data Collection*, FHWA-RD-01-027. < www.fhwa.dot.gov/publications/research/infrastructure/pavements/ltpp/01027/01027.pdf>

Federal Highway Administration (FHWA) (2004). *Pavement Smoothness Methodologies*, FHWA-HRT-04-061 145-91. <23we>

Flintsch, G.W., Al-Qadi, I.L., Park, Y., Brandon, T.L., and Appea, A. (2003). Relation between Back-calculated and Laboratory Measured Resilient Modulus of Unbound Materials, *Transportation Research Record*, 1849, 1177-182.

Fredlund, D. G., Bergan, A. T., and Wong, P. K. (1977). Relation between Resilient Modulus and Stress Research Conditions for Cohesive Subgrade Soils, Transportation Research Record: *Journal of Transportation Research Board*, 642, 73-81.

Garg, N., Larkin, A., and Brar, H. (2009). A Comparative Subgrade Evaluation using CBR, Vane Shear, Light Weight Deflectometer, and Resilient Modulus Tests. *Proceedings of the 8th International Conference on the Bearing Capacity of Roads, Railways and Airfields*, 5, 57-64.

Gassman, S.L., and Rahman, M.M. (2016). *Calibration of the AASHTO Pavement Design Guide to South Carolina Conditions-Phase I.* Publication FHWA-SC-16-02. FHWA, U.S. Department of Transportation.

George, K.P. (2004). Prediction of Resilient Modulus from Soil Properties, *Final Project Report*, Submitted to the Mississippi State Highway Department and the Federal Highway Administration.

Graves, R.C., and Mahboub, K.C. (2006). Pilot Study in Sampling-Based Sensitivity Analysis of NCHRP Design Guide for Flexible Pavements, *Transportation Research Record*, 1947, 123-135.

Guan, Y., Drumm, E.C., and Jackson, N.M. (1998). Weighting Factor for Seasonal Subgrade Resilient Modulus, *Transportation Research Record*, 1821, 47-55.

Gulen, S., Zhu, K., Weaver, J., Shan, J., and Flora, W. F. (2001). *Development of Improved Pavement Performance Prediction Models for the Indiana Pavement Management System*, Federal Highway Administration, Report FHWA/IN/JTRP-2001/17.

Gupta, A., Kumar, P., and Rastogi, R. (2014). Critical Review of Flexible Pavement Performance Models. *KSCE Journal of Civil Engineering*, 18(1), 142–148.

Hasan, M. R. M., Hiller, J. E., and You, Z. (2015). Effects of Mean Annual Temperature and Mean Annual Precipitation on the Performance of Flexible Pavement using ME Design. *International Journal of Pavement Engineering* (forthcoming).

Henning, T. F. P., Costello, S. B., Dunn, R. C. M., Parkman, C. C., and Hart, G. (2004). The Establishment of A Long-Term Pavement Performance Study on the New Zealand State Highway Network. *Road and Transport Research*, 13(2), 17–32.

Heukelom, W., and Klomp, A.J.G., (1962). Dynamic Testing as a Means of Controlling Pavement during and after Construction. *Proceedings of the 1st International Conference on the Structural Design of Asphalt Pavement*, University of Michigan, Ann Arbor, MI.

Heydinger, A.G. (2003). Evaluation of Seasonal Effects on Subgrade Soils. *Journal of Transportation Research Record*, 1619, 94-101.

Hicks, R.G., and Monismith, C.L. (1971). Factors Influencing the Resilient Response of Granular Materials. *Highway Research Record*, 34, 15-31.

Hong, H. P., and Wang, S. S. (2003). Stochastic Modeling of Pavement Performance. *International Journal of Pavement Engineering*, 4(4), 235–243.

Hossain, M.S. (2008). Characterization of Subgrade Resilient Modulus for Virginia Soils and Its Correlation with the Results of other Soil Tests, *Final Project Report*, Submitted to the Virginia State Highway Department and the Federal Highway Administration.

Hossain, M.S. (2010). Estimation of Subgrade Resilient Modulus for Virginia Soil, *Transportation Research Record*, 2101, 98-109.

Hossain, M., Romanoschi, S., and Gisi, A.J. (2000). Seasonal and Spatial Variations of Subgrade Response, *Geotechnical Special Publication*, 98, 150-167.

Hossain, Z., Zaman, M., Doiron, C., and Solanki, P. (2011). Evaluation of Mechanistic-Empirical Design Guide Input Parameters for Resilient Modulus of Subgrade Soils in Oklahoma, *Journal of Testing and Evaluation*, 39(5), 803-814.

Huang, J. (2001). Degradation of Resilient Modulus of Saturated Clay Due to Pore Water Pressure Buildup Under Cyclic Loading, *M.S Thesis, Ohio State University.*

Isa, A. H. M., Ma'soem, D. M., and Hwa, L. T. (2005). Pavement Performance Model for Federal Roads. *Proceedings of the Eastern Asia Society for Transportation Studies*, 5, 428–440.

ISSEM4, (1987). Description of and Users Guide for the Dynatest ISSEM4 Computer Program (IBM PC (DOS) Version), *Dynatest Consulting, Inc.*, Ojai, California.

Jadoun, F.M., and Kim, Y.R. (2012). Calibrating Mechanistic-Empirical Pavement Design Guide for North Carolina, *Transportation Research Record*, 2305, 131-140.

Ji, R., Siddiki, N., Nantung, T., and Kim, D. (2015). Field and Laboratory Determination of Subgrade Resilient Modulus and its Application in Pavement Design. In *Journal of Testing and Evaluation*, 43(5), 1009-1119.

Johanneck, L., and Khazanovich, L. (2010). Comprehensive Evaluation of Effect of Climate in Mechanistic Empirical Pavement Design Guide Predictions. *Transportation Research Record: Journal of the Transportation Research Board*, No. 2170, 45–55.

Johnson, A.M. (1992). Design of Flexible Pavement Overlays by Dynamic Deflections. *PhD Dissertation*, University of South Carolina.

Johnson, K. D., and Cation, K. A. (1992). Performance Prediction Development using Three Indexes for North Dakota Pavement Management System. *Transportation Research Record: Journal of the Transportation Research Board*, 1344, 22–30.

Jong, D., Bosscher, P.J., and Benson, C.H. (1998). Field Assessment of Changes in Pavement Moduli Caused by Freezing and Thawing. *Transportation Research Record: Journal of the Transportation Research Board*, 1615, 41-48.

Keith, T. Z. (2015). *Multiple Regression and Beyond: An Introduction to Multiple Regression and Structural Equation Modeling*, Routledge, Taylor and Francis, New York, USA.

Khazanovich, L.K., Celauro, C., Chadbourn, B., Zollars, J., and Dai, S. (2006). Evaluation of Subgrade Resilient Modulus Predictive Model for use in Mechanistic-Empirical Pavement Design Guide, *Transportation Research Record*, 1947, 155-166.

Khoury, N.N., and Zaman, M.M. (2004). Correlation Between Resilient Modulus, Moisture Variation, and Soil Suction for Subgrade Soils, *Transportation Research Record*, 1874, 99-107.

Kim, S.-H., and Kim, N. (2006). Development of Performance Prediction Models in Flexible Pavement using Regression Analysis Method. *KSCE Journal of Civil Engineering*, 10(2), 91–96.

Kim, D., Ji, Y., and Siddiki, N.Z. (2010). Evaluation of in-situ Stiffness of Subgrade by Resilient and FWD Modulus, *Final Project Report*, Submitted to the Indiana Department of Transportation and the Federal Highway Administration.

Ksaibati, K., Armaghani, J., and Fisher, J. (2000). Effects of Moistures on Modulus Values of Base and Subgrade Materials, *Transportation Research Record*, 1716, 20-29.

Lee, W., .C., Altschaeffl, A.G., and White, T.D. (1997). Resilient Modulus of Cohesive Soils. *Journal of Geotechnical and Geoenvironmental Engineering*, 123(2), 85-95.

Lee, S.W., Mahoney, J.P., and Jackson, N.C. (1988). Verification of Backcalculation of Pavement Moduli. *Journal of Transportation Research Record*, 1196, 131-135.

Lekarp, F., Isacsson, U., and Dawson, A. (2000). State of the Art. I: Resilient Response of Unbound Aggregates. *Journal of Transportation Engineering*, 126(1), 66-75.

Li, X. Y., Zhang, R., Zhao, X., and Wang, H. N. (2014). Sensitivity Analysis of Flexible Pavements Parameters by Mechanistic-Empirical Design Guide. *Applied Mechanics and Materials*, 590, 539–545.

Lu, D. Y., Lytton, R. L., and Moore, W. M. (1974). *Forecasting Serviceability Loss of Flexible Pavements*, Federal Highway Administration, Report. TTI-2-8-74-57-1F.

Madanat, S. (1993). Incorporating Inspection Decisions in Pavement Management. *Transportation Research Part B: Methodological*, 27(6), 425–438.

Maher, A., Bennert, T., Gucunski, N., and Papp, W.J. (2000). Resilient Modulus of New Jersey Subgrade Soils, FHWA Report No. 2000-01, Washington D.C.

Malla, R. B., and Joshi, S. (2007). Resilient Modulus Prediction Models Based on Analysis of LTPP Data for Subgrade Soils and Experimental Verifications. *International Journal of Transportation Engineering*, 133(9), 491–504.

Malla, R. B., and Joshi, S. (2008). Subgrade Resilient Modulus Prediction Models for coarse and fine-grained soils based on long-term pavement performance data. *International Journal of Pavement Engineering*, 9(6), 431–444.

May, R.W., and Witczak, M.W. (1981). Effective Granular Modulus to Model Pavement Responses, *Transportation Research Record: Journal of Transportation Research Board*, 810, 1-9.

Meegoda, J. N., and Gao, S. (2014). Roughness Progression Model for Asphalt Pavements using Long-Term Pavement Performance Data. *Journal of Transportation Engineering*, 140(8), 1–7.

Meshkani, A., Abdallah, I. N., and Nazarian, S. (2003). Feasibility of Backcalculation of Nonlinear Flexible Pavement Layer Parameters from Nondestructive Testing, In *Transportation Research Record: Journal of Transportation Research Board*, Washington, D.C., 1860, 16-25.

Mfinanga, D. A., H. Ochiai, N. Yasufuku, and H. Yokota. (1996). Traffic Loading and Environmental Effects on Asphalt Pavement Rutting, *Memoirs of the Kyushu University*, Faculty of Engineering. 56(3), 149-169.

Mikhail, M. Y., Mamlouk, M. S. (1999). Effect of Traffic Load on Pavement Serviceability. *ASTM Special Technical Publication*, 1348, 7–20.

Mills, L. N. O., Attoh-Okine, N. O., and McNeil, S. (2012). Developing Pavement Performance Models for Delaware. *Transportation Research Record: Journal of the Transportation Research Board*, 2304, 97–103.

Mohammad, L., Herath, A., Abu-Farsakh, M., and Gaspard, K., and Gudishala, R. (2007). Prediction of Resilient Modulus of Cohesive Subgrade Soils from Dynamic Cone Penetrometer Test Parameters. *Journal of Materials in Civil Engineering*, 19(11), 986-992.

Mohammad, L. N., Huang, B., Puppala, A. J., and Allen, A. (1999). Regression Model for Regression Modulus of Subgrade Soils. *Transportation Research Record: Journal of Transportation Research Board*, 1687, 47-54.

Mohammad, L. N., Puppala, A. J., and Alavilli, P. (1994). Influence of Testing Procedure and LVDT Location on Resilient Modulus of Soils. *Transportation Research Record: Journal of Transportation Research Board*, 1462, 91-101.

Nassiri, S., and Bayat, A. (2013). Evaluation of MEPDG Seasonal Adjustment Factors for the Unbound Layers' Moduli using Field Moisture and Temperature Data. *International Journal of Pavement Research and Technology*, 6(1), 45–51.

National Centers for Environmental Information (NCEI) (2015). *National Oceanic and Atmospheric Administration.* <www.ncdc.noaa.gov>

Nazzal, M.D., and Mohammad L.N. Nazarian, S., and Yuan, D. (2008). Variation in Moduli of Base and Subgrade with Moisture, *GeoCongress 2008*, Geosustainability and Geohazard Mitigation.

Nazzal, M.D., and Mohammad L.N. (2010). Estimation of Modulus Resilient of Subgrade Soils using Falling Weight Deflectometer, *Transportation Research Record*, 2186, 1-10.

NCHRP 1-28A (2004). Laboratory Determination of Resilient Modulus for Flexible Pavement Design. Digest No. 285, 2004, 1-52.

Neter, J., and Wasserman, W. (1996). *Applied Linear Statistical Models*. Irwin, Chicago.

Newcomb, D.E., Chadbourn, B.A., Van Deusen, D. A., and Burnham, T. R. (1995). Initial Characterization of Subgrade Soils and Granular Base Materials at the Minnesota Road Research Project, *Report No. MN/RC-96/19*. Minnesota Department of Transportation, St. Paul, Minn.

Ng, K., Henrichs, Z. R., Ksaibati, K., and Wulff, S. S. (2016). Measurement and Estimation of the Resilient Modulus of Subgrade Materials for Mechanistic-Empirical Pavement Design Guide in Wyoming, *Transportation Research Board Annual Meeting*, 1-17.

Orobio, A., and Zaniewski, J.P. (2011). Sampling-Based Sensitivity Analysis of the Mechanistic-Empirical Pavement Design Guide Applied to Material Inputs, *Transportation Research Record*, 2226, 95-93.

Paterson, W. D. O. (1986). International Roughness Index: Relationship to other Measures of Roughness and Riding Quality. *Transportation Research Record: Journal of the Transportation Research Board*, 1084, 49–59.

Pierce, C. E., Gassman, S. L., and Ray, R. P. (2011). *Geotechnical Materials Database for Embankment Design and Construction*, Federal Highway Administration, Report FHWA-SC-11-02.

Ping, W.V., Yang, Z., and Gao, Z (2002). Field and Laboratory Determination of Granular Subgrade Moduli. *Journal of Performance of Constructed Facilities*, ASCE, 16(4), 149-159.

Puppala, A. J., Saride, S., and Chomtid, S. (2009). Experimental and Modeling Studies of Permanent Strains of Subgrade Soils. *Journal of Geotechnical and Geoenvironmental Engineering*, ASCE, 135(10), 1379-1389.

PMS Inc. (1990). PMS Final Specification Report. South Carolina Department of Transportation, Columbia, SC.

Prozzi, J. A., and Madanat, S. M. (2004). Development of Pavement Performance Models by Combining Experimental and Field Data. *Journal of Infrastructure Systems*, 10(1), 9–22.

Rahim, A., and George, K.P. (2003). Falling Weight Deflectometer for Estimating Subgrade Elastic Moduli. *Journal of Transportation Engineering*, 129(1), 100-107.

Rahman, M., and Tarefder, R. (2015). "Assessment of Molding Moisture and Suction on Resilient Modulus of Lime Stabilized Clayey Subgrade Soils." *Geotechnical Testing Journal*, 38(6), pp. 840-850.

Rahman, M.M., and Tarefder, R. (2015). "PCI and non-PCI-based Pavement Evaluation." *Journal of Airport Management*, 9(6), pp. 185-196.

Rahman, M.M., and Gassman, S.L. (2017). Effect of Resilient Modulus of Undisturbed Subgrade Soils on Pavement Rutting. *International Journal of Geotechnical Engineering*, (forthcoming).

Rahman, M.M., Uddin, M.M., and Gassman, S.L. (2017). Pavement Performance Evaluation Models for South Carolina. *KSCE Journal of Civil Engineering*, (forthcoming).

Ramos Garcia, J. A., and M. Castro. (2011). Analysis of the Temperature Influence on Flexible Pavement Deflection. *Construction & Building Materials*. 25(8), pp. 3530-3539.

Salama, H. K., Chatti, K., Lyles, R. W. (2006). Effect of Heavy Multiple Axle Trucks on Flexible Pavement Damage using In-Service Pavement Performance Data. *Journal of Transportation Engineering*, 132(10), 763–770.

Saxena, P., Tompkins, D., Khazanovich, L., and Balbo, T. (2010). Evaluation of Characterization and Performance Modeling of Cementitiously Stabilized Layers in the Mechanistic-Empirical Pavement Design Guide, *Transportation Research Record*, 2186, 111-119.

Scullion, T., Uzan, J., and Paredes, M. (1990). MODULUS: A Microcomputer-based Backcalculation System., *Presented at the 69th Annual Meeting of the Transportation Research Board.*

Seed, H. B., Chan, C. K., Lee, C. E. (1962). Resilience Characteristics of Subgrade Soils and their Relations to Fatigue Failures in Asphalt Pavements. *Proceedings of the International Conference on the Structural Design of Asphalt Pavements*, Ann Arbor, MI, 77–113.

Serigos, P. A., M., Murphy, and J. A., Prozzi. (2013). Evaluation of Rut-Depth Accuracy and Precision Using Different Automated Systems for Texas Consditions, *Transportation Research Board Annual Meeting*, 1-15.

Shahin, M. Y. (2005). Pavement Management for Airports, Roads, and Parking Lots, *Springer Publication*, New York, USA.

Singh, D., Zaman, M., and Commuri, S. (2011). Evaluation of Measured and Estimated Dynamic Moduli for Selected Asphalt Mixed, *Journal of ASTM International*, 8(9), 19.

South Carolina Department of Transportation (SCDOT) (2010). *Geotechnical Design Manual Version 1.1*. < http://www.scdot.org/doing/structural_geotechnical.aspx >

Souliman, M., Mamlouk, M., El-Basyouy, M., and Zapata, C. (2010). Calibration of the AASHTO MEPDG for Flexible pavement for Arizona conditions, *Compendium of Papers of the 89th TRB Annual Meeting (CD-ROM), Transportation Research Board*, Washington, DC.

Tarefder, R., and Rahman, M.M. (2016). Development of System Dynamic Approaches to Airport Pavements Maintenance, *Journal of Transportation Engineering*, 142(8), 04016027.

Tarefder, R., and Rodriguez-Ruiz, J.I. (2013). Local Calibration of MEPDG for Flexible Pavements in New Mexico, *Journal of Transportation Engineering*, 139(10), 981-991.

Thomson, M. R., and Robnett, Q. L. (1979). Resilient Properties of Subgrade Soils. *Journal of Transportation Engineering,* 105(1), 71-89.

Thyagarajan, S., Sivaneswaran, N., Muhunthan, B., and Petros, K. (2010). Statistical Analysis of Critical Input Parameters in Mechanistic Empirical Pavement Design Guide. *Journal of the Association of Asphalt Paving Technologists,* Vol. 79, pp. 635–662.

Tian, P., Zaman, M. M., and Laguros, J. G. (1998). Gradation and Moisture Effects on Resilient Moduli of Aggregate Bases, *Transportation Research Record*, 1619, 75-84.

Titi, H. H. (2011). Determination of Resilient Modulus Values for Typical Plastic Soils in Wisconsin, *Final Project Report*, Submitted to the Wisconsin State Highway Department and the Federal Highway Administration.

Titi, H. H., Elias, M. B., and Helwany, S. (2006). Determination of Typical Resilient Modulus Values for Selected Soils in Wisconsin, University of Wisconsin-Milwaukee, Office of Research Services and Administration, Mitchell Hall, Milwaukee, WI.

Titi, H.H., English, R., and Faheem, A. (2015). Resilient Modulus of Fine-Grained Soils for Mechanistic-Empirical Pavement Design. *Transportation Research Record*, 2510, 24-35.

Uddin, M. M., and Huynh, N. (2015). Freight Traffic Assignment Methodology for Large-Scale Road-Rail Intermodal Networks. *Transportation Research Record: Journal of the Transportation Research Board*, 2477, 50–57.

Von Quintus, V.H., and Killingsworth, B. (1997). *Design Pamphlet for the Determination of Design Subgrade in Support of the AASHTO Guide for the Design of Pavement Structures*. FHWA-RD-97-083, Federal Highway Administration, VA.

Von Quintus, V.H., and Killingsworth, B. (1998). *Analysis Relating to Pavement Material Characterizations and their Effects on Pavement Performance*. FHWA-RD-97-085, Federal Highway Administration, VA.

Wang, D. J. (2002). *Evaluating Pavement Performance Prediction Models for the Interstate Highway System in South Carolina*, M.S. Thesis, University of South Carolina, Columbia, SC.

Wang, T., Harvey, J., Lea, J., and Kim, C. (2014). Impact of Pavement Roughness on Vehicle Free-Flow Speed. *Journal of Transportation Engineering*, 140(9), 1–11.

Waseem, A., and Yuan, X. (2013). Longitudinal Local Calibration of MEPDG Permanent Deformation Models for Reconstructed Flexible Pavements Using PMS Data, *International Journal of Pavement Research and Technology*, 6(4), 304-312.

Witczak, W.M., Qi, X, and Mirza, W.M. (1995). Use of Non Linear Subgrade Modulus in AASHTO Design Procedure, *Journal of Transportation Engineering*, 121(3), 273-282

Webb, W. M., and Campbell, B. E. (1986). Preliminary Investigation into Resilient Modulus Testing for New AASHTO Pavement Design Guide, *Office of Materials and Research, Georgia Department of Transportation*.

Wu, Z., and Yang, X. (2012). Evaluation of the MEPDG Permanent Deformation Models in Louisiana Conditions, *Geocongress 2012 State of Art and Practice in Geotechnical Engineering*, pp. 1438-1447.

Xu, G., Bai, L., and Sun, Z. (2014). Pavement Deterioration Modeling and Prediction for Kentucky Interstate and Highways. *Proceedings of the 2014 Industrial and Systems Engineering Research Conference*, Montreal, QC, Canada.

Xu, Q., Ruiz, M., Moravec, M., and Rasmussen, R.O. (2013). Simulation of Unbound Material Resilient Modulus Effects on Mechanistic-Empirical Pavement Designs, *Material and Structures*, 46(7), 1089-1100.

Yau, A., and Von Quintos, H.L. (2004). Predicting Elastic Response Characteristics of Unbound Materials and Soils. *Transportation Research Record*, 1874, 47-56.

Zaghloul, S., Ayed, A., Halim, A.A., Vitillo, N., and Sauber, R. (2006). Investigations of Environmental and Traffic Impacts on Mechanistic-Empirical Pavement Design Guide Predictions, *Transportation Research Record*, 1967, 148-159.

Zapata, C.E., Andrei, D., Witczak, M.W., and Houston, W.N. (2007). Incorporation of Environmental Effects in Pavement Design, *Transportation Research Record*, 2282, 22-23.

Zhou, H., (2000). Comparison of Backcalculated and Measured Moduli on AC and Granular Base Layer Materials, In *Nondestructive Testing of Pavements and Backcalculation of Moduli*, ASTM STP 1375, West Conshohocken, PA, 3, 161-173.

Zhou, H., Hicks, R.G., and Bell, C.A., (1990). BOUSDEF: A Backcalculation Program for Determining Moduli of a Pavement Structure, *Presented at the 69th Annual Meeting of the Transportation Research Board.*

Zhou, C., Huang, B., Drumm, E., Xiang, S., Qiao, D., and Udeh, S (2014). Soil Resilient Modulus Regressed from Physical Properties and Influence of Seasonal Variation on Asphalt Pavement Performance, In *Journal of Transportation Engineering*, 141(1), 0414069.

APPENDIX A –RESILIENT MODULUS VERSUS CYCLIC STRESS (UNDISTURBED)

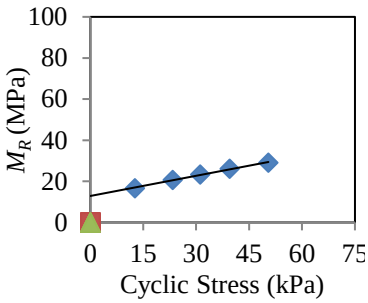

Figure A-1
(Orangeburg Sam. 111:
SM/A-2-4)

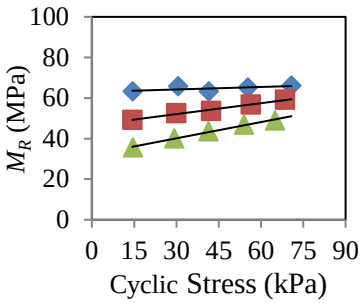

Figure A-2
(Orangeburg Sam. 121:
SM/A-2-4)

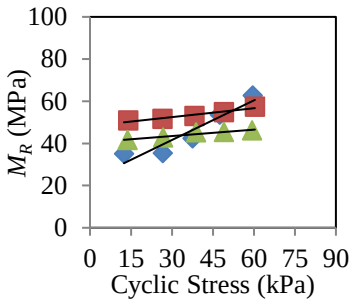

Figure A-3
(Orangeburg Sam. 211:
SC-SM/A-2-4)

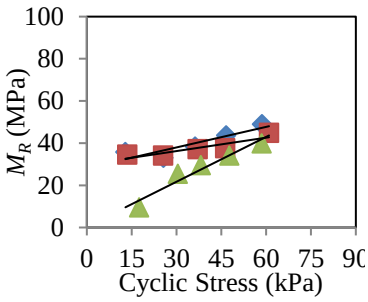

Figure A-4
(Orangeburg Sam. 221:
SC-SM/A-2-4)

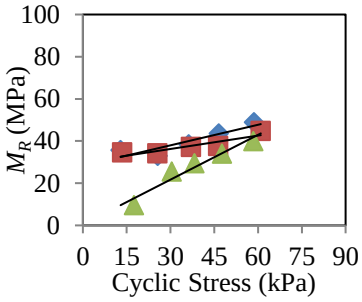

Figure A-5
(Orangeburg Sam. 223:
SM/A-2-4)

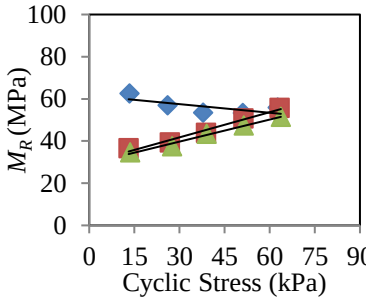

Figure A-6
(Orangeburg Sam. 312:
SC/A-2-4)

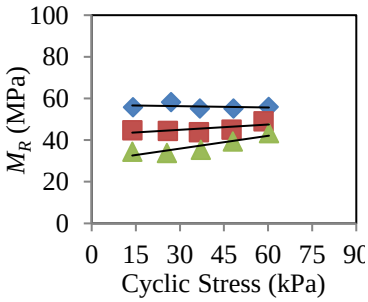

Figure A-7
(Orangeburg Sam. 313:
SC/A-2-4)

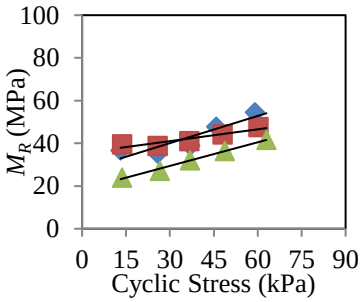

Figure A-8
(Orangeburg Sam. 411:
SM/A-2-4)

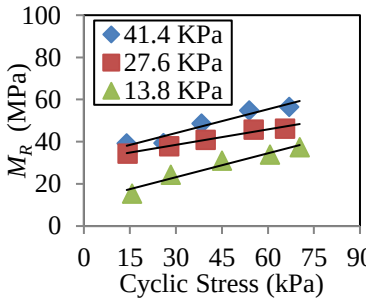

Figure A-9
(Orangeburg Sam. 412:
SM/A-2-4)

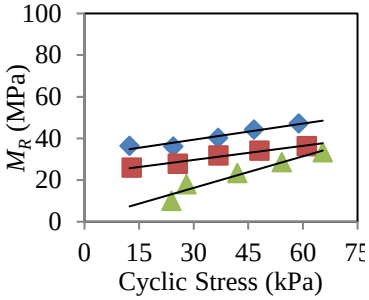

Figure A-10
(Orangeburg Sam. 511:
SM/A-2-4)

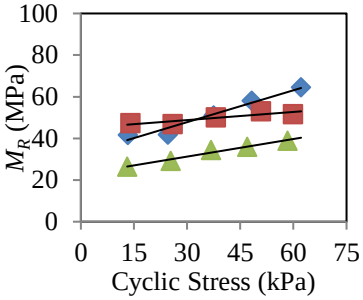

Figure A-11
(Orangeburg Sam. 512:
SM/A-2-4)

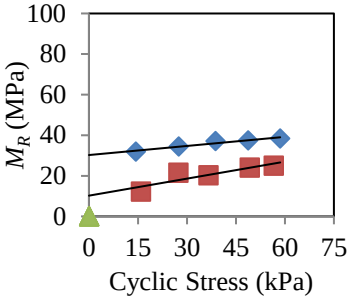

Figure A-12
(Orangeburg Sam. 513:
SC-SM/A-2-4)

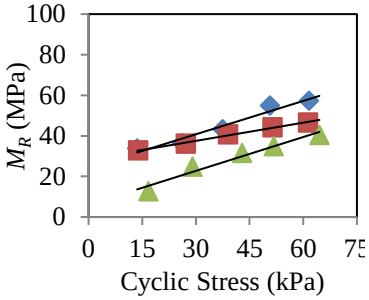

Figure A-13
(Orangeburg Sam. 612:
SM/A-2-4)

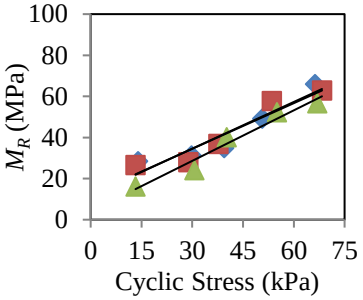

Figure A-14
(Orangeburg Sam. 613:
SM/A-2-4)

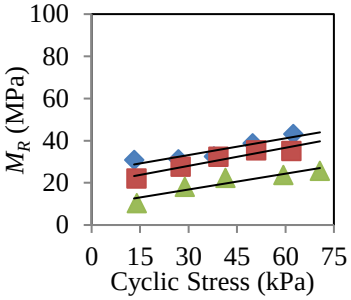

Figure A-15
(Orangeburg Sam. 711:
SM/A-2-4)

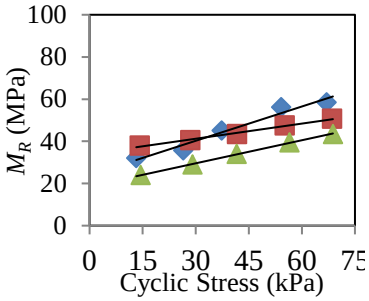

Figure A-16
(Orangeburg Sam. 712:
SM/A-2-4)

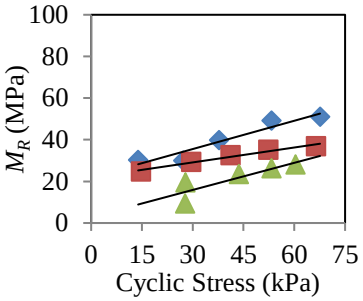

Figure A-17
(Orangeburg Sam. 713:
SM/A-2-4)

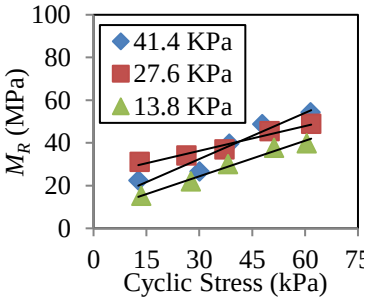

Figure A-18
(Orangeburg Sam. 811:
SC-SM/A-2-4)

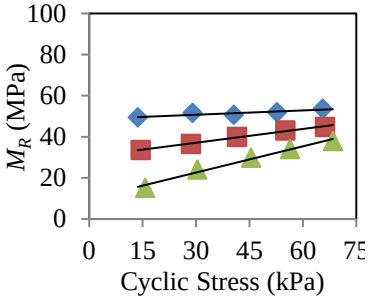

Figure A-19
(Orangeburg Sam. 812:
SC-SM/A-2-4)

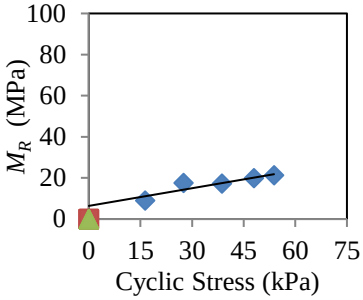

Figure A-20
(Orangeburg Sam. 821:
SC-SM/A-2-4)

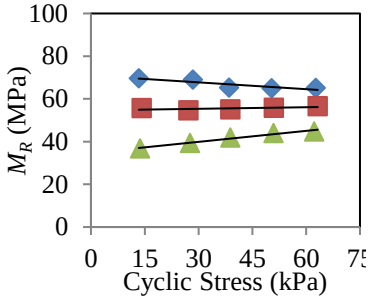

Figure A-21
(Orangeburg Sam. 822:
SC-SM/A-2-4)

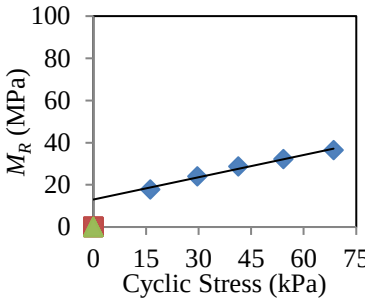

Figure A-22
(Orangeburg Sam. 911:
SC/A-2-4)

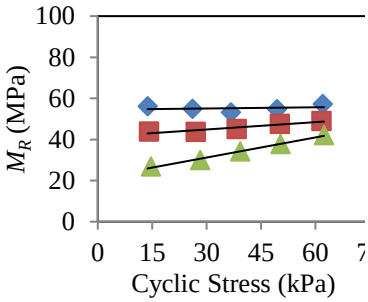

Figure A-23
(Orangeburg Sam. 912:
SC/A-2-4)

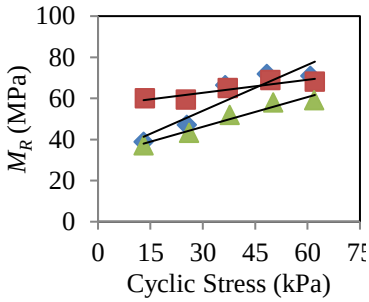

Figure A-24
(Orangeburg Sam. 1011:
SM/A-2-4)

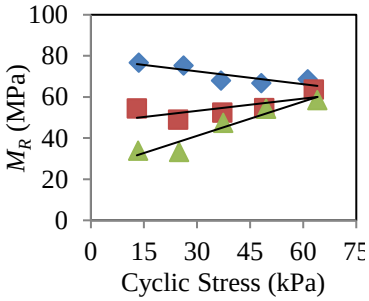

Figure A-25
(Orangeburg Sam. 1012:
SM/A-2-4)

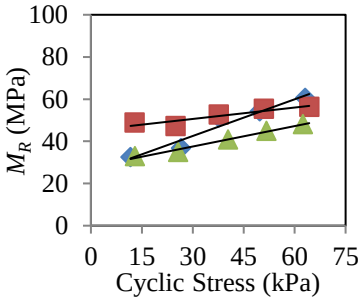

Figure A-26
(Orangeburg Sam. 1013:
SM/A-2-4)

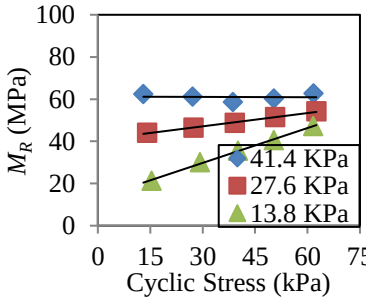

Figure A-27
(Orangeburg Sam. 1014:
SM/A-2-4)

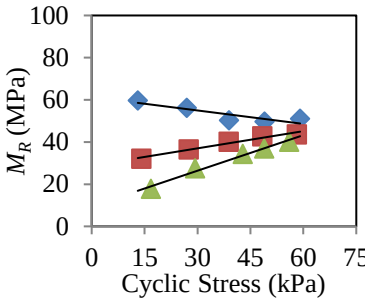

Figure A-28
(Orangeburg Sam. 1111:
SC/A-2-4)

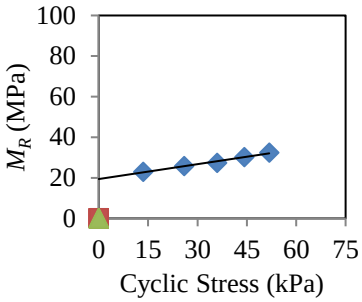

Figure A-29
(Orangeburg Sam. 1121:
SC/A-2-4)

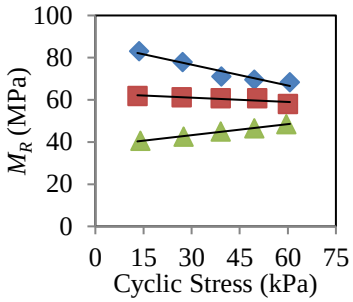

Figure A-30
(Orangeburg Sam. 1122:
SC/A-2-4)

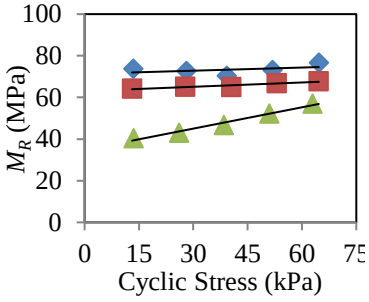

Figure A-31
(Orangeburg Sam. 1123:
SC/A-2-4)

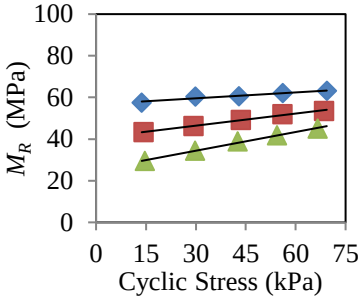

Figure A-32
(Orangeburg Sam. 1211:
SC-SM/A-2-4)

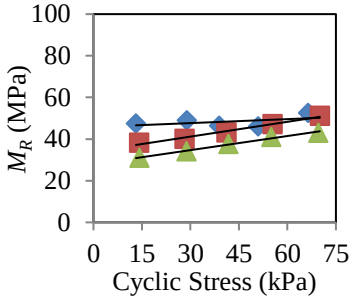

Figure A-33
(Orangeburg Sam. 1212:
SC-SM/A-2-4)

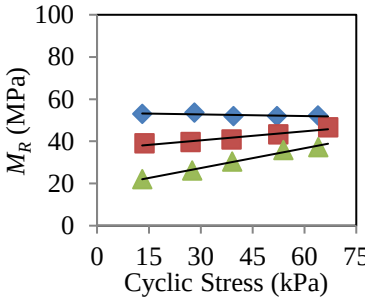

Figure A-34
(Orangeburg Sam. 1221:
SC-SM/A-2-4)

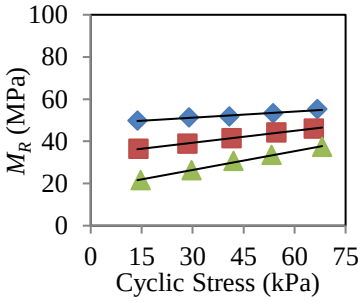

Figure A-35
(Orangeburg Sam. 1313:
SM/A-2-4)

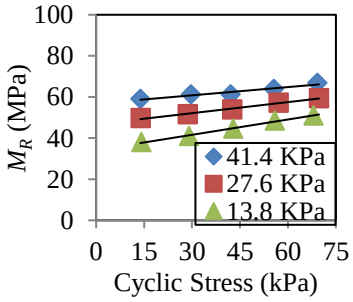

Figure A-36
(Orangeburg Sam. 1312:
SM/A-2-4)

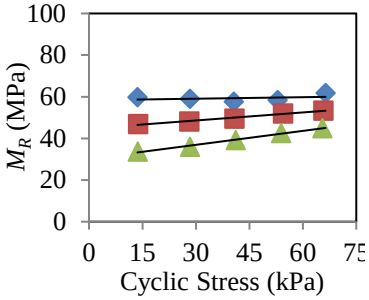

Figure A-37
(Orangeburg Sam. 1321:
SM/A-2-4)

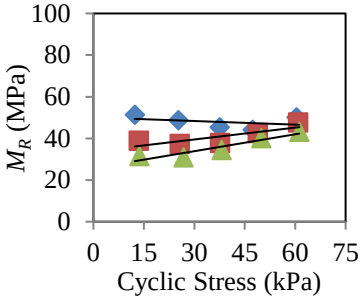

Figure A-38
(Georgetown Sam. 111:
SP/A-1-b)

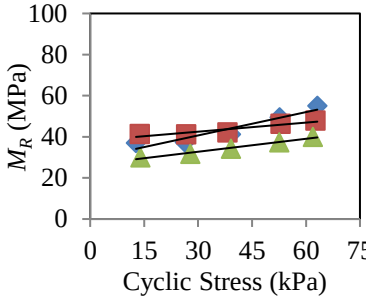

Figure A-39
(Georgetown Sam. 112:
SP/A-1-b)

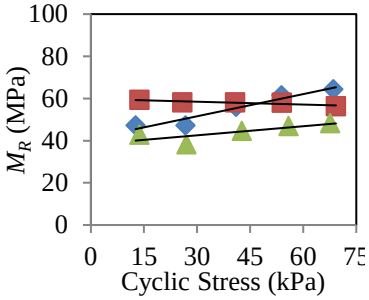

Figure A-40
(Georgetown Sam. 113:
SP/A-1-b)

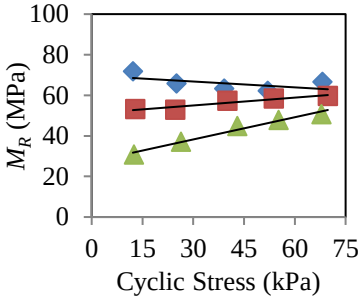

Figure A-41
(Georgetown Sam. 114:
SP/A-1-b)

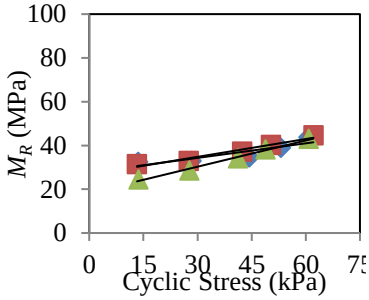

Figure A-42
(Georgetown Sam. 211:
SP/A-3)

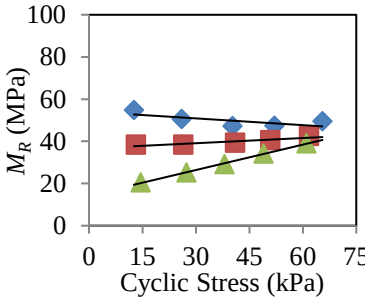

Figure A-43
(Georgetown Sam. 221:
SP/A-3)

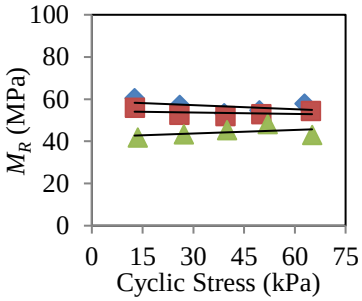

Figure A-44
(Georgetown Sam. 222:
SP/A-3)

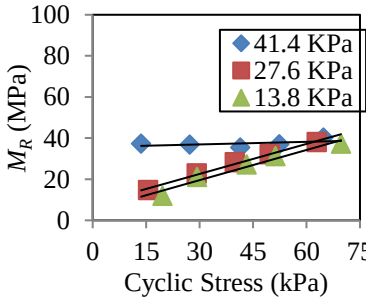

Figure A-45
(Georgetown Sam. 223:
SP/A-3)

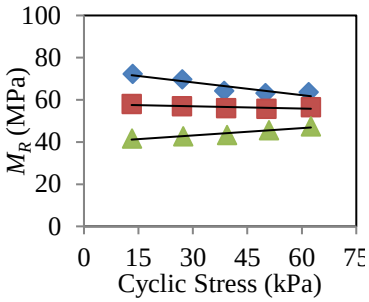

Figure A-46
(Georgetown Sam. 311: SP/A-3)

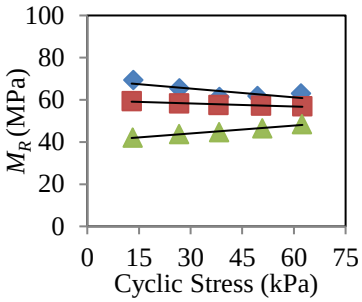

Figure A-47
(Georgetown Sam. 321: SP/A-3)

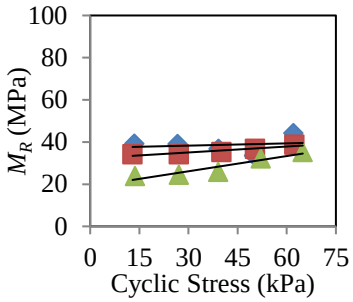

Figure A-48
(Georgetown Sam. 322: SP/A-3)

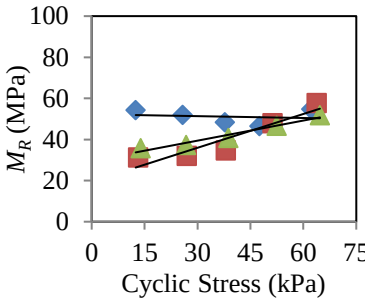

Figure A-49
(Georgetown Sam. 411: SP/A-3)

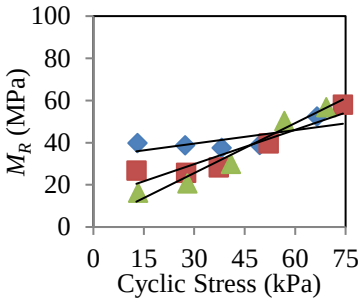

Figure A-50
(Georgetown Sam. 511: SP/A-3)

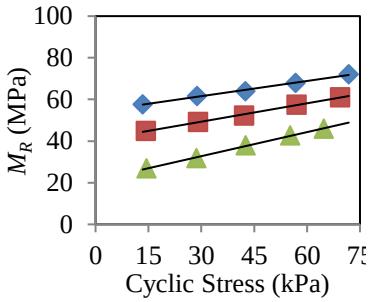

Figure A-51
(Georgetown Sam. 512: SP/A-3)

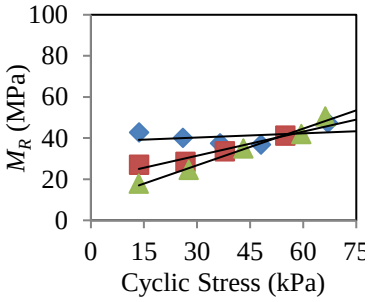

Figure A-52
(Georgetown Sam. 513: SP/A-3)

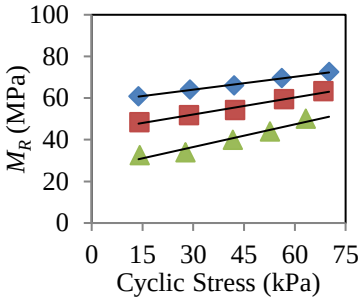

Figure A-53
(Georgetown Sam. 611: SP/A-3)

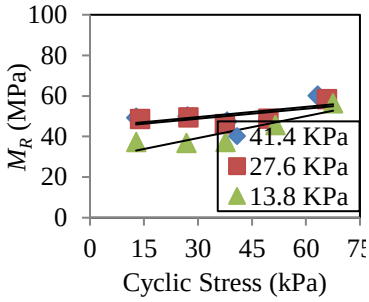

Figure A-54
(Georgetown Sam. 613: SP/A-3)

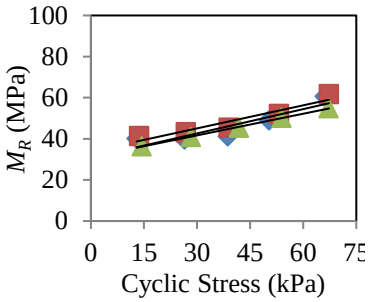

Figure A-55
(Georgetown Sam. 721:
SP/A-3)

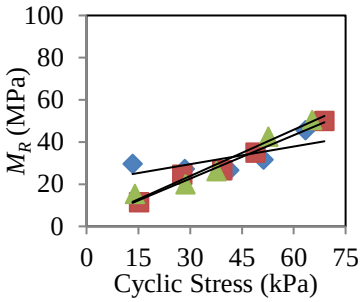

Figure A-56
(Georgetown Sam. 722:
SP/A-3)

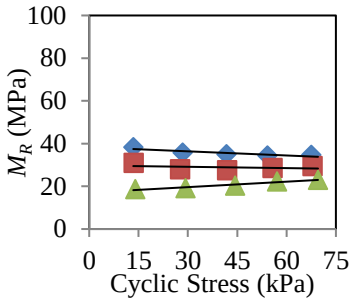

Figure A-57
(Pickens Sam. 111:
SC/A-7-6)

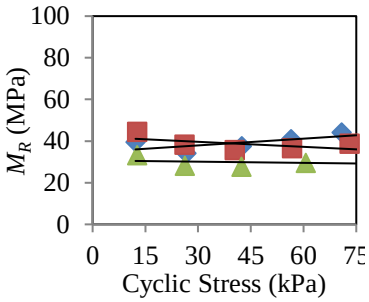

Figure A-58
(Pickens Sam. 112:
SC/A-7-6)

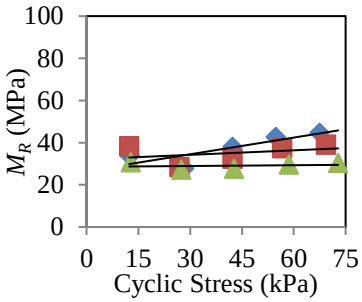

Figure A-59
(Pickens Sam. 113:
SC/A-7-6)

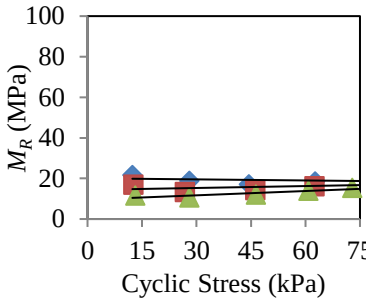

Figure A-60
(Pickens Sam. 114:
SC/A-7-6)

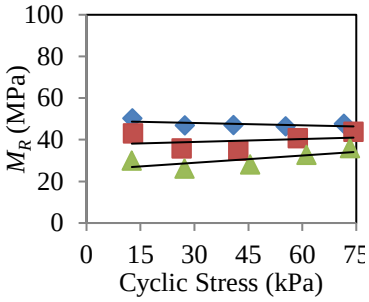

Figure A-61
(Pickens Sam. 115:
SC/A-7-6)

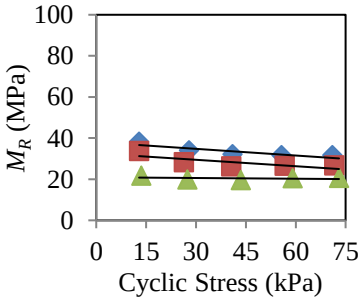

Figure A-62
(Pickens Sam. 211:
SC/A-7-6)

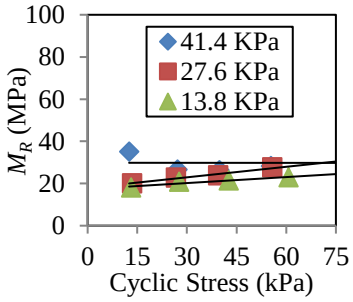

Figure A-63
(Pickens Sam. 212:
SC/A-7-6)

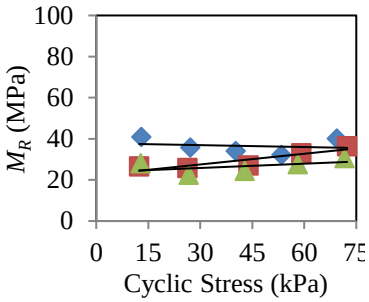

Figure A-64
(Pickens Sam. 213:
SC/A-7-6)

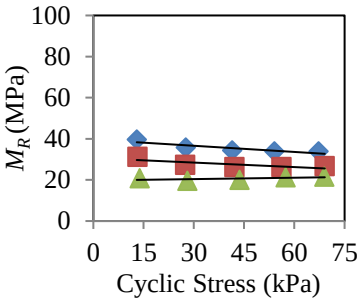

Figure A-65
(Pickens Sam. 214:
SC/A-7-6)

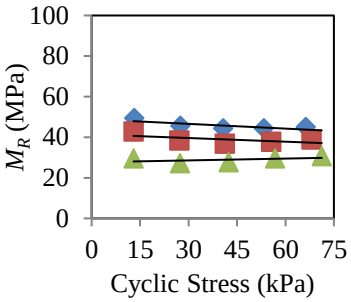

Figure A-66
(Pickens Sam. 215:
SC/A-7-6)

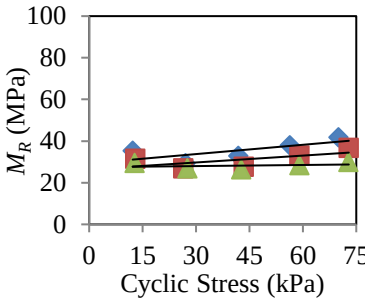

Figure A-67
(Pickens Sam. 311:
SC/A-7-6)

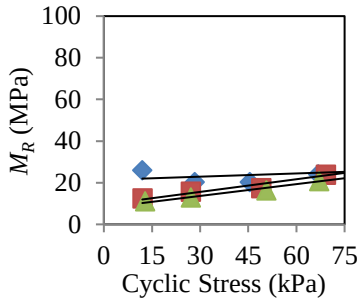

Figure A-68
(Pickens Sam. 312:
SC/A-7-6)

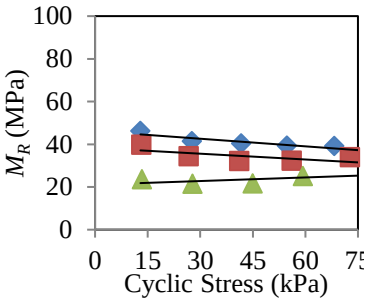

Figure A-69
(Pickens Sam. 313:
SC/A-7-6)

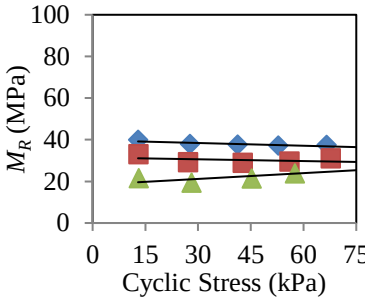

Figure A-70
(Pickens Sam. 314:
SC/A-7-6)

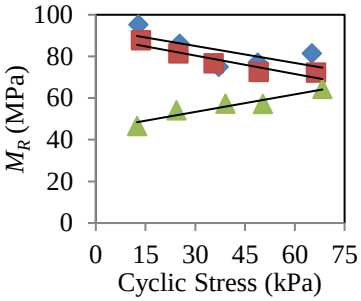

Figure A-71
(Pickens Sam. 411:
ML/A-4)

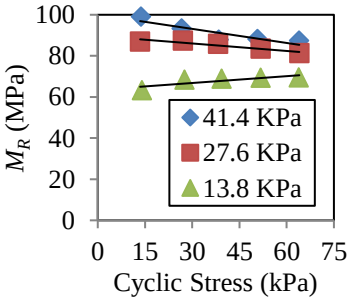

Figure A-72
(Pickens Sam. 412:
ML/A-4)

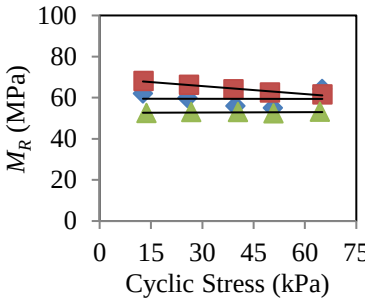

Figure A-73
(Pickens Sam. 413:
ML/A-4)

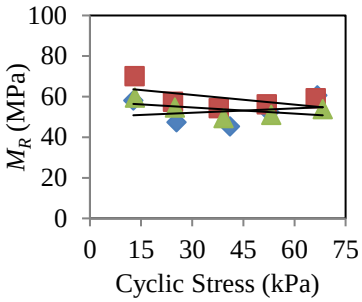

Figure A-74
(Pickens Sam. 414:
ML/A-4)

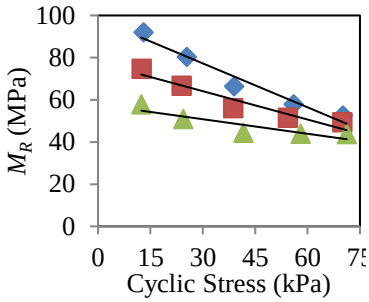

Figure A-75
(Pickens Sam. 415:
ML/A-4)

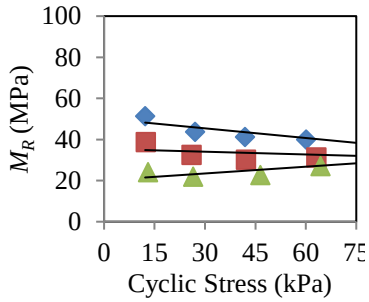

Figure A-76
(Pickens Sam. 511:
SC/A-7-6)

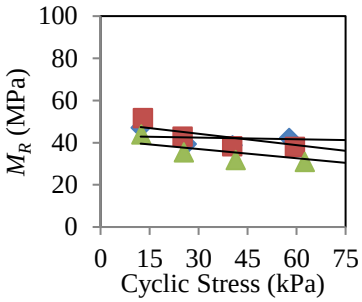

Figure A-77
(Pickens Sam. 512:
SC/A-7-6)

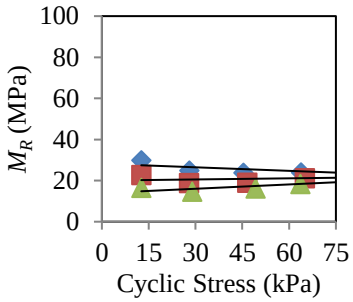

Figure A-78
(Pickens Sam. 521:
SC/A-7-6)

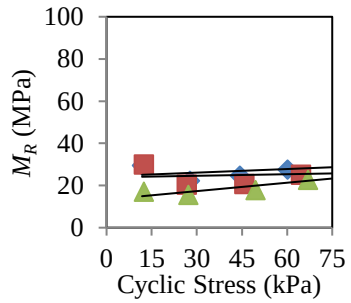

Figure A-79
(Pickens Sam. 522:
SC/A-7-6)

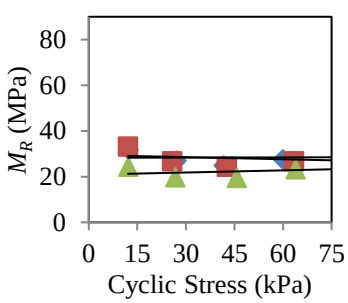

Figure A-80
(Pickens Sam. 523:
SC/A-7-6)

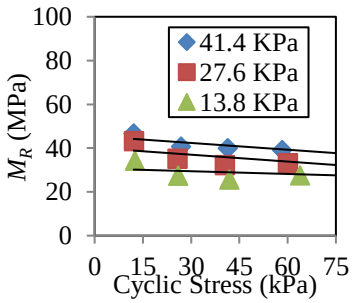

Figure A-81
(Pickens Sam. 524:
SC/A-7-6)

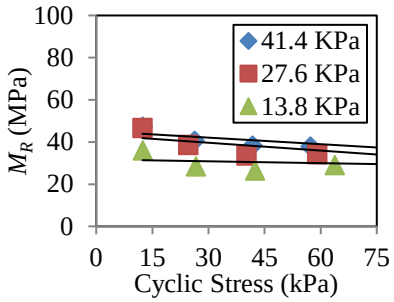

Figure A-82
(Pickens Sam. 525:
SC/A-7-6)

APPENDIX B –RESILIENT MODULUS VERSUS CYCLIC STRESS (REMOLDED)

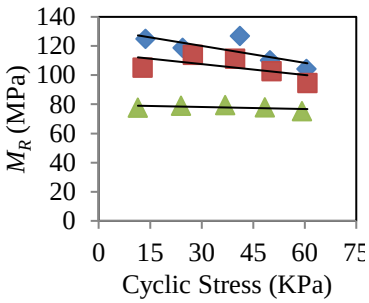

Figure B-1: 2% Dry Side (Orangeburg B-3: SC/A-2-4)

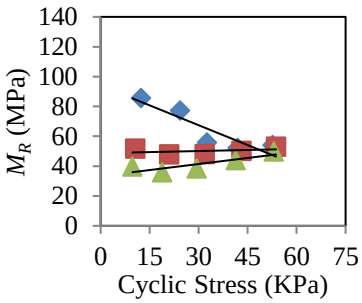

Figure B-2: OMC (Orangeburg B-3: SC/A-2-4)

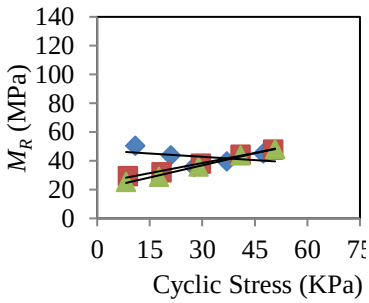

Figure B-3: 2% Wet Side (Orangeburg B-3: SC/A-2-4)

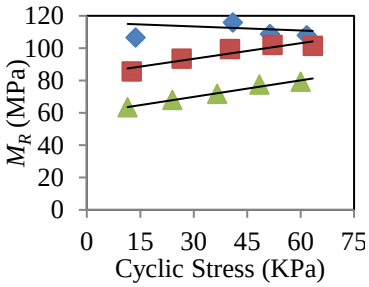

Figure B-4: 2% Dry Side (Orangeburg B-6: SM/A-2-4)

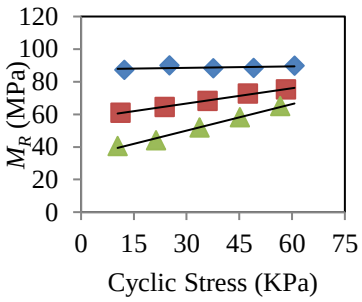

Figure B-5: OMC (Orangeburg B-6: SM/A-2-4)

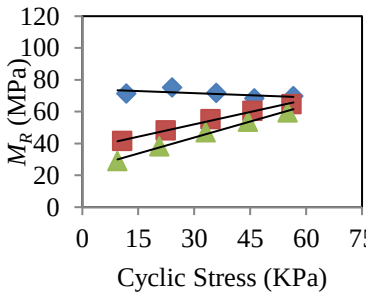

Figure B-6: 2% West Side (Orangeburg B-6: SM/A-2-4)

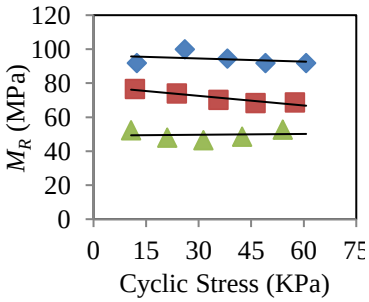

Figure B-7: 2% Dry Side (Orangeburg B-8: SC-SM/A-2-4)

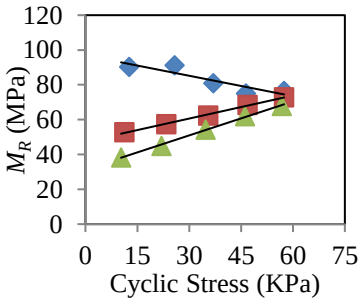

Figure B-8: OMC (Orangeburg B-8: SC-SM/A-2-4)

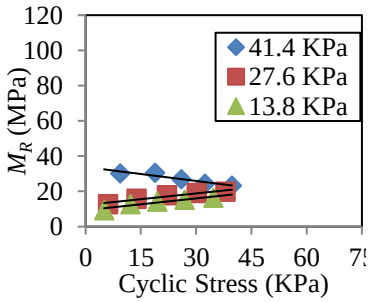

Figure B-9: 2% Wet Side (Orangeburg B-8: SC-SM/A-2-4)

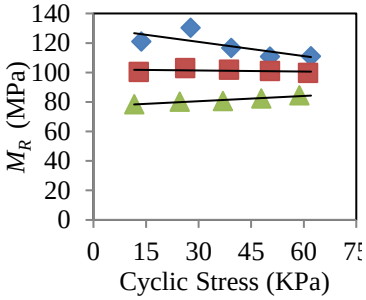

Figure B-10: 2% Dry Side (Georgetown B-1: SP/A-1-b)

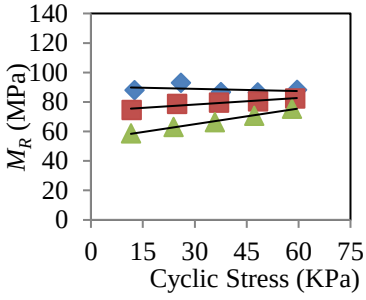

Figure B-11: OMC (Georgetown B-1: SP/A-1-b)

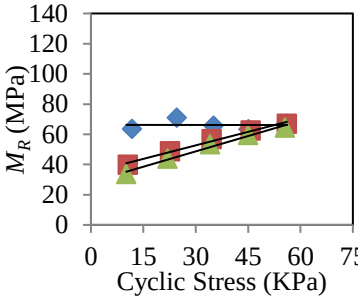

Figure B-12: 2% Wet Side (Georgetown B-1: SP/A-1-b)

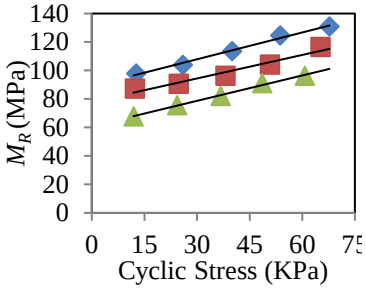

Figure B-13: 2% Dry Side (Georgetown B-4: SP/A-3)

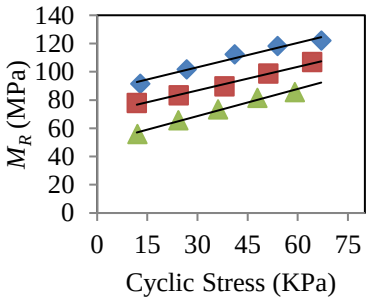

Figure B-14: OMC (Georgetown B-4: SP/A-3)

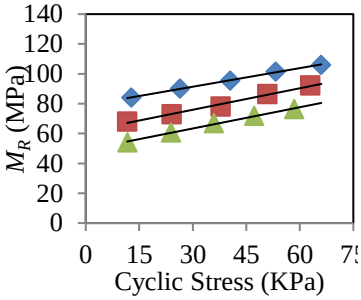

Figure B-15: 2% Wet Side (Georgetown B-4: SP/A-3)

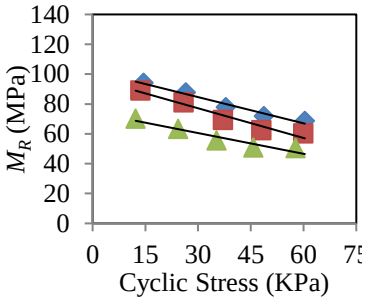

Figure B-16: 2% Dry Side (Pickens B-2: SM/A-7-6)

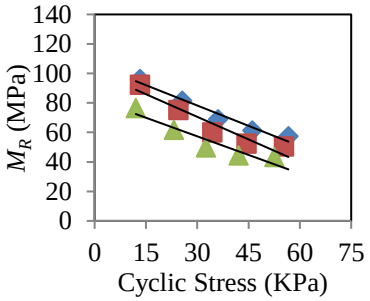

Figure B-17: OMC (Pickens B-2: SM/A-7-6)

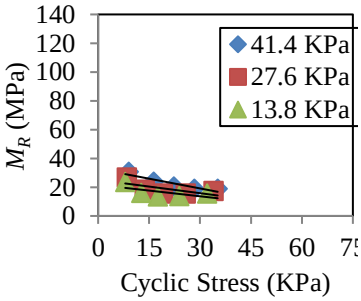

Figure B-18: 2% Wet Side (Pickens B-2: SM/A-7-6)

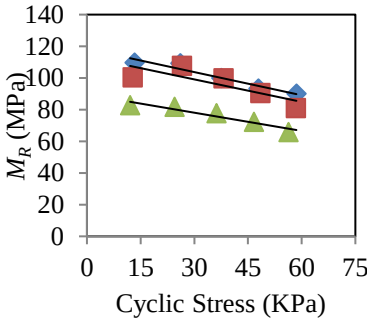

Figure B-19: 2% Dry Side (Pickens B-4: ML/A-4)

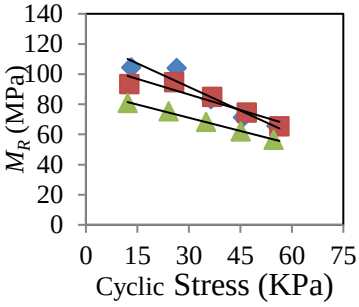

Figure B-20: OMC (Pickens B-4: ML/A-4)

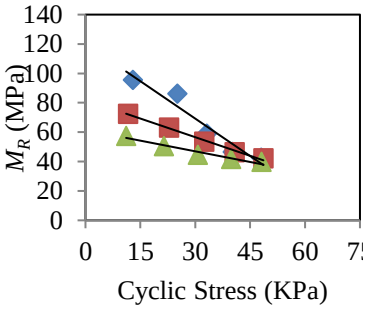

Figure B-21: 2% Wet Side (Pickens B-4: ML/A-4)

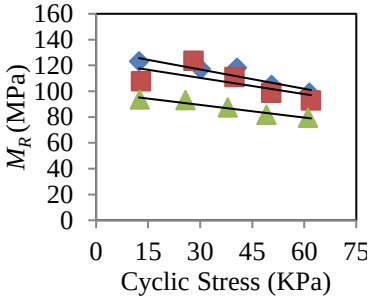

Figure B-22: 2% Dry Side (Pickens B-5: SC/A-7-6)

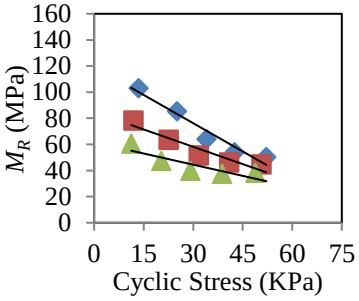

Figure B-23: OMC (Pickens B-5: SC/A-7-6)

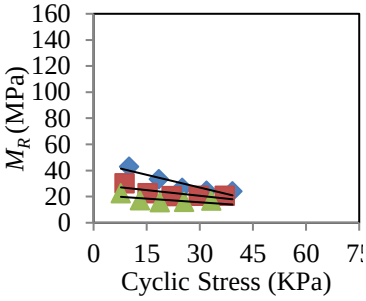

Figure B-24: 2% Wet Side (Pickens B-5: SC/A-7-6)

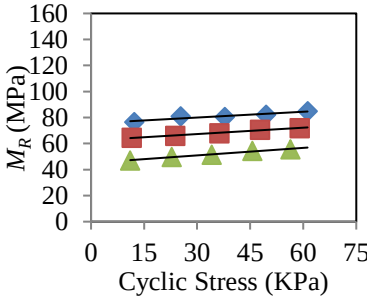

Figure B-25: 2% Dry Side (Orangeburg B-6: SC/A-2-4)

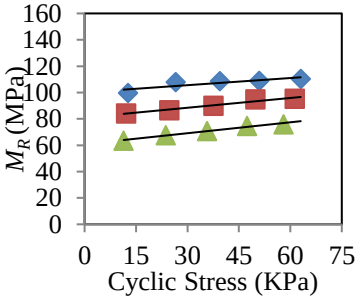

Figure B-26: 2% OMC (Orangeburg B-6: SC/A-2-4)

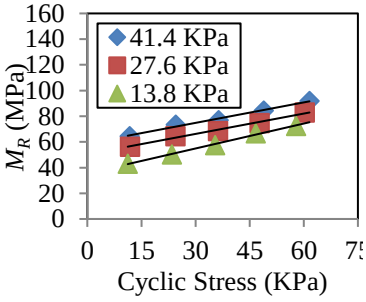

Figure B-27: 2% Dry Side (Georgetown B-4: SP/A-3)

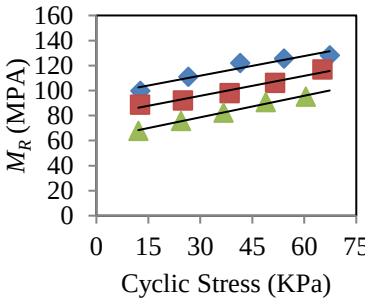

Figure B-28: OMC (Georgetown B-4: SP/A-3)

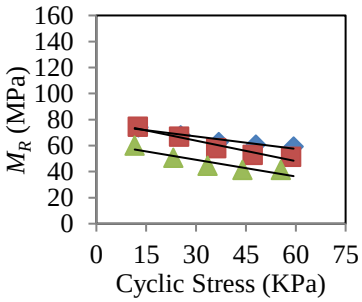

Figure B-29: 2% Dry Side (Pickens B-2: SM/A-7-6)

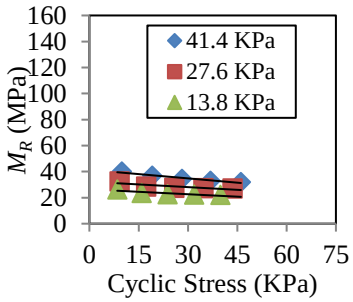

Figure B-30: 2% Dry Side (Pickens B-5: SC/A-7-6)

APPENDIX C –PERMISSION OF REPRINT

License Number	4175091251305
License date	Aug 23, 2017
Licensed Content Publisher	Springer
Licensed Content Publication	KSCE Journal of Civil Engineering
Licensed Content Title	Pavement performance evaluation models for South Carolina
Licensed Content Author	Md Mostaqur Rahman
Licensed Content Date	Jan 1, 2017
Type of Use	Thesis/Dissertation
Portion	Full text
Number of copies	1
Author of this Springer article	Yes and you are the sole author of the new work
Order reference number	
Title of your thesis / dissertation	Characterization of Subgrade Resilient Modulus for MEPDG and the Effects on Pavement Rutting
Expected completion date	Dec 2017
Estimated size(pages)	200

Figure C-1: Copyright Release for Chapter 2

Figure C-2: Copyright Release for Chapter 3